The Dissertation Committee for Abigail Devin Ondeck
certifies that this is the approved version of the following dissertation:

The Economic Feasibility of Combined Heat and Power as a Utility Producer for the Residential Sector

Committee:

Thomas F. Edgar, Co-Supervisor

Michael Baldea, Co-Supervisor

Ross Baldick

Atila Novoselac

Thomas Truskett

The Economic Feasibility of Combined Heat and Power as a Utility Producer for the Residential Sector

by

Abigail Devin Ondeck, B.S. CH.E.; M.S.E.

DISSERTATION

Presented to the Faculty of the Graduate School of

The University of Texas at Austin

in Partial Fulfillment

of the Requirements

for the Degree of

DOCTOR OF PHILOSOPHY

THE UNIVERSITY OF TEXAS AT AUSTIN

May 2017

Dedicated to my family.

Acknowledgments

I first want to thank with all my heart my parents, Pam and Tom, and my brother and sister, Nathaniel and Mariah, for all of their constant support. They were always there for me 24/7, and made the distance from Pittsburgh to Austin feel a lot shorter.

To my advisor, Thomas Edgar, it has always been reassuring to know that I can come to you with questions and you were there to give a guiding hand. You have been very giving in support and opportunities, and have demonstrated how a person can be a leader with a good sense of humor.

To my advisor, Michael Baldea, thank you for giving me the independence and room to create my own research area and follow it to its conclusion. With your guidance and support, the quality of my written reports has increased greatly from the time I started the program. More importantly, you have taught me there is not one path to completing a Ph.D.; each person has their own timeline.

A special thank you to my undergraduate professor, Ignacio Grossmann, for encouraging me to study in the field of optimization and being a trusted reference along the way.

To Austin Lane, thank you for being such a great source of ambition and laughter.

I also want to thank my fellow group members, especially the people I was lucky to share an office with (Matthew Walters, Bo Lu, Wesley Cole, Jong Kim, Corey James, and Ankur Kumar). You were great sources of enjoyment, patient listeners, and valuable contributors to my time at UT Austin.

Lastly, my work would not have been possible without the financial support provided by the Cockrell School of Engineering and IGERT.

The Economic Feasibility of Combined Heat and Power as a Utility Producer for the Residential Sector

Publication No. _____

Abigail Devin Ondeck, Ph.D.
The University of Texas at Austin, 2017

Co-Supervisors: Thomas F. Edgar
Michael Baldea

Combined heat and power (CHP) plants are a very promising prospect to reducing CO_2 emissions and increasing efficiency in the power generation sector, especially when combined with residential solar photovoltaic (PV) power generation. By utilizing natural gas, a cleaner fuel than coal, CHP plants can reduce CO_2 emissions, while exploiting the waste heat from electricity production to generate a useful thermal energy, increasing the overall efficiency of the plant. While incorporating residential solar PV power generation has important environmental benefits, it can - if not properly managed - lead to an over-generation situation with very high power plant ramp rates. Most current power plants are unlikely to be able to withstand such rapid changes in generation rates. If PV generation is incorporated into the design and operation of the CHP plant, both thermal and electrical energy storage

systems can be included, opening the door to more strategies for controlling photovoltaic generation and increased PV power generation.

The ability to combine thermal and electrical energy generation in an efficient manner, on a medium to large scale, suggests that CHP plants with rooftop PV panels and energy storage are an appealing choice as an integrated utility supplier for the neighborhood of the future. Yet, there are currently no CHP plants that serve exclusively residential neighborhoods in the United States. Thus, the objective of this research was to determine the most economical design and operation of a CHP plant with integrated residential solar PV power generation to meet all the energy demands of a residential neighborhood. After determining that a CHP plant could meet all the electricity, heating, and cooling demands of a residential neighborhood, a multi-scale economical optimization formulation to simultaneously determine the design and operation of a CHP plant with PV generation was constructed. The optimal CHP plant produced extra energy, so the optimization formulation was updated to include both thermal and electrical energy storage. Utilizing the results from these optimizations, the monetary values of PV generation and energy storage were evaluated, giving a guide for future economic targets for these technologies.

Table of Contents

List of Tables

List of Figures

Chapter 1

Introduction

1.1 Motivation

Everything in our lives runs on energy, with a large amount of this energy found in the form of electricity. Without electricity, it would be much harder to run state-of-the-art hospitals and labs, obtain clean water, run manufacturing facilities, and cool/heat our buildings and homes. With so many things running off of electricity, electricity is now viewed more as a necessity, and less a commodity.

In order to meet the current and future electricity demands in the industrial, commercial, and residential sectors, the electricity sector must carefully observe the current state of the grid, while simultaneously looking ahead to the future to make important decisions that will affect the grid's reliability, flexibility, and capacity. While maintaining and regulating the real and reactive power in the time span of seconds to minutes, independent system operators (ISOs) and regional transmission organizations (RTOs) have to decide who will generate how much of power to meet a predicted electricity demand in the time span of hours to days. Also, reliability coordinators must consider long-term planning, in the time span of years to decades, to decide which kind

of generation, using which types of fuels, at certain capacities and specific locations, should be added to the grid so that the future electricity demand can be met in an economic and efficient manner. With such a high level of uncertainty and an expansive time period of operation to cover, from seconds to decades, there is never a shortage of problems to be solved in the electricity sector.

Due to importance of energy and the large number of problems to be solved in the electricity sector, many initiatives and groups have been formed to find ways to increase energy efficiency. In 2015, the Department of Defense established a goal of deploying 3 GW of renewable energy on their Army, Navy, and Air Force installations by 2025 [13]. Also, the Smart Manufacturing Leadership Coalition (SMLC) received a grant from the Department of Energy's Energy Efficiency and Renewable Energy as part of the Clean Energy Manufacturing Initiative (CEMI) to research methods to improve manufacturing energy efficiency [14]. While these two initiatives were made to address the low penetration of renewable technology and the high energy consumption in the industrial sector, there are other problems that need to be addressed. For example, in Texas, the energy demand is highly dependent on the weather temperature. On Thursday, March 12^{th}, 2015, when the temperature in Dallas was 69^{o}, the electricity load for ERCOT was 32,955 MW at 5 PM. Skipping forward to August 10^{th}, 2015, when the temperature in Dallas was 107^{o}, the ERCOT electricity load was 69,659 MW. While the electricity demand from the industrial and commercial sectors increased slightly between the two days,

a majority of the increased electricity load was from the residential sector, which went up 248%, from 8,634 MW on March 12^{th} to 30,108 MW on August 10^{th} [15]. This extreme variability in daily and seasonal demand, mostly created by the residential sector, often leads to inefficient electricity generation. When there is an extreme peak in electricity generation, as seen on August 10^{th}, peaker plants, known for their ability to turn on and produce power quickly, as well as their low efficiencies, are used to meet the high demand.

In this dissertation, we address this problem by proposing a solution of utilizing a natural gas-fired Combined Heat and Power (CHP) plant with rooftop photovoltaic (PV) generation and energy storage to meet all of the energy utilities (heating, cooling, and electricity) of a residential neighborhood. With the overarching goals of increasing the efficiency of energy generation and lowering demand peaks common to the residential sector, optimization techniques are employed to 1) determine the physical capabilities of the CHP plant (i.e., if it is able to meet the heating, cooling, and electricity demands of the neighborhood at all hours), and 2) to calculate the cost-effectiveness of the solution in the residential sector.

1.2 Dissertation Outline

The dissertation is organized as follows:

- Chapter 2: Model-based scheduling of a district-level CHP plant with rooftop PV generation making use of the generic operation problem

- Chapter 3: Solving the simultaneous optimization of the design and operational strategy of a CHP plant with rooftop PV generation using the temporal Lagrangean decomposition method
- Chapter 4: Solving the simultaneous optimization of the design and operational strategy of a CHP plant with rooftop PV generation and energy storage using a bilevel decomposition method
- Chapter 5: Optimizing the operation of a CHP plant with PV generation and energy storage as a participant in the day ahead market, using a moving-horizon scheduling technique
- Chapter 6: Conclusions and recommendations

Chapter 2

Model-Based Scheduling of a Tri-Generation CHP Plant

This material has been published in [16] [1].

2.1 Introduction

Of the energy consumed in the United States, 20.10 quadrillion BTU (21% of the total energy consumption) are delivered for residential use. According to the data provided by the U.S. Energy Information Administration, a staggering 9.68 quadrillion BTU are lost [17]. Approximately 48% of these losses are due to electricity related inefficiencies. This number, calculated using data from all across the United States, and can vary from region to region. Shown in Figure 2.1, Austin, TX can experience energy losses of over 67% from coal power plants, and additional losses can be incurred during transmission and heating, cooling, and ventilation for residential homes.

Government agencies, industry, and academic researchers been working

[1] This chapter is based primarily on the following work, of which Abigail Ondeck is the primary contributor and Thomas Edgar and Michael Baldea supervised: A.D. Ondeck, T.F. Edgar, and M. Baldea. "Optimal operation of a residential district-level combined photovoltaic/natural gas power and cooling system". *Applied Energy*, 2015.

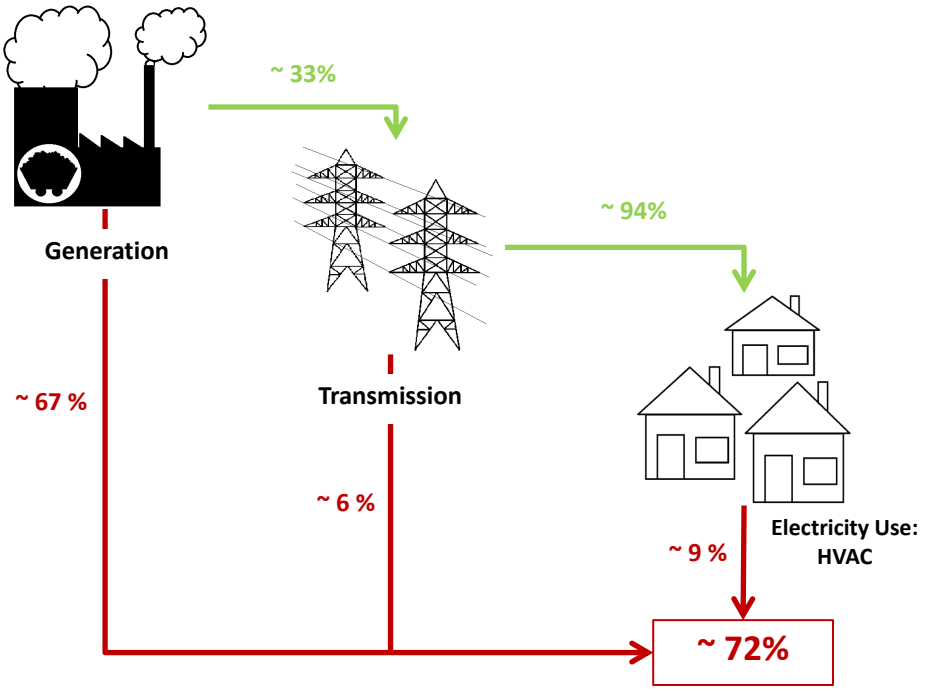

Figure 2.1: Residential Electricity Supply Chain Example: Some of the electricity used in Austin is produced at the coal-fired Fayette Power Plant with a generation efficiency of 33% [3]. The electricity produced from the plant must then be transported over long distances, where 6% of the electricity is lost [4]. Finally, once the electricity reaches residential end-users, incorrectly sized HVAC units can account for an additional 9% energy loss [5]. Overall, the total energy loss for residential homes, from generation to use, is approximately 72%.

to increase efficiency at the household level (e.g. energy-efficient appliances, retrofitting older homes) and shift energy demand from peak times to periods of lower demand. One possible solution to improve efficiency is to use Combined Heat and Power (CHP) with district cooling for residential neighborhoods. CHP plants are over twice as efficient than coal-fired power plants, reaching efficiencies of 80% [18]. The CHP plant can be located near the neighborhood, minimizing transmission losses. Finally, with district heating

and cooling produced from the plant, efficiency losses caused by oversizing or undersizing of HVAC units are eliminated.

In the industrial sector, CHP is commonly used with processes that have large concurrent concurrent heat and power demands, such as chemical [19, 20], pulp and paper [21], food [22], textile [23], and minerals [24]) [25]. In the commercial buildings sector, CHP plants can be found in areas with many businesses and lodging in close proximity, such as hotels [26], hospitals [27], university campuses [28], and large urban office buildings [29].

Despite only 8% of the world's electricity being generated by CHP, Europe has embraced this technology and continues to promote installation of new plants in the residential sector. In Denmark, 52% of the electricity demand (5,690 MW) is met by CHP, with most of the heat produced used for district heating systems, and more than half of Western Europe's CHP plants are connected to district heating and cooling systems [30].

While CHP appears to be economically feasible in a cold climate where heating is primarily used –as is the case in many European cities– the same may not be true for a hot climate. The climate, and consequently the location of the plant and the neighborhood to be supplied, has an effect on the electricity, heating, and cooling demands that need to be met. For example, in Sweden, the average summer temperature is between 55^oF and 63^oF [31], and this is reflected in typical energy use profiles (Figure 2.2: Top); heating is still used in the summer. On the other hand, in the predominantly cooling climate typical for the Southwestern United States, there is little need for heating, and the

energy use is dominated by cooling and electricity for lighting and appliances. Another key difference between heating and cooling climates is variability in energy demands: instead of the relatively constant demand profile of a house in a heating climate, the load profile in a cooling-dominant area is low in the morning and peaks in the evening. These differences in heating/cooling and the load profiles strongly impact the design and operation of a district CHP plant, and the feasibility of transplanting such district level technology in hot climates is thus far an open question.

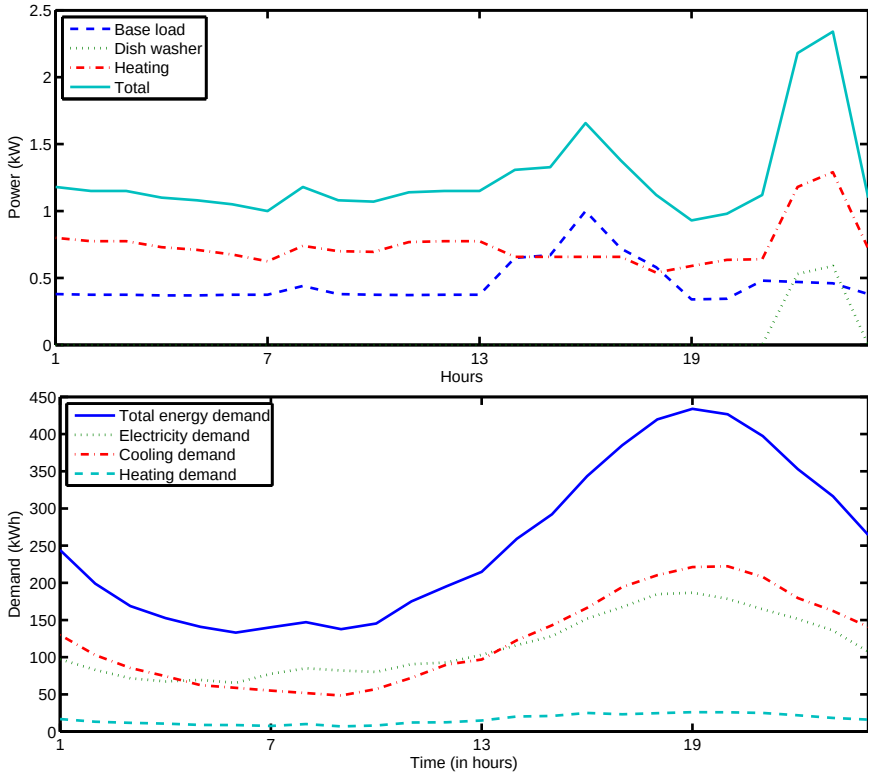

Figure 2.2: Top: Load profile for a home during the summer in Sweden (data from [6]); Bottom: Energy demand (electricity, cooling, and heating) for a home during the summer in Austin, Texas (data from WikiEnergy).

As a further requirement, if district-level CHP is to become feasible and economical in a cooling climate, the CHP plant must be able able to operate in conjunction with energy generation from renewable resources. For example, in 2011, the residential sector in the US consumed 610 Trillion BTU of renewable energy, with 140 trillion BTU coming from solar photovoltaic (PV) sources [32]. States such as Arizona [33], Texas [34], and New Mexico [35], have created aggressive rebate and tax incentive structures for residences that have installed renewables (e.g. solar PV panels), and four out of the top eight top states (in terms of solar PV panel capacity) are located in the Southwestern United States, where cooling demand is high [36].

High solar generation capacities can lead to grid-integration problems. Specifically, residential electricity and cooling demands are low in the morning (Figure 2.3) and rise to their highest level at the same time in the evening. However, the electricity generated by residential photovoltaic panels is desynchronized from the household energy demand. When the PV panels are generating electricity, the residential energy demand is near its lowest level, until the PV generation decreases in the evening, just when residential energy demand typically begins to increase. Thus, the operation of a district-level CHP plant must account for high PV generation in the afternoon when energy demand is low, and high energy demands in the evening when PV generation is not available, as well as meet the electricity, cooling, and heating demands of the residential neighborhood at all times.

Motivated by the above, in this paper, we address the following specific

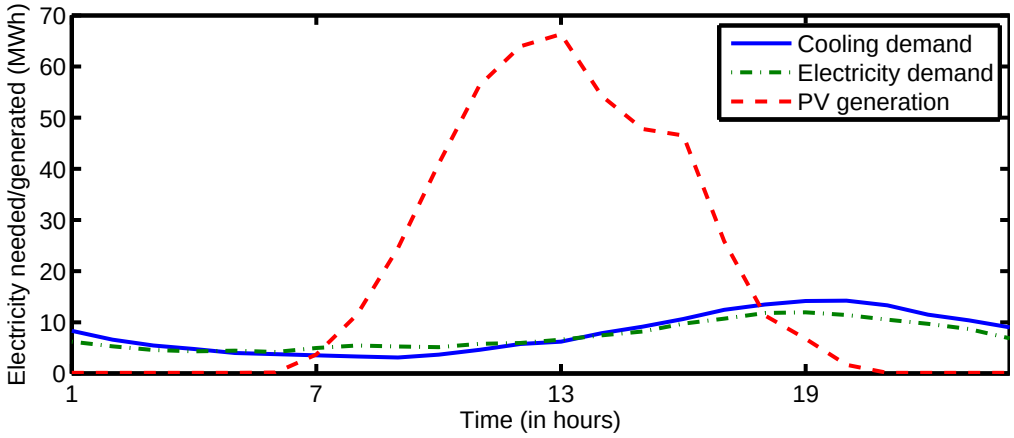

Figure 2.3: The amount of energy needed to supply both the electricity and cooling demands for a residential neighborhood in Austin, TX in the summer, as well as the PV generation if the entire neighborhood has PV panels. Heating, though present, is minimal in the summer and is not shown.

questions:

1. *Is CHP a viable means for providing district-level cooling in a predominantly cooling climate?*

2. *What is the optimal operating strategy for an integrated CHP/solar utility and what is the impact of photovoltaic generation on plant operation and operating profit?*

Our approach consists of developing a mathematical model for a district level CHP plant, followed by formulating the (generic) operation problem of this facility as an optimal scheduling problem that accounts for fluctuations in the energy prices, ambient conditions and residential demand. We also account for the potential to use photovoltaics, implemented as an electrical generation

source for the CHP plant, and determine its implication on the operation of the CHP system. The optimal operation problem is then solved for a particular case: a potential plant located in Austin, TX. In this case study, we rely on experimental residential demand data collected from WikiEnergy (owned and operated by Pecan Street Research Institute in Austin, TX).

2.2 Background

To our knowledge, district-level CHP plants that exclusively serve entire neighborhoods in a predominantly cooling climate have, thus far, not received any attention from researchers and practitioners.

When considering CHP plants used in a residential setting, a majority of the literature findings concentrate on micro-CHP for a single residential home, and not an entire neighborhood. There is a multitude of papers on the selection of the prime mover and sizing of the micro-CHP plant to provide heating, electricity [37–40], and cooling [41, 42]. Bianchi et al. also studied the scheduling of micro-CHP [43]. The optimization of the design from the economic versus energy savings perspective [44–46] and time horizon of the optimization [47] for micro-CHP has been studied. Finally, micro-CHP has been tested using different prime movers in test facilities [48, 49].

The papers that discuss district-level CHP often only consider European towns, due to the close proximity of the houses [50, 51], and many works concentrate on improving district heating, without additionally considering cooling. Different energy sources, such as natural gas and woodchips [52], and

incorporating heat storage [53, 54], have been studied to supply towns in Europe. Other authors have compared heating vs. electricity generation as the driving factor for CHP operation [55].

Outside the residential domain, the economics of designing and installing a trigeneration plant at hospitals [56, 57] were studied. Size optimization was also considered for CHP systems serving commercial building complexes [58] and hotels [59]. The feasibility of cogeneration for the food industry [60] and of CHP plants for supplying chemical complexes [61] has also been studied.

In this paper, we investigate district-level CHP plants that provide utilities for neighborhoods in predominantly cooling climates. We begin by describing the model of the system under consideration, followed by formulating the optimal operating problem for the CHP plant. We then present the results of a case study based on real-life data, and conclude with some final remarks, recommendations and future directions for research.

2.3 System Description

2.3.1 District System Arrangement

To deliver steam and chilled water for district cooling, the HVAC system for the residential neighborhood must be altered. In a cooling climate, most homes have their own centralized HVAC units that run on electricity (Figure 2.4: Top). With the new system, heating is delivered to the neighborhood by steam, cooling is delivered by chilled water, and electricity is

delivered using power lines, but as previously mentioned, there are minimal transmission losses (Figure 2.4: Bottom). Since the cost to retrofit an already existing neighborhood with district heating and cooling infrastructure is likely prohibitive, this project is aimed at future neighborhoods, where the needed infrastructure can be incorporated into the neighborhood design.

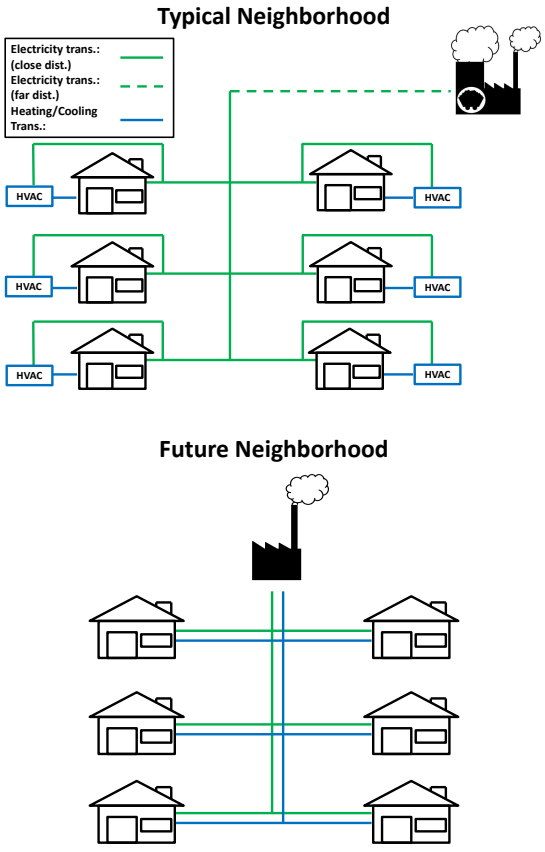

Figure 2.4: Residential Energy Production Problem & Solution: Current energy production methods can lead to large inefficiencies.

2.3.2 Residential District

The district energy load model was developed based on real data collected from the Mueller neighborhood in Austin, TX. The Mueller neighborhood is an urban redevelopment of the Robert Mueller Municipal Airport. It contains a collection of yard, row, and garden court houses and condominiums, where all buildings are designed with the goal to promote energy and water efficiency, water protection, and green space preservation. In 2009, the Mueller Megawatt Project was established with the goal to install 1 MW of PV panels in the neighborhood [62]. By 2011, the goal of having 1 MW of installed capacity was reached, and currently there are 254 homes with PV panels installed on their rooftops [63]. Pecan Street collects energy data from over 500 homes, including whole-home electricity, water, and natural gas data [8]. Data on PV panel generation from the panels installed on the home rooftops are also available.

The CHP plant is expected to meet the electricity, heating, and cooling demand for an entire neighborhood, but the available data on energy use and PV generation are limited to a small number of homes. Thus, either more homes need to be monitored to collect additional data, which is currently not available, or the current data loads need to be scaled up by an appropriate factor to simulate the loads for an entire neighborhood. Since the Mueller neighborhood is planned to have over 5,000 residential homes, the demands are scaled as followed, with the bolded values being the scaling factors. The scaling factors are different for each item because the number of homes with

available electricity, heating, and PV generation data vary:

Electricity Load: 88 homes × **64** = 5,632 homes

Cooling Load: 88 homes × **64** = 5,632 homes

Heating Load: 19 homes× **296** = 5,624 homes

PV Generation: 25 homes × **225** = 5,625 homes

15-minute data on residential electricity use were available for 88 homes in the Mueller neighborhood. From these residential electricity data, the electricity used by the HVAC unit to provide cooling was disaggregated [64] and converted to cooling by assuming that all homes have HVAC units with a seasonal energy efficiency ratio (SEER) of 18. Heating data, in 15-minute intervals, were available for only 19 homes. The electricity used to provide heating for each house was converted to heating needed, assuming that all homes have a heating efficiency of 97%. Finally, 15-minute data on PV generation were available for 25 homes. The PV generation was multiplied by 225 to calculate the amount of electricity generated by an entire neighborhood if all homes have PV panels installed on the rooftops.

2.3.3 CHP Plant

In this study, we consider the CHP plant (Figure 2.5) as the sole provider of electricity, heating, and cooling for the residential neighborhood. Part of the CHP plant model is based on the Carl J. Eckhardt Heating and

Power Complex located at the University of Texas at Austin. The UT Austin CHP plant is run in island mode, meeting all of the university's electricity, heat, and cooling demands throughout the year for all 17 million square feet of classroom, laboratory, and office space. The 137 MW plant runs at an efficiency over 80% [65], and can produce 1,282,000 lbs/hr of steam, 48,000 tons of chilled water, and also has 39,00 ton-hours of thermal energy storage (TES) to store chilled water [28]. Data obtained from the plant, including equipment parameters, inlet pressure, pressure drops, and inlet water and air temperatures, are used to more accurately model and schedule the inlet air cooler, gas turbine, heat recovery steam generator, and boiler, highlighted by the dotted orange box in Figure 2.5.

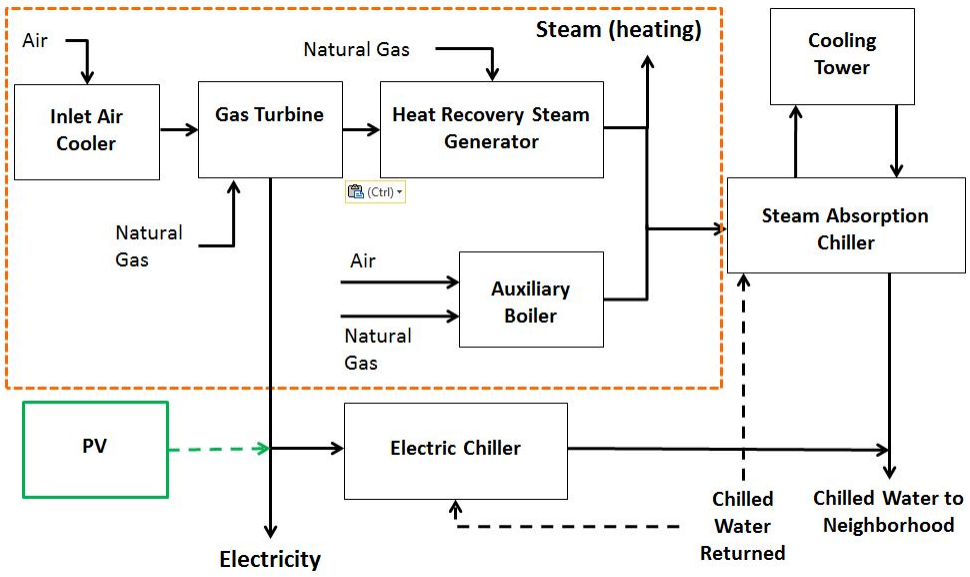

Figure 2.5: Diagram of the CHP plant to be modeled, with equipment highlighted by the orange box modeled using data from the University of Texas at Austin's CHP plant.

First, air enters the inlet air cooler where it is cooled using water. The hot air entering the cooler is controlled by the inlet guide vanes (IGV). Then chilled water is sprayed in the inlet air using an atomizer; any extra water droplets in the air are then removed before the cool air is sent to the gas turbine. The temperature of the air entering the gas turbine affects the power output from the gas turbine. By decreasing the temperature of the air entering the gas turbine, less fuel can be used to generate the same amount of power, improving the efficiency of the overall plant.

The cool air from the inlet air cooler is combined with natural gas in the gas turbine, and combusted to produce electricity. The exhaust gas from the gas turbine is sent to the heat recovery steam generator (HRSG) where it is used to convert water into superheated steam. If necessary, natural gas can be supplied to the HRSG via an in-duct burner to either produce more steam or to increase the temperature of the steam if the exhaust gas from the gas turbine is not hot enough. The steam produced by the HRSG can either be used to provide heating for the neighborhood or can be sent to the steam absorption chiller to provide cooling for the neighborhood. If the HRSG cannot produce enough steam, or if the gas turbine is not on, an auxiliary boiler, powered by natural gas, can be used to supply additional steam.

The first piece of equipment used to provide cooling for the residential neighborhood in the form of chilled water is the two-stage steam absorption chiller. A two-stage absorption chiller was selected over a single stage unit because the single stage units run using low pressure steam and have much

lower coefficients of performance (COPs) compared to the two-stage units. The two-stage units operate using hot exhaust gas at high pressures, and the COPs are almost 50% larger than a single stage unit.

The steam absorption chiller, using the maximum amount of steam produced from both the HRSG and the boiler, is unable to produce enough cooling to meet the entire neighborhood cooling demand. To help meet the demand, an electric chiller is included to provide additional chilled water.

Finally, electricity generated by the PV panels located in the neighborhood is incorporated into the plant model to be used by the CHP plant. The electricity can either be sold for profit (to the neighborhood or the grid), or to help provide power for the electric chiller.

2.4 CHP System Modeling

2.4.1 Equipment Models

We rely on the work by Kim et al. [66] to develop a system model. The original models developed by Kim et al. for the inlet air cooler, gas turbine, and HRSG are highly nonlinear. In order to make the optimization tractable, we obtain linear approximations of the behavior of these components. The corresponding nonlinear models can be are described in Appendix B and more information on the linear approximations is presented in Appendix C.

2.4.1.1 Inlet Air Cooler

The inlet air cooler model is used to determine the mass (m^h_{air}) and temperature ($T^h_{air,out}$) of air exiting the cooler before it is sent to the gas turbine. The volume of air entering the cooler at ambient temperature and pressure is controlled by the Inlet Guide Vane (IGV^h), and the temperature of the air can be changed by altering the volume of water (Vw^h) entering the cooler. The mass and temperature of the air are calculated using two manipulated variables (IGV^h, Vw^h) and two input parameters ($T^h_{w,in}$, $T^h_{air,in}$):

$$m^h_{air} = (\alpha_1 \times IGV^h) + (\alpha_2 \times Vw^h) + y^h_{GT,on} \times \left[(\alpha_3 \times T^h_{w,in}) + (\alpha_4 \times T^h_{air,in}) + \alpha_5\right] \quad (2.1)$$

$$T^h_{air,out} = (\beta_1 \times IGV^h) + (\beta_2 \times Vw^h) + y^h_{GT,on} \times \left[(\beta_3 \times T^h_{w,in}) + (\beta_4 \times T^h_{air,in}) + \beta_5\right] \quad (2.2)$$

with

$$IGV^{min} \times y^h_{GT,on} \leq IGV^h \leq IGV^{max} \times y^h_{GT,on} \quad (2.3)$$

$$0 \leq Vw^h \leq Vw^{max} \times y^h_{GT,on} \quad (2.4)$$

where α_i and β_i, i=1,2,...,5, are the coefficient values obtained from approximating the nonlinear inlet air cooler model. The inlet guide vane is limited to minimum (IGV^{min}) and maximum (IGV^{max}) angles by Equation (2.3). The volume of water used to cool the air must be greater than or equal to zero, and is constrained to a maximum value, Vw^{max}, in Equation (2.4).

2.4.1.2 Gas Turbine

The gas turbine combines the air from the inlet air cooler with natural gas, and combusts them to produce electricity with exhaust gas as a by-product. The amount of natural gas used in the gas turbine is controlled by the fuel signal, Fd^h. The power generated from the gas turbine, P^h_{GT}, as well as the firing temperature (T^h_f) and exhaust temperature (T^h_e), are functions of the fuel signal and the mass and temperature of air exiting the inlet air cooler:

$$P^h_{GT} = (\gamma_1 \times Fd^h) + (\gamma_2 \times m^h_{air}) + (\gamma_3 \times T^h_{air,out}) + \left(y^h_{GT,on} \times \gamma_4\right) \tag{2.5}$$

$$T^h_f = (\delta_1 \times Fd^h) + (\delta_2 \times m^h_{air}) + (\delta_3 \times T^h_{air,out}) + \left(y^h_{GT,on} \times \delta_4\right) \tag{2.6}$$

$$T^h_e = (\zeta_1 \times Fd^h) + (\zeta_2 \times m^h_{air}) + (\zeta_3 \times T^h_{air,out}) + \left(y^h_{GT,on} \times \zeta_4\right) \tag{2.7}$$

with

$$Fd^{min} \times y^h_{GT,on} \leq Fd^h \leq Fd^{max} \times y^h_{GT,on} \tag{2.8}$$

where γ_j, δ_j and ζ_j, j=1,2,...,4, are the coefficient values obtained from approximating the nonlinear gas turbine model. Equation (2.8) is used to bound the amount of natural gas entering the gas turbine by limiting the fuel signal to be between the minimum (Fd^{min}) and maximum (Fd^{max}) values.

2.4.1.3 Heat Recovery Steam Generator

As described in Section 2.3.3, the HRSG uses the exhaust heat from the gas turbine to produce steam. Natural gas can be used, if necessary, to power a duct burner to increase the temperature of the exhaust gas or to increase the

amount of steam produced. The approximated HRSG models for the steam produced, $W^h_{sh,HRSG}$, and the temperature of the exhaust leaving the HRSG, $T^h_{e,raised}$, are functions of the fuel entering the HRSG, $W^h_{f,HRSG}$, the fuel signal of the gas turbine, and the mass and temperature of air exiting the inlet air cooler:

$$W^h_{sh,HRSG} = (\kappa_1 \times W^h_{f,HRSG}) + (\kappa_2 \times Fd^h) + (\kappa_3 \times m^h_{air}) + (\kappa_4 \times T^h_{air,out}) + \left(y^h_{GT,on} \times \kappa_5\right) \quad (2.9)$$

$$T^h_{e,raised} = (\lambda_1 \times W^h_{f,HRSG}) + (\lambda_2 \times Fd^h) + (\lambda_3 \times m^h_{air}) + (\lambda_4 \times T_{air,out}6h) + \left(y^h_{GT,on} \times \lambda_5\right) \quad (2.10)$$

with

$$0 \leq W^h_{f,HRSG} \leq W^{max}_{f,HRSG} \times y^h_{GT,on} \quad (2.11)$$

where κ_k and λ_k, k=1,2,...,5, are the coefficient values obtained from approximating the nonlinear HRSG model. The flow of natural gas must be less than the maximum flow, $W^{max}_{f,HRSG}$, as stipulated by Equation (2.11).

2.4.1.4 Auxiliary Boiler

The steam output from the boiler, $W^h_{sh,BR}$, is directly proportional to the amount of natural gas ($W^h_{f,BR}$) supplied to the boiler:

$$W^h_{sh,BR} = \frac{(\eta_{BR} \times \rho_{NG} \times LHV) \times W^h_{f,BR}}{\hat{H}_{sh,BR} - \hat{H}_{i,BR}} \quad (2.12)$$

with

$$W_{f,BR}^{min} \times y_{BR,on}^{h} \leq W_{f,BR}^{h} \leq W_{f,BR}^{max} \times y_{BR,on}^{h} \tag{2.13}$$

where the parameters are defined as: η_{BR} is the efficiency of the boiler, ρ_{NG} is the density of natural gas, LHV is the lower heating value of natural gas, $\hat{H}_{sh,BR}$ is the enthalpy of the steam exiting the boiler, and $\hat{H}_{i,BR}$ is the enthalpy of the water entering the boiler. The fuel entering the boiler, must be greater than the minimum fuel flow, $W_{f,BR}^{min}$, and less than the maximum fuel flow, $W_{f,BR}^{max}$, whenever the boiler is in "on" mode.

2.4.1.5 Steam Absorption Chiller

The steam absorption chiller takes the steam from the HRSG and, if necessary, the auxiliary boiler, to create cooling for the neighborhood in the form of chilled water. The steam absorption chiller is modeled using a simplified model, where the coefficient of performance (COP) is kept constant and the temperature of the steam entering and the steam leaving are known and constant. The only manipulated variable that determines the amount of cooling produced (Q_{SA}^{h}) is the amount of steam entering the chiller, $W_{sh,SA}^{h}$:

$$Q_{SA}^{h} = COP_{SA} \times W_{sh,SA}^{h} \times \left(\hat{H}_{sh,HRSG} - \hat{H}_{sh,SA}\right) \tag{2.14}$$

with

$$W_{sh,SA}^{min} \times y_{SA,on}^{h} \leq W_{sh,SA}^{h} \leq W_{sh,SA}^{max} \times y_{SA,on}^{h} \tag{2.15}$$

where COP_{SA} is the coefficient of performance for the chiller, $\hat{H}_{sh,HRSG}$ is the enthalpy of the steam exiting the HRSG, and $\hat{H}_{sh,SA}$ is the enthalpy of the

steam exiting the chiller. Equation (2.15) stipulates that the amount of steam entering the chiller must be between the minimum ($W^{min}_{sh,SA}$) and maximum ($W^{max}_{sh,SA}$) amounts of steam that can be processed by the chiller when in "on" mode.

2.4.1.6 Electric Chiller

The cooling produced by the electric chiller, Q^h_{EC}, is proportional to the amount of power supplied to the chiller, P^h_{EC}:

$$Q^h_{EC} = COP_{EC} \times P^h_{EC} \tag{2.16}$$

with

$$P^{min}_{EC} \times y^h_{EC,on} \leq P^h_{EC} \leq P^{max}_{EC} \times y^h_{EC,on} \tag{2.17}$$

where COP_{EC} is the coefficient of performance for the electric chiller. The COP of the electric chiller is assumed to be a constant across the whole cooling load range and is not affected by partial loads. Equation (2.17) stipulates that the amount of electricity supplied to the electric chiller must be between the minimum (P^{min}_{EC}) and maximum (P^{max}_{EC}) values.

2.4.2 Equipment Operating Constraints

Each component c in the CHP plant can operate in one of four modes (m): on, off, warm startup, or cold startup [61,67]. If the component has been off for five hours or less, the component can turn on via warm startup mode. However, if the component has been off for more than five hours, then the

component can only turn on in cold startup mode. The binary variable $y^h_{c,m}$ is used to keep track of the mode, where h is the hour, c is the component, and m is the mode.

Even though the CHP plant contains six different pieces of equipment, there are only four different components (Table 2.1). The inlet air cooler, gas turbine, and HRSG are all interconnected. If the gas turbine is running, the inlet air cooler will also be running to supply air to the gas turbine, and the HRSG will be running to turn the exhaust gas into steam. Thus, all three pieces of equipment will be in the same mode at the same time.

Component (c)	Equipment
GT	Inlet Air Cooler Gas Turbine HRSG
BR	Boiler
EC	Electric Chiller
SA	Steam Absorption Chiller

Table 2.1: CHP plant equipment broken into component groups.

In addition to the constraints already mentioned for the operation of the equipment, the gas turbine and the HRSG are subject to further constraints. The power generated by the gas turbine, P^h_{GT}, is constrained by Equation (2.18), to the maximum capacity of the gas turbine (P^{max}_{GT}). Also to prevent damage to the gas turbine, the exhaust temperature must be below T^{max}_e (Equation 2.20). In order to manage Nitrogen Oxide (NO_x) emissions, the

turbine's firing temperature is kept below T_f^{max} (Equation 2.19).

$$P_{GT}^h \leq P_{GT}^{max} \times y_{GT,on}^h \tag{2.18}$$

$$T_f^h \leq T_f^{max} \tag{2.19}$$

$$T_e^h \leq T_e^{max} \tag{2.20}$$

For the HRSG, the amount of steam is constrained to a maximum flow, $W_{sh,HRSG}^{max}$ (Equation 2.21) and the temperature of the steam leaving must be ΔT_{min} above the superheated temperature of steam, $T_{sh,HRSG}$ (Equation 2.22).

$$W_{sh,HRSG}^h \leq W_{sh,HRSG}^{max} \tag{2.21}$$

$$T_{e,raised}^h \geq T_{sh,HRSG} + \Delta T_{min} \tag{2.22}$$

2.4.3 Transition and Timing Constraints

Logic constraints are used to control and track transitions from one mode to the next. As mentioned previously, each component has four different modes. Equation (2.23) stipulates that each component c can only be in one mode m at hour h:

$$\sum_m y_{c,m}^h = 1 \quad \forall c \in C, h \in H \tag{2.23}$$

2.4.3.1 Prohibited Transition Constraints

Certain transitions from mode *m'* at hour *h-1* to mode m at hour h are allowed while others are not. The transitions that are prohibited (and allowed) are shown in Table 2.2.

	Off	On	Cold Startup	Warm Startup
Off	✓	X	✓	✓
On	✓	✓	X	X
Cold Startup	X	✓	✓	X
Warm Startup	X	✓	X	X

Table 2.2: Prohibited (X) and allowed (✓) transitions for the four CHP plant component groups, described in Table 2.1.

Prohibited and allowed transitions are modeled by the inequality constraints in Equations 2.24 and 2.25. If component c is allowed to move from mode *m'* at hour *h-1* to mode m at hour h, then the sum of the two binary variables is less than or equal to two (Equation 2.24). On the other hand, if a transition is not allowed, such as a component transitioning directly to "on" mode at hour h from "off" mode at hour *h-1*, the sum of the corresponding binary variables must be less than or equal to 1 (Equation 2.25).

$$y_{c,m'}^{h-1} + y_{c,m}^{h} \leq 2 \quad \forall\, c \in C, h > 1 \tag{2.24}$$

$$y_{c,m'}^{h-1} + y_{c,m}^{h} \leq 1 \quad \forall\, c \in C, h > 1 \tag{2.25}$$

2.4.3.2 Warm Startup vs. Cold Startup: Downtime

The distinguishing point to determine whether a piece of equipment is allowed to turn on in warm startup mode is the amount of time the equipment has been off. Any component can startup in warm startup mode if it was on for at least one hour within the past five hours. If the equipment was off for more than five consecutive hours, then the equipment must turn on via its cold startup mode. To model this behavior, the binary variable for each

component c at hour h in mode *warm startup* is constrained, so that if the equipment wasn't on in the past five hours, $y^h_{c,warmstartup}$, must equal 0:

$$y^h_{c,warmstart} \leq \sum_{\theta=1}^{5} y^{h-\theta}_{c,on} \quad \forall\, c \in C, h > 5 \tag{2.26}$$

2.4.3.3 Minimum Stay Constraints

When the equipment is in some modes, the equipment must stay in that mode for a designated amount of time, before it can transition to another mode. The minimum stay constraint is used for the cold startup only in this CHP plant model. When the equipment has been off for more than five hours, the equipment must be warmed up over a longer period of time. This time is incorporated into the model through the following constraint:

$$y^h_{c,on} + y^{h-1}_{c,coldstartup} \geq 2 \times y^{h-2}_{c,coldstart} + 2 \times y^{h-3}_{c,off} - 2 \quad \forall\, c \in C, h > 3 \tag{2.27}$$

All components, when turning on at hour h through cold startup mode, must be in cold startup mode for the previous two hours (*h-1* and *h-2*), before they can turn on (Equation 2.27).

2.4.3.4 Cost to Turn On

Each startup, warm or cold, comes with an associated cost, which varies for each piece of equipment. The cold startup is typically more costly than the warm startup because it places more stress on the equipment, and thus the maintenance factor is higher. In Table 2.3, the warm ($WarmCost_c$) and cold startup ($ColdCost_c$) costs for each piece of equipment are shown.

	$WarmCost_c$	$ColdCost_c$
Gas Turbine	\$180	\$360
Boiler	\$300	\$600
Electric Chiller	\$100	\$200
Steam Absorption Chiller	\$100	\$200

Table 2.3: Costs associated with turning on different components via a warm startup or cold startup.

The total cost for transitioning equipment ($Cost\ Time\ Lost_c^h$) from off to on, either through a warm or cold startup is calculated as follows:

$$Cost\ Time\ Lost_c^h = \left(ColdCost_c \times V_{c,cold}^h\right) + \left(WarmCost_c \times V_{c,warm}^h\right) \quad \forall\ c \in C, h > 2 \quad (2.28)$$

where $V_{c,cold}^h$ and $V_{c,warm}^h$ are two binary variables constrained by the mode of component *c*. When a warm startup has occurred, the equipment is in warm startup mode at hour *h-1* and turned on at hour *h*. Likewise, when a cold startup has occurred, the equipment must be in cold startup mode at hours *h-1* and *h-2* (since it takes two hours for a cold startup), and on at hour *h*. $V_{c,cold}^h$ and $V_{c,warm}^h$ are thus constrained as follows so that if a warm or cold startup has happened, the binary variable will be equal to 1, and equal to 0 otherwise:

$$V_{c,cold}^h \geq y_{c,cold}^h + y_{c,cold}^{h-1} - 1 \quad \forall\ c \in C, h > 2 \quad (2.29)$$

$$y_{c,warmstart}^{h-1} \leq V_{c,warm}^h \quad \forall\ c \in C, h > 1 \quad (2.30)$$

$$V_{c,warm}^h \leq y_{c,on}^h \quad \forall\ c \in C, h > 1 \quad (2.31)$$

2.5 Optimal Operating Schedule

In this section, we discuss the optimal operating solution for the district CHP system, which is formulated and solved as an optimal scheduling problem.

The objective of the scheduling problem consists of two parts:

1. Meet the neighborhood electricity, heating, and cooling demands
2. Maximize the profit of the CHP plant by selling electricity to the grid (P^h_{ext})

To ensure that the first requirement is met, the following constraints are used to reflect balances on electricity, steam, and chilled water:

$$P^h_{int} + P^h_{EC} + P^h_{ext} \leq P^h_{GT} + P^h_{solar} \tag{2.32}$$

$$Q^h_{cool,int} \leq Q^h_{EC} + Q^h_{SA} \tag{2.33}$$

$$W^h_{sh,HT} + W^h_{sh,SA} \leq W^h_{sh,HRSG} + W^h_{sh,BR} \tag{2.34}$$

The first equation requires that the electricity needed by the neighborhood (P^h_{int}) and the electric chiller, and the electricity sold to the grid must be less than or equal to the amount of electricity produced by the gas turbine and the PV panels in the neighborhood. The second equation requires that the cooling needed by the neighborhood ($Q^h_{cool,int}$) must be met by the electric chiller and the steam absorption chiller. The third constraint imposes that the steam provided to the neighborhood ($W_{sh,HT}$) and used by the steam absorption chiller for cooling must be less than or equal to the amount of steam produced by the HRSG and the boiler.

The objective of the scheduling is to maximize the total operating profit for the CHP plant. The CHP plant has four sources of revenue:

1. Selling electricity to the neighborhood ($Power\ Rev.\ Int.^h$)
2. Selling cooling to the neighborhood ($Cooling\ Rev.^h$)
3. Selling heating to the neighborhood ($Heating\ Rev.^h$)
4. Selling electricity to the grid ($Power\ Rev.\ Ext.^h$)

The first three revenue streams are predetermined from the demand data from the neighborhood, and are calculated as follows:

$$Power\ Rev.\ Int.^h = AE_{cost} \times P^h_{int} \tag{2.35}$$

$$Cooling\ Rev.^h = Cool_{cost} \times Q^h_{cool,int} \tag{2.36}$$

$$Heating\ Rev.^h = Heat_{cost} \times Q^h_{heat,int} \tag{2.37}$$

where AE_{cost} is the price for a home to purchase electricity from the local utility, $Cool_{cost}$ is the price for a home to purchase 1 BTU of cooling via district cooling, and $Heat_{cost}$ is the price for a home to purchase 1 kWh of heating via district heating. The final source of revenue, $Power\ Rev.\ Ext.^h$, is to be determined by the scheduling. The profit from selling electricity to the grid is calculated using past day-ahead market prices, $Grid^h_{cost}$, and the amount of electricity sold to the grid, P^h_{ext}, which is unbounded:

$$Power\ Rev.\ Ext.^h = Grid^h_{cost} \times P^h_{ext} \tag{2.38}$$

The two sources of cost to the CHP plant in the scheduling are from transitioning from off to on ($Cost\ Time\ Lost^h$) and from purchasing fuel for the plant. Since the entire plant runs on natural gas, the cost to purchase natural gas ($Fuel\ Cost^h$) is:

$$Fuel\ Cost^h = NG_{cost} \times \left(W^h_{f,GT} + W^h_{f,HRSG} + W^h_{f,BR}\right) \tag{2.39}$$

where NG_{cost} is the cost to purchase natural gas. The economic values used to calculate the profits and costs are shown in Table 2.4.

The overall objective to maximize is thus:

$$\begin{aligned} Profit = \sum_h (&Power\ Rev.\ Int.^h + Cooling\ Rev.^h + Heating\ Rev.^h \\ &+ Power\ Rev.\ Ext.^h - Fuel\ Cost^h - Cost\ Time\ Lost^h) \end{aligned} \tag{2.40}$$

Variable	Value	Description
AE_{cost}	\$0.11/kWh	Austin Energy summer prices in Tier 3 (1001-1500 kWh per month) [68]
$Cool_{cost}$	\$6.11 $\times 10^{-6}$/BTU	Calculated using Austin Energy prices and a SEER of 18
$Heat_{cost}$	\$.07/kWh	Average cost in NYC using district heating [69]
$Grid^h_{cost}$	Varies (\$/kWh)	Day-ahead market prices from ERCOT for Austin, TX [70]
NG_{cost}	\$4.39/ft^3	Industrial price for natural gas in Texas [71]

Table 2.4: Economic values used in calculating the plant revenues and costs.

2.6 Case Study

2.6.1 Maximizing Profit

The optimization problem was solved for a one week period, from July 1^{st} to July 7^{th}. This week was selected because the data on energy demand are representative of energy use in the area during the summer months. Each day, the CHP plant was able to generate a significant amount of profit, with the maximum profit coming from selling electricity to the grid, as shown in Figure 2.6. The profits from selling electricity, cooling, and heating to the neighborhood are cyclic, which is expected since the profit follows the path of the residential energy demand. The heating revenue for this case is minimal because little heating is needed in the summer in Austin. In total, the profit from July1^{st} to July 7^{th} was \$421,434.

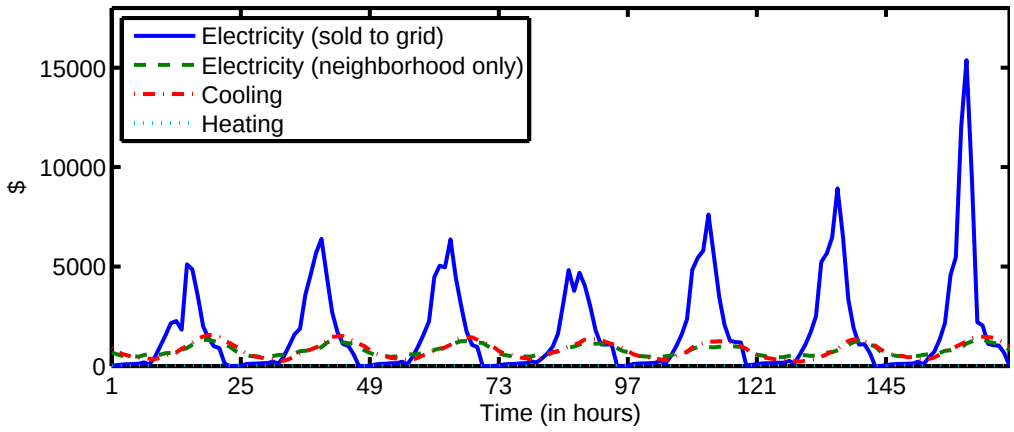

Figure 2.6: Revenue from selling electricity, cooling, and heating to the neighborhood, and electricity to the grid.

There are two important factors that determine when electricity is to

be sold to the grid: the availability of electricity and the day-ahead market prices. Shown in Figure 2.7, electricity sales to the grid start when the PV panels generate sufficient energy to provide electricity for the neighborhood. At this time, the gas turbine is in "off" mode. Once the day-ahead electricity prices become sufficiently high, the gas turbine is turned on to the maximum capacity so the plant can make the most profit. In the evening, solar decreases when the sun sets and the gas turbine continues to run at maximum capacity until it becomes not economical to sell electricity to the grid. Once it is not economical to sell electricity to the grid, the gas turbine production is lowered to the minimum production capacity, so that it may provide electricity to the neighborhood and any extra electricity can be sold to the grid, but at an economic loss.

2.6.2 Meeting Cooling Demand

In order to meet the cooling demand for the residential neighborhood, many pieces of equipment were used to help produce the chilled water. Cooling demand was near its highest around 6:00 PM everyday but just the electric chiller was unable to meet the total cooling needs for the neighborhood. At this point, additional cooling from the steam absorption chiller was needed, as seen in Figure 2.8. The gas turbine was already running at maximum capacity so the HRSG was producing steam at its maximum capacity. However, this was not enough steam for the steam absorption chiller, so the steam production rate of the less efficient boiler was increased to generate enough steam to meet

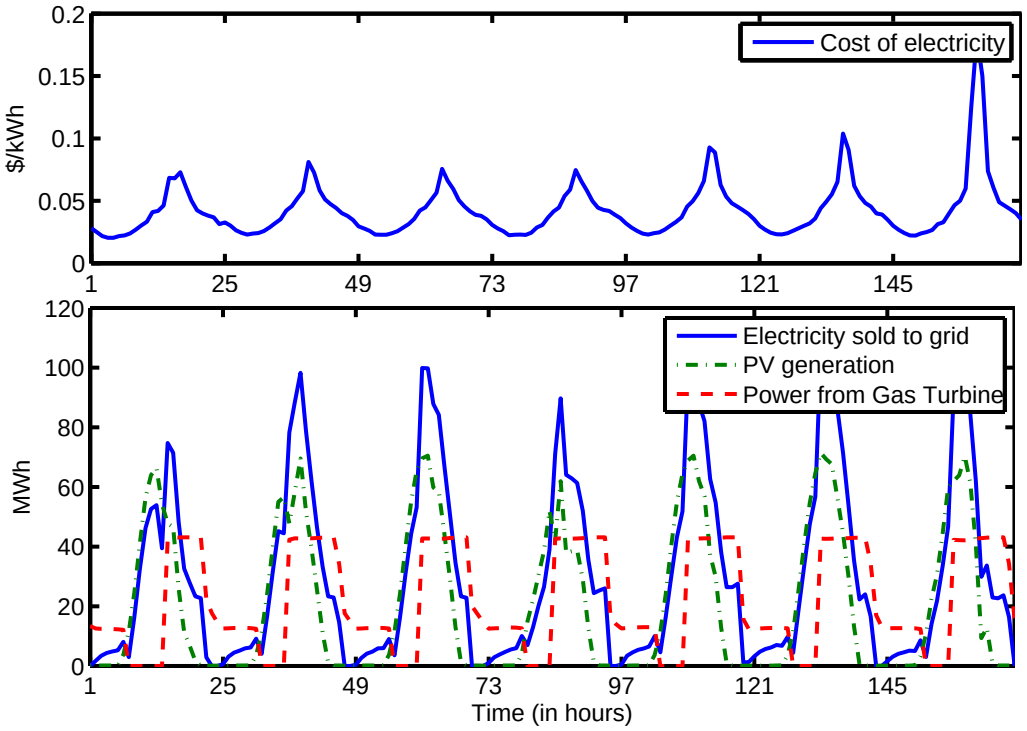

Figure 2.7: Cost-driven electricity production: Electricity sold to the grid is driven by availability and the day-ahead market prices.

all of the cooling demand for the neighborhood, shown in the bottom graph of Figure 2.8.

2.6.3 Effect of PV Integration on Plant Operation

As mentioned in the introduction, one goal of this research is to determine the impact of using PV-generated electricity as an additional source of electricity for the CHP plant. In the original model, electricity generated by the PV panels in the neighborhood can be used by the CHP plant to power the electric chiller, help meet the neighborhood electricity demand, or can be sold

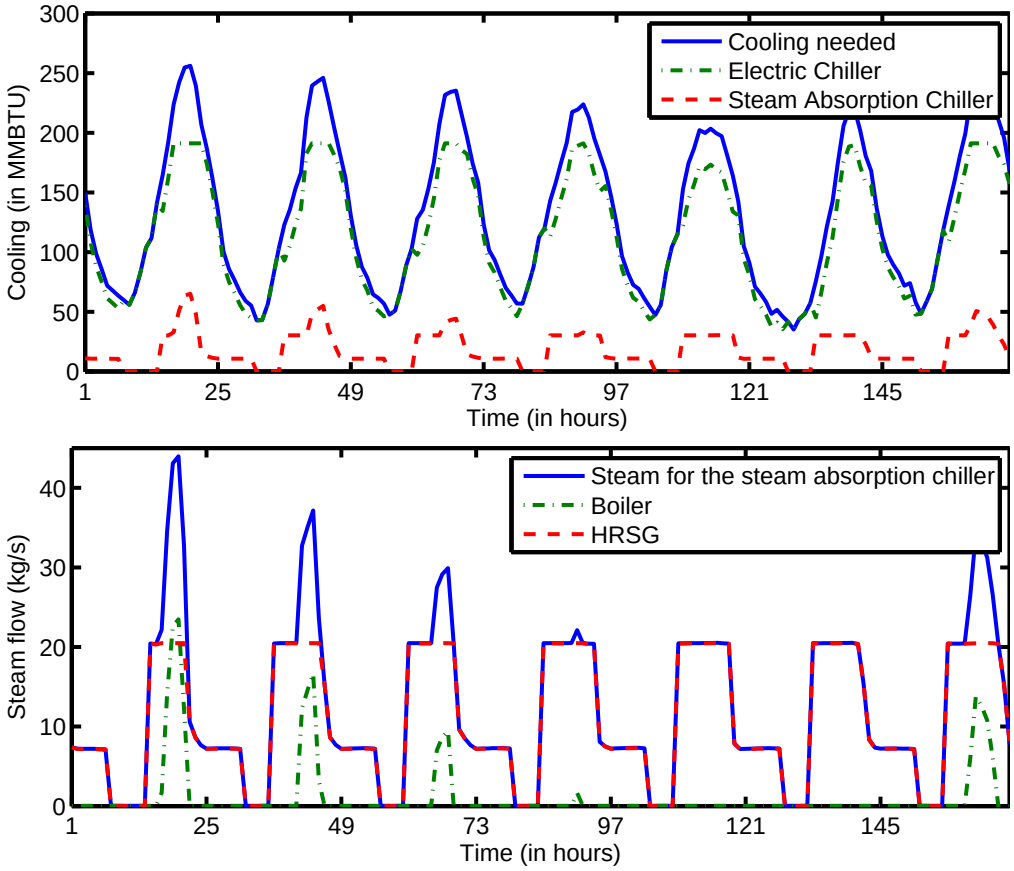

Figure 2.8: Cooling Sources: Since residential cooling demand is so high in the summer, both the electric chiller and the steam absorption chiller were needed

to the grid. To identify the effect of PV integration on plant operation, the optimization problem of maximizing plant profit was again solved for the same one week period, from July 1^{st} to July 7^{th}, but this time without integration of electricity generated by the neighborhood PV panels (Figure 2.9). In the original optimization problem, a majority of the profit came from selling electricity generated by the PV panels to the grid (Figure 2.7). However, without

PV panel generation, less electricity was available and thus less electricity was sold to the grid (Figure 2.10).

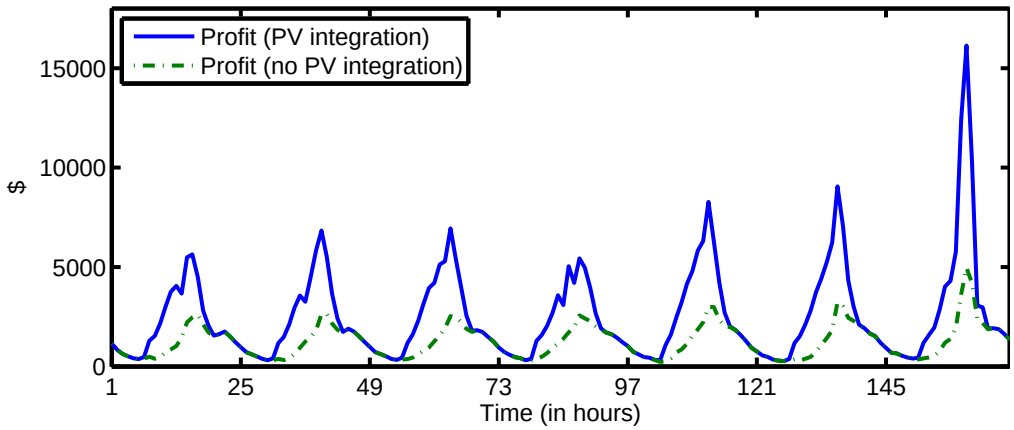

Figure 2.9: Without integrating PV generated electricity, the overall profit of the plant for the 1^{st} week of July is approximately half of the original profit.

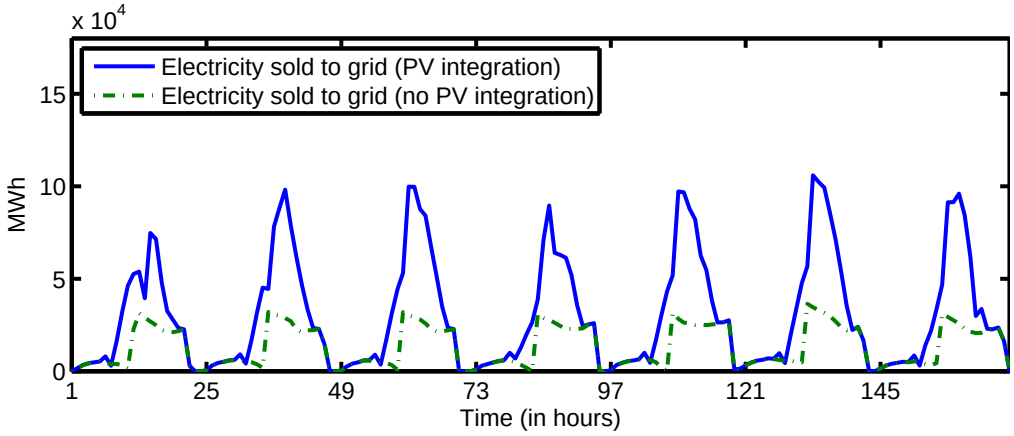

Figure 2.10: The amount of electricity sold to the grid greatly decreases when PV generated electricity is not integrated into the CHP plant.

Another noticeable change in the operation of the CHP plant is related to the gas turbine generation. To cover the morning electricity demand that

was originally supplied by the PV panels, the gas turbine must be on at all hours (Figure 2.11).

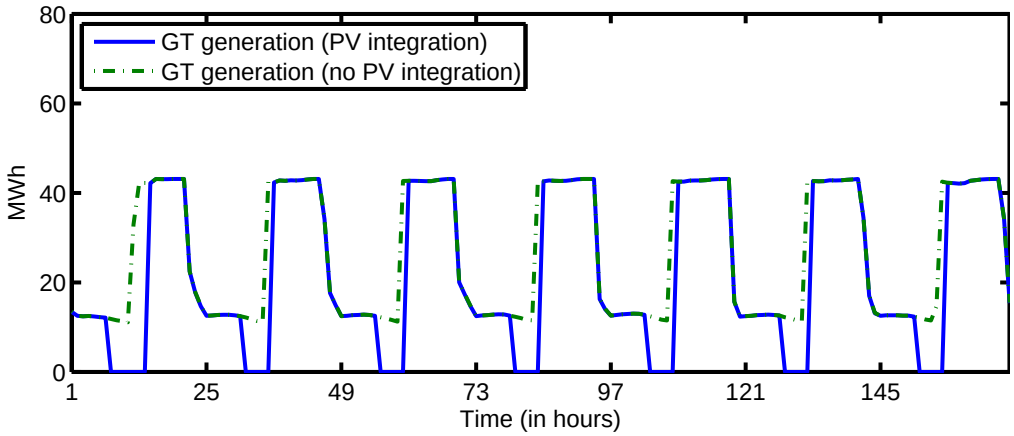

Figure 2.11: Without the incorporation of electricity generated by the PV panels, the gas turbine must be on at all times.

The one week linear scheduling features 12,097 variables, of which 4,032 were binary. There were a total of 27,802 equations/constraints. The optimization was solved with GAMS 24.3.2 using the commercial solver CPLEX 12.6.0.1 on a PC Intel Core i5, 2.50 GHz, 8 GB RAM, 64 bit and Windows 7, with a 0% optimality gap, and was solved in 1 second.

2.7 Conclusions

In conclusion, a CHP plant with PV generation is able to meet all of the electricity, heating, and cooling demands of a residential neighborhood. Despite the decoupling of PV with the residential energy demand, the scheduling shows that the PV generation can be used to supply the electricity and cool-

ing demands for the neighborhood in the morning when it is uneconomical to use the gas turbine to provide electricity and heating. In the afternoon when day-ahead electricity prices increase, running the gas turbine becomes economically beneficial for the plant, and a majority of the $421,434 profit from July 1^{st} to July 7^{th} can be made from selling electricity to the grid. Without PV integration, the overall profit is approximately half of the original profit, and the gas turbine must be on at all hours to meet the neighborhood energy demand.

Practically, using CHP with district cooling can greatly improve the efficiency of the energy production process. Instead of using only electricity to power individual HVAC units to meet the cooling demand of the neighborhood, the scheduling shows that the steam absorption chiller can and should be used to provide chilled water, using the waste heat from the gas turbine and occasional steam from from the auxiliary boiler to power the absorption chiller.

Chapter 3

A Multi-Scale Framework for the Optimal Design and Operation of CHP/PV Systems

The material in this chapter has been submitted for publication [72].

3.1 Introduction

The United States is currently generating, transmitting, and distributing electricity using an aging system, with parts dating back to the 1880s [73]. According to the U.S. EIA, this system is predicted to receive updates, with 90 GW of capacity retired and 287 GW added by 2040, primarily consisting of natural gas-fired and renewable technologies (Figure 3.1) [7]. This evolving generation capacity must be able to meet the expanding electricity demand, which is expected to increase by 24% by 2040, from approximately 4 trillion kWh to over 5 trillion kWh [7]. One possible way to incorporate these predicted increases of natural gas and renewables in an efficient manner is by using Combined Heat and Power (CHP) with photovoltaic (PV) integration to provide heating, cooling, and electricity to residential consumers.

Combined Heat and Power is not a new technology, and has been applied in numerous instances in the industrial sector to help meet the electricity

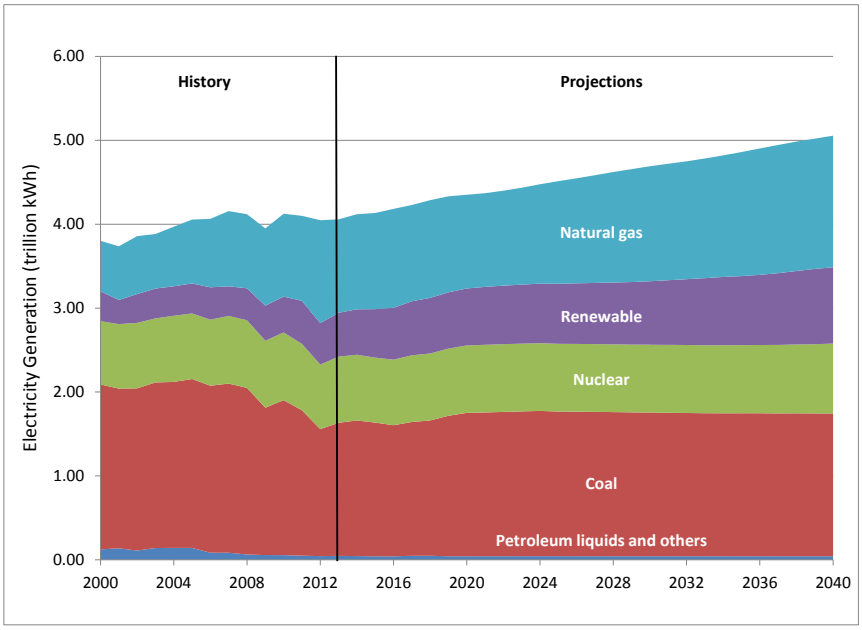

Figure 3.1: Historic and predicted electricity generation by fuel source (data from [7]).

and high heating demands of, e.g., chemical processes [74]. We cannot, however, assume that the CHP technology will be equally as successful in the residential sector. As mentioned in the previous chapter, in the industrial sector, the plants are typically run at or around steady state, leading to a relatively flat electricity profile throughout the day. On the other hand, the residential electricity demand profile does not have similar stability. In the morning, electricity consumption is at its lowest, and then continually rises to its highest value in the evening (Figure 3.2). Moreover, rooftop photo-

voltaic (PV) generation is increasingly present in the residential sector, and the addition of PV generation into the energy mix will only exacerbate the sharp increase in electricity demand in the evening, as seen in California with the infamous "Duck Curve" [75]. Without storage, PV cannot stand alone as the solo generation source. The electricity system still needs the support of conventional generation. However, these sharp changes in demand and PV generation push the ramp rate and capacity limits of large hydrocarbon based generation systems.

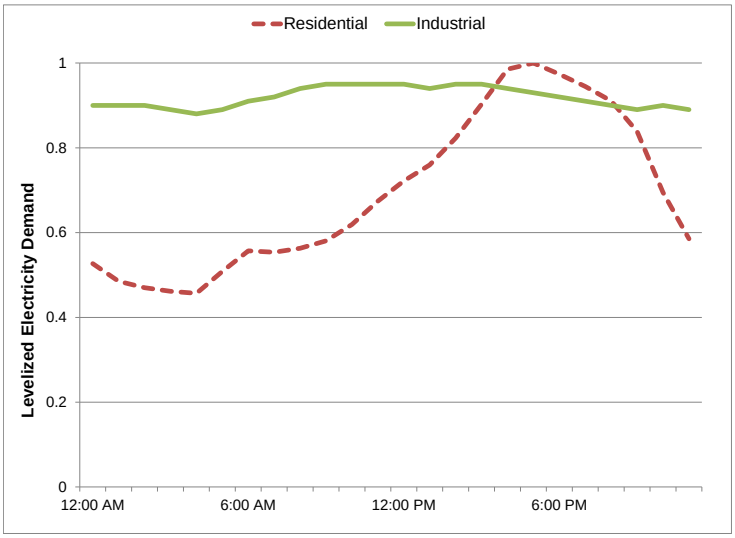

Figure 3.2: Comparison of electricity consumption by sector (data from [8, 9]).

In the previous chapter [16], we have found that the size of the equipment in a CHP plant plays an important role in minimizing the total plant

cost, and optimally sized equipment can lead to improvements in equipment efficiency through a reduction of excess capacity. In the study, we showed that a CHP plant with district cooling is able to meet all of the heating, electricity, and cooling demands of a residential neighborhood. However, we considered equipment sizes based on an existing facility, which were severely oversized for the demand of the average neighborhood.

Motivated by the quest to improve energy generation efficiency and the results of the previous study, the question to be answered in this chapter is *What is the most cost effective design and operation strategy of a CHP plant with distributed PV panel generation to meet the variable utility demands of a residential neighborhood?* This integrated design/operation approach entails solving a large-scale optimization problem that accounts for the long-term variability in weather conditions as well as daily fluctuations in energy demand and PV generation.

In this chapter, we begin by describing the CHP plant model with multiple, discrete sizes of equipment and inter-hour equipment operation constraints, followed by formulating the optimal design and operation problem for the CHP plant, and the Lagrangean decomposition method used to decrease the computational effort needed to solve the problem. Creating a residential neighborhood model from real house utility demand data and PV panel generation in Austin, Texas, we present a case study of the simultaneous design and operational optimization, and conclude with final remarks.

3.2 Background

Over the past several years, there has been an increased interest in improving energy generation efficiency and decreasing energy consumption. Two methods people have been studying to increase energy savings are the integration of thermal and electrical energy production (e.g., the combined generation of electricity and heating), and the integration of design and scheduling. However, as we will show, most of these applications in the integrated optimization of design and operating strategies in the energy sector are either in the industrial sector or at the residential micro-grid scale. To our knowledge, there is little research on the integrated optimization of the design/operating strategy for a medium-scale CHP system, subject to highly variable and uncertain energy demands.

The integrated optimization of design and operating strategies is easier to solve when the inputs (e.g. energy demand profile) are flat, such as seen in the industrial sector. However, when inputs with high variability (e.g. residential heating, electricity, and cooling demands) are introduced, the optimization becomes harder to solve [76]. While many works have been solved without decomposition [77–82], the most recent research trends in solving the integrated optimization of design and operational strategies have focused on incorporating various decomposition methods. With the increase in the number of methods available to generate energy, and the ability (or need) to run processes to meet variable inputs, more variables are being included in the optimizations, while still trying to compute the "most global, optimal" solution.

There are various methods used by researchers to decompose the integrated optimization of design and operating strategies. The two most common divisions used in the decompositions for these types of problems are: 1. long-term/short-term variable separation, and 2. temporal separation. The partition of the long-term investment costs (i.e., equipment selection) and short-term operational costs (i.e., equipment scheduling) allows the researcher to reduce the computation time by reducing or eliminating the binary variables. This is usually done by a) fixing the number and sizes of equipment used, and optimizing the operation of all possible equipment combinations [83,84], or b) optimizing the selection of equipment to be fixed and optimizing the operation of the selected equipment [85–87]. In the second cartegory, temporal separation, the time horizon to be scheduled is divided, producing smaller mixed integer problems that are easier to solve. Lagrangian decomposition, one such method used to solve the time-separated optimization, is an efficient way to generate a lower bound for a large scale MILP/MINLP minimization [88], and has been used in many areas to solve the simultaneous optimization of design and operating strategies [88–92].

Looking at the energy sector, most of the research on the simultaneous optimization of design and operating strategies is concentrated on microgrid applications, targeting either the commercial sector (hotels [82, 84, 89, 93], individual commerical buildings [94–96], and hospitals [59, 97]) or a small group of residential homes [98, 99]. At this scale of energy generation capacity, a few optimization models already exist to simultaneously optimize the design

and operating strategies of the microgrid, such as Berkeley Lab's Distributed Energy Resources Customer Adoption Model (DER-CAM), which was used by Marnay, et.al., to design the optimal microgrid for a hotel in San Francisco [100] and W-ECoMP, which was used to determine the optimal design and operation of a microgrid for a school campus in Italy [85]. At the larger scale of energy generation capacity (greater than 5 MW), the small number of papers published concentrated on apartment complexes, using simplified equipment models to allow the consideration of a larger number of scenarios for the economic optimization of the CHP plants [83, 101]. To our knowledge, the simultaneous optimization of the design and operational strategy for larger CHP systems is still an open problem.

3.3 CHP Plant Model

For this chapter, the role of the CHP plant is to provide all of the heating, electricity, and cooling to an entire residential neighborhood. The starting point for the design is the superstructure, shown in Figure 3.3. The electricity demand can be met by using any combination of PV panel generation, steam turbines, and gas turbines; the heating demand can be met by using any combination of steam from the heat recovery steam generators (HRSG) and boilers; the cooling demand can be met by using any combination of the electric chillers or steam absorption chillers. One important restriction we impose is that the plant is to operate in island mode, i.e., no connection to the grid, so electricity can not be purchased from or sold to the grid.

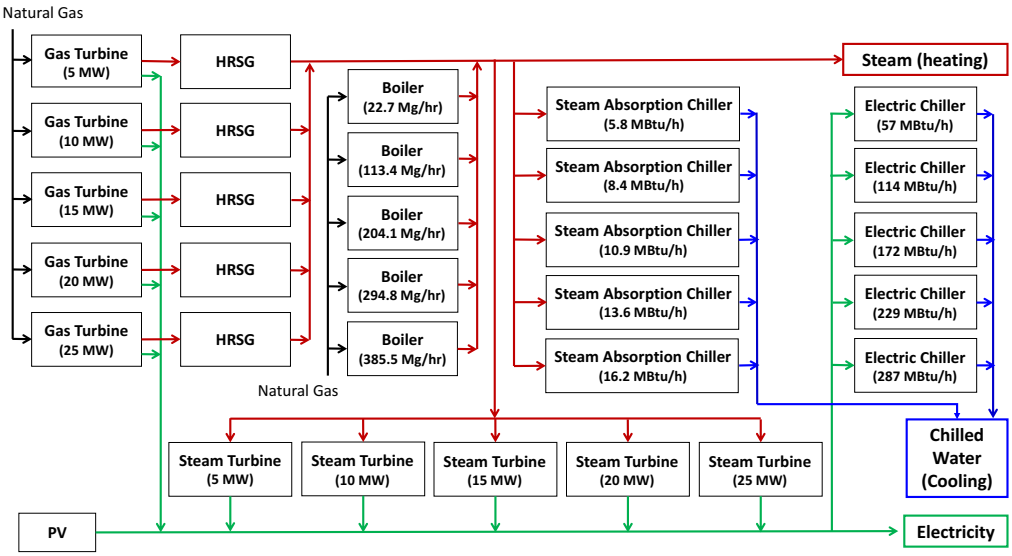

Figure 3.3: Superstructure of the CHP plant to be modeled, with the red lines representing steam, blue lines representing chilled water, and green lines representing electricity. The plant contains five of each piece of equipment, in varying sizes.

All equipment models were derived using data from journals and equipment manufacturers via the LINEST function.

3.3.1 Gas Turbine Model

The gas turbine, powered by natural gas, is used to generate electricity with exhaust gas as a by-product. The multiple sized models are identified based on their maximum electricity generation ($P_{GT,\upsilon}^{max}$), where $\upsilon = [1, 2, 3, ..., N_{GT}]$ is the integer set used to track the different size gas turbines.

The efficiency of the gas turbine is strongly influenced by three elements: nominal capacity, inlet air temperature, and instantaneous load. The

gas turbine model developed (linear in variables and quadratic in parameters), must take all three factors into consideration in order to accurately predict the operation of different sized turbines under varying inlet air temperatures and partial loads. The first aspect incorporated in the model is the effect of size on the nominal efficiency. Data was collected to relate the electrical efficiency to the nominal capacity (data located in Appendix D), generating the following nominal efficiency model:

$$\eta_{GT,v}^{nom} = -8 \times 10^{-5} \left(P_{GT,v}^{max}\right)^2 + 0.0065 P_{GT,v}^{max} + 0.2556 \tag{3.1}$$

where $\eta_{GT,v}^{nom}$ is the nominal efficiency of the gas turbine.

The next impact on efficiency incorporated in the gas turbine model was the outdoor air temperature. A quadratic line was fit to data from Solar Turbine's Mercury 50 [102] to generate the following equation, accounting for an adjustment based on the gas turbine's nominal efficiency:

$$\begin{aligned}\eta_{GT,T,v}^{h} = -1.4 \times 10^{-5} \left(T_{air}^{h}\right)^2 - 0.0007 T_{air}^{h} \\ + \left(\eta_{GT,v}^{nom} + 1.4 \times 10^{-5} (T_{air,nom})^2 + 0.0007 T_{air,nom}\right)\end{aligned} \tag{3.2}$$

where T_{air}^{h} is the temperature of the air entering (i.e., the temperature outside), $T_{air,nom}$ is the temperature of the air used to calculate the nominal efficiency ($T_{air,nom} = 15\ ^{o}$C), and $\eta_{GT,T,v}^{h}$ is the efficiency after taking the outdoor air temperature into consideration.

The final component taken into account when calculating the efficiency of the gas turbine is the instantaneous load on the gas turbine, which can lead to lower investment costs and better part-load efficiencies [87]. The partial load ($P^h_{GT,pr,\upsilon}$) is equal to the current production of electricity from a gas turbine at hour h ($P^h_{GT,\upsilon}$) divided by the size of the gas turbine. Data from three arbitrarily selected industrial turbines [103], were averaged, and a line was fit to the data:

$$\eta^h_{GT,pr,\upsilon} = 0.4613 P^h_{GT,pr,\upsilon} + 55.975 \tag{3.3}$$

where

$$\eta^h_{GT,pr,\upsilon} = 100 \times \left(\frac{\eta^h_{GT,\upsilon}}{\eta^h_{GT,T,\upsilon}} \right) \tag{3.4}$$

$$P^h_{GT,pr,\upsilon} = 100 \times \left(\frac{P^h_{GT,\upsilon}}{1000 \times P^{max}_{GT,\upsilon}} \right) \tag{3.5}$$

with the following limits:

$$50 \leq P^h_{GT,pr,\upsilon} \leq 100 \tag{3.6}$$

$$77.28 \leq \eta^h_{GT,pr,\upsilon} \leq 100 \tag{3.7}$$

where $\eta^h_{GT,\upsilon}$ is the efficiency of the gas turbine at hour h. From the above equations, the efficiency of the gas turbine and the power supplied by the gas turbine can be calculated.

With the power supplied by the gas turbine known, the flow rate of natural gas to drive the gas turbine is calculated by:

$$P^h_{GT,v} = \alpha_{GT} \times W^h_{f,GT,v} \times \eta^h_{GT,v} \tag{3.8}$$

where $W^h_{f,GT,v}$ is the fuel flow rate and α_{GT} is a constant. To calculate α_{GT} for the gas turbine model, information on five different gas turbines (data from [104]) was substituted into Equation 3.8 to calculate individual α_{GT} values, and then all five values were averaged.

Since the fuel flow rate ($W^h_{f,GT,v}$) and the efficiency of the gas turbine ($\eta^h_{GT,v}$) are decision variables, Equation 3.8 is linearized using a McCormick relaxation (see Appendix E for relaxation details).

3.3.2 Heat Recovery Steam Generator (HRSG)

The hot exhaust gas expelled from the gas turbine is sent to the HRSG to generate steam that can be used to power a steam turbine and/or steam absorption chiller, and/or provide heating for the neighborhood. A linear model was developed to calculate the nominal amount of steam produced by the HRSG ($W^{nom}_{HRSG,v}$) when the gas turbine is operating at maximum capacity (data from [104]):

$$W^{nom}_{HRSG,v} = 2.79 P^{max}_{GT,v} + 17004 \tag{3.9}$$

The amount of steam produced ($W^h_{HRSG,v}$) is allowed to vary in time, based on the gas turbine load at hour h:

$$W^h_{HRSG,v} = W^{nom}_{HRSG,v} \times \frac{P^h_{GT,pr,v}}{100} \tag{3.10}$$

3.3.3 Steam Turbine

The back-pressure steam turbine is modeled using the Willan's model [105, 106], which describes the shaft power as a function of the steam flow. Discrete steam turbine sizes were used to retain a linear model, with N_{ST} different sizes, $\phi = [1, 2, 3, ..., N_{ST}]$, based on the maximum power produced by the steam turbine ($P^{max}_{ST,\phi}$). The power supplied from each size of steam turbine is calculated as follows:

$$P^{h}_{ST,\phi} = n_{\phi} \times W^{h}_{ST,\phi} - \left(W_{int,\phi} \times y^{h}_{ST,\phi}\right) \tag{3.11}$$

where

$$n_{\phi} = \frac{1.2}{B_{\phi}} \left(\Delta h_{\phi} - \frac{A_{\phi}}{W^{max}_{ST,\phi}}\right) \tag{3.12}$$

$$W_{int,\phi} = \frac{.2}{B_{\phi}} \left(\Delta h_{\phi} \times W^{max}_{ST,\phi} - A_{\phi}\right) \tag{3.13}$$

$P^{h}_{ST,\phi}$ is the power generated by the steam turbine at hour h, n_{ϕ} is the slope of the Willan's model, $W^{h}_{ST,\phi}$ is the flow rate of steam entering the steam turbine, $P_{int,\phi}$ is the intercept of the Willan's model, and Δh_{ϕ} is the isentropic enthalpy change. Parameters A_{ϕ} and B_{ϕ} are calculated using Equations 3.14 and 3.15, with the values of $a_{i,\phi}$ ($i = [1, 2, 3, 4]$) obtained from [106]:

$$A_{\phi} = a_{0,\phi} + a_{1,\phi} T_{sat,in,\phi} \tag{3.14}$$

$$B_{\phi} = a_{2,\phi} + a_{3,\phi} T_{sat,in,\phi} \tag{3.15}$$

where $T_{sat,in,\phi}$ is the temperature of the steam entering the steam turbine.

The maximum amount of steam consumed by the steam turbine ($W^{max}_{ST,\phi}$) is calculated using a linear model generated from data [104], based on the maximum capacity of the steam turbine:

$$W^{max}_{ST,\phi} = 3.9539 P^{max}_{ST,\phi} + 3.636 \tag{3.16}$$

Additionally, data from [104] were used to create models that relate the temperature of steam entering ($T_{sat,in,\phi}$) and theisentropic enthalpy change to the maximum capacity of the steam turbine:

$$T_{sat,in,\phi} = 3.7178 P^{max}_{ST,\phi} + 288 \tag{3.17}$$

$$\Delta h_{\phi} = 0.0054 P^{max}_{ST,\phi} + 0.1755 \tag{3.18}$$

Lastly, the amount of power produced by the steam turbine (Equation 3.19) and the steam consumed (Equation 3.20) is constrained as follows:

$$P^{h}_{ST,\phi} \leq P^{max}_{ST,\phi} \tag{3.19}$$

$$.5 * W^{max}_{ST,\phi} \leq W^{h}_{ST,\phi} \leq W^{max}_{ST,\phi} \tag{3.20}$$

3.3.4 Auxiliary Boiler

An auxiliary boiler is included in the CHP plant to produce additional steam. The linear model found in [16, 66] is used, and is broken into discrete sizes based on the maximum amount of steam generated, $W^{max}_{BR,\chi}$ where χ = [1, 2, 3, ..., N_{BR}], with the following model as a result:

$$W^{h}_{BR,\chi} = \frac{\eta_{BR} \times LHV \times W^{h}_{f,BR,\chi}}{H_{BR,out} - H_{BR,in}} \tag{3.21}$$

$$.2 \times W^{max}_{f,BR,\chi} \leq W^{h}_{f,BR,\chi} \leq W^{max}_{f,BR,\chi} \tag{3.22}$$

where $W^h_{BR,\chi}$ is the amount of steam produced, $W^h_{f,BR,\chi}$ is the fuel consumed, $H_{BR,out}$ is the enthalpy of the steam exiting the boiler, and $H_{BR,in}$ is the enthalpy of the water entering the boiler. The efficiency of the boiler, η_{BR}, is assumed to be constant for all sizes. Equation 3.22 limits the minimum and maximum amount of fuel supplied for each size boiler. $W^{max}_{f,BR,\chi}$ was calculated for each size steam turbine by solving Equation 3.21 for $W^h_{f,BR,\chi}$, when $W^h_{BR,\chi}$ is equal to $W^{max}_{BR,\chi}$.

3.3.5 Steam Absorption Chiller

A steam absorption chiller is available to generate cooling (in the form of chilled water) for the neighborhood using steam produced from the HRSG and boiler. A two-stage chiller was selected over a one-stage chiller because of its higher coefficient of performance (COP), and its ability to operate with higher pressure and temperature steam. In order to maintain a linear model, the steam absorption chiller model was divided into N_{SA} discrete equipment sizes based on the amount of cooling provided ($Q^{max}_{SA,\psi}$), where $\psi = [1, 2, 3, ..., N_{SA}]$. The COP ($COP_{SA}$), and enthalpy of steam entering ($H_{s,in}$) and exiting ($H_{s,out}$), are assumed to be constant and the same for all sizes. The cooling provided by the steam absorption chiller ($Q_{SA,\psi}$) is modeled as follows:

$$Q^h_{SA,\psi} = COP_{SA} \times (H_{s,in} - H_{s,out}) \times W^h_{SA,\psi} \tag{3.23}$$

$$0.1 \times W^{max}_{SA,\psi} \leq W^h_{SA,\psi} \leq W^{max}_{SA,\psi} \tag{3.24}$$

where $W^h_{SA,\psi}$ is the flow rate of steam consumed. The maximum steam consumed ($W^{max}_{SA,\psi}$) is calculated by solving Equation 3.23 using the sizes of the

steam absorption chiller ($Q^{max}_{SA,\psi}$). Lastly, the amount of steam consumed is limited using Equation 3.24

3.3.6 Electric Chiller

We consider an electric chiller in the model superstructure in order to ensure that the most efficient structure is selected. An electric chiller has a COP approximately four times higher than the steam absorption chiller. The model is broken into discretized based on the maximum amount of cooling provided ($Q^{max}_{EC,\omega}$), where ω = [1, 2, 3, ..., N_{EC}]. The COP (COP_{EC}) for all sizes is assumed to be the same for all sizes of chiller, and constant over the chiller operating region. The amount of cooling produced by the electric chiller ($Q_{EC,\omega}$) is calculated as follows:

$$Q^{h}_{EC,\omega} = P^{h}_{EC,\omega} \times COP_{EC} \times 3412 \tag{3.25}$$

$$0.28 \times P^{max}_{EC,\omega} \leq P^{h}_{EC,\omega} \leq P^{max}_{EC,\omega} \tag{3.26}$$

where $P^{h}_{EC,\omega}$ is the amount of electricity supplied to the electric chiller. The maximum amount of power for each size electric chiller is calculated by substituting the maximum amount of cooling provided (i.e., the size of the chiller) into Equation 3.25 and solving for the power needed. This value is used to constrain the power supplied to the electric chiller, with the minimum amount of electricity being calculated as an average of the ratio of minimum to maximum cooling capacity collected using data (Appendix F) [2].

3.4 Operation Scheduling

In order to more accurately represent the dynamics of the CHP plant and their role in the plant design, scheduling allows for the seasonal operation of the plant to be considered and operating costs to be estimated. Of the six different equipment models developed earlier, the gas turbine and HRSG operate together. This means, that the HRSG, which runs on the exhaust gas from the gas turbine, can not be scheduled independently from the gas turbine.

3.4.1 Equipment operating modes

All equipment can operate in one of four modes: on, off, cold startup and warm startup. A single binary variable $y^h_{e,s}$ is used to track the on/off operation of equipment e of size s at hour h, where one indicates that the component is on and zero indicates that the component is off [107]. $y^h_{e,s}$ can then be used to determine when a cold ($cold^h_{e,s}$) and warm ($warm^h_{e,s}$) startup is occurring for equipment e of size s at hour h by using a set of mode transition constraints.

3.4.2 Mode transitions

It is necessary to track the mode transition of equipment so that both warm and cold modes can be assigned, and any prohibited transitions can be prevented. Equipment is turned on either via cold startup or warm startup between consecutive hours *h-1* and *h*. Two continuous positive variables, $warm^h_{e,s}$

and $cold^h_{e,s}$, are used to indicate when the piece of equipment of size s is in the warm or cold startup mode, where $warm^h_{e,s}$ is equal to one if the equipment is in the last hour of a warm startup at hour h, and $cold^h_{e,s}$ is equal to one if the equipment is in the last hour of a cold startup at hour h. The following constraint assures that the equipment is not turned on instantaneously, rather, either a warm or cold startup procedure is followed:

$$y^h_{e,s} - y^{h-1}_{e,s} \leq warm^{h-1}_{e,s} + cold^{h-1}_{e,s} \quad \forall\, e \in E, s \in S, h > 1 \tag{3.27}$$

A warm startup can only occur if the equipment has been on for at least one hour in the past t^{ws}_e hours. If a piece of equipment has been off for more than t^{ws}_e consecutive hours, it can only turn on via a cold startup. This constraint is imposed by restricting $warm^h_{e,s}$ so that it must equal zero if the equipment has not been on for at least one hour in the past t^{ws}_e hours:

$$warm^h_{e,s} \leq \sum_{\theta=1}^{t^{ws}_e} y^{h-\theta}_{e,s} \quad \forall\, e \in E, s \in S, h > 5 \tag{3.28}$$

Only one inter-hour constraint is needed to prohibit a transition between modes: a piece of equipment can not alternate from on to off to on. When a piece of equipment is turning on, it must go through a warm or cold startup, and for the purpose of the plant operation is constrained to still be in the "off" state. Thus, to prevent a piece of equipment from turning directly on without a startup period, the following constraint is used:

$$y^{h-2}_{e,s} + y^h_{e,s} - y^{h-1}_{e,s} \leq 1 \quad \forall\, e \in E, s \in S, h > 2 \tag{3.29}$$

3.4.3 Start-up penalties

Each startup comes with an associated penalty, whose value depends on the type of equipment and startup mode. A warm startup typically takes less time and causes less wear and tear on the equipment, and is thus less costly than a cold startup. The total penalties accrued from startups at each hour, $start^h_{e,s}$, are calculated by the following:

$$startcost^h_{e,s} = \left(\kappa_e \times warm^h_{e,s}\right) + \left(\gamma_e \times cold^h_{e,s}\right) \quad \forall\, e \in E, s \in S, h \in H \quad (3.30)$$

where κ_e is the penalty associated with a warm startup and γ_e is the penalty associated with a cold startup for equipment e. The penalties, located in Table 3.1, are assumed to be constant for all equipment sizes.

Equipment	γ_e (\$)	κ_e (\$)
GT	300	150
ST	400	200
BR	600	300
SA	400	200
EC	200	100

Table 3.1: Cost (in \$) to turn on equipment via a warm or cold startup.

Note that (5.4) is the equation that forces the positive continuous variables $warm^h_{e,s}$ and $cold^h_{e,s}$ to act as binary. The constraint (3.27) creates a lower bound of zero or one. Given the objective of minimizing ultimate goal to minimize the plant cost, the optimal solution entails minimizing the penalties that are associated with turning equipment on.

3.5 Capital Investment and Maintenance Costs

If CHP with district cooling is to be practical in a residential neighborhood, the plant must economically meet all the neighborhood utility demands, i.e., the cost of utilities from the CHP plant must be equal or less than the current cost. To calculate the total plant price over the lifetime of the plant, maintenance fees, and operational and capital costs are included, in addition to the transition penalties.

3.5.1 Capital Cost Models

The capital cost of the gas turbine, ($C_{GT,\upsilon}$), which includes the capital cost of the HRSG, is a function of the size of the gas turbine. The cost relation below includes the cost of installation, using data from [104]:

$$C_{GT,\upsilon} = P_{GT,\upsilon}^{max} \times \left(59289 \times \left(P_{GT,\upsilon}^{max}\right)^{-0.365}\right) \tag{3.31}$$

The steam turbine capital and installation cost ($C_{ST,\phi}$) model, also developed using data from [104], is:

$$C_{ST,\phi} = P_{ST,\phi}^{max} \times \left(2846.2 \times \left(1000 \times P_{ST,\phi}^{max}\right)^{-0.159}\right) \tag{3.32}$$

The capital cost of the boiler, $C_{BR,\chi}$, is assumed to be linearly dependent on the amount of energy used by the boiler to generate steam [108]:

$$C_{BR,\chi} = Cost_{BR} \times \left(\frac{W_{BR,\chi}^{max}\left(H_{BRout} - H_{BRin}\right)}{\eta_{BR}}\right) \tag{3.33}$$

where $Cost_{BR}$ is the cost per heat input per hour.

Using data from [109], a line of best fit was used to generate a the steam absorption chiller capital cost model, based on the cost per ton of chilling capacity:

$$C_{SA,\psi} = Q^{max}_{SA,\psi} \times \left(0.0006 \left(Q^{max}_{SA,\psi}\right)^2 - 1.0839 Q^{max}_{SA,\psi} + 1133.1\right) \tag{3.34}$$

Lastly, the capital cost of the electric chiller ($C_{EC,\omega}$) is assumed to be a constant price per unit cooling produced ($Cost_{EC}$), which does not change based on the size of the chiller [110]:

$$C_{EC,\omega} = Cost_{EC} \times \left(Q^{max}_{EC,\omega}\right) \tag{3.35}$$

3.5.2 Maintenance Cost Models

For the gas turbine maintenance cost, a linear model was fitted to data from [104]. The model determines the price of maintenance per kWh of energy produced by the turbine ($M^h_{GT,\upsilon}$), and accounts for turbine size:

$$M^h_{GT,\upsilon} = P^h_{GT,\upsilon} \times \left(\left(-9 \times 10^{-8}\right) \times P^{max}_{GT,\upsilon} + 0.0126\right) \tag{3.36}$$

The steam turbine maintenance cost model assumes a constant maintenance charge ($M_{ST,\phi}$) every year. The cost is determined by the size of the steam turbine ($P^{max}_{ST,\phi}$), and was developed using data from [104]:

$$M_{ST,\phi} = \left(-3 \times 10^{-7}\right) \times \left(1000 \times P^{max}_{ST,\phi}\right) + 0.01 \tag{3.37}$$

The maintenance cost for the boiler ($M^h_{BR,\chi}$), like the gas turbine, is based on the production of the boiler [108]:

$$M^h_{BR,\chi} = MC_{BR} \times \left(\frac{W^h_{BR,\chi}\left(H_{BRout} - H_{BRin}\right)}{\eta_{BR}}\right) \tag{3.38}$$

where MC_{BR} is the cost per energy input per hour ($/MBtu/hr).

For the steam absorption chiller, the maintenance cost ($M_{SA,\psi}$) is expressed in terms of a constant amount per year (MC_{SA}), based on the capacity of the chiller [111]:

$$M_{SA,\psi} = MC_{SA} \times Q^{max}_{SA,\psi} \tag{3.39}$$

Lastly, the electric chiller maintenance cost, $M_{EC,\omega}$, is computed as a function of a specified amount per ton of cooling ($MC_{EC,\omega}$), but changes based on the overall capacity of the chiller (Table 3.2).

$Q^{max}_{EC,\omega}$ (tons of cooling)	$MC_{EC,\omega}$ ($/ton)
<450	6.00
450 - 1500	4.50
>1500	2.50

Table 3.2: Costs of maintenance based on cooling capacity of the electric chiller [1].

Specifically, the cost of of maintenance for the electric chiller each year is calculated as follows:

$$M_{EC,\omega} = MC_{EC,\omega} \times Cool^{max}_{EC,\omega} \tag{3.40}$$

3.5.3 Equipment Selection

The purpose of the simultaneous optimization of the design and operational strategy is to determine the optimal plant equipment to meet all electricity, heating, and cooling demands. While many pieces are available

to be used in the design of the CHP plant, as shown in the CHP plant superstructure (Figure 3.3, only those pieces of equipment that generate energy (i.e., are turned "on") should be included in the calculation of the total cost of the plant.

To determine if a piece of equipment of size s is used, the positive continuous variable $U_{e,s}$ is constrained such that if a piece of equipment was turned on at any hour, $U_{e,s}$ must have a value of one or greater:

$$U_{e,s} \geq y^h_{e,s} \quad \forall \quad h \in H, e \in E, s \in S \tag{3.41}$$

With this calculation, the exact pieces of equipment turned on can be determined, and their costs (maintenance and capital) can be counted towards the total cost of the plant.

3.5.4 Capital and Maintenance Costs

The total capital cost for all pieces of equipment used ($Capital$), is calculated using the following equation:

$$Capital = \sum_e \sum_s (U_{e,s} \times C_{e,s}) \tag{3.42}$$

With the goal of minimizing the overall cost of the plant, $U_{e,s}$, which is a positive continuous variable acting as a binary, will take on a value of zero when the corresponding equipment is not used, or 1 when the equipment is used.

As seen in Section 4.6.2, the maintenance cost is either a constant fee each year (steam turbine, electric chiller, and steam absorption chiller) or can

change based on hourly equipment use (gas turbine/HRSG and boiler). For the equipment with a constant value each year, the total maintenance cost ($Main_1$) must be calculated incorporating $U_{e,s}$, so that only the equipment used is included:

$$Main_1 = \sum_e \sum_s (U_{e,s} \times M_{e,s}) \quad \forall \quad e \neq \{GT, BR\}, s \in S \tag{3.43}$$

The total maintenance cost for the gas turbines and boilers, which is a function of equipment load, is calculated as follows for one day of operation ($Main_{2,d}$):

$$Main_{2,d} = \sum_{h=24(d-1)+1,\ldots,24*d} \left(\sum_{\upsilon} M^h_{GT,\upsilon} + \sum_{\chi} M^h_{BR,\chi} \right) \quad \forall \quad s \in S, d \in D \tag{3.44}$$

where d is one day of demand data and D is the total number of days optimized.

3.6 Simultaneous Design and Operational Optimization

3.6.1 Meeting Neighborhood Utility Demand

All electricity, heating, and cooling demands of the neighborhood must be met by the CHP plant at all hours. In order to make sure that all utility requirements are met, balances on electricity, steam, and chilled water are needed when scheduling plant operation. The electricity produced by the gas turbines, steam turbines, and solar panels (PV^h) must be equal to the

electricity demand of the neighborhood ($Elec^h$) and of the electric chillers:

$$Elec^h + \sum_{\omega} P^h_{EC,\omega} = PV^h + \sum_{\upsilon} P^h_{GT,\upsilon} + \sum_{\phi} P^h_{ST,\phi} \quad \forall h \in H \tag{3.45}$$

For heating, there must be enough steam produced by the HRSG and boiler to either match or be greater than the amount of energy needed to heat the neighborhood ($Heat^h$), operate the steam absorption chillers, and power the steam turbines:

$$Heat^h + \sum_{\phi} W^h_{ST,\phi} + \sum_{\psi} W^h_{SA,\psi} \leq \sum_{\upsilon} W^h_{HRSG,\upsilon} + \sum_{\chi} W^h_{BR,\chi} \quad \forall h \in H \tag{3.46}$$

Lastly, the steam absorption chillers and electric chillers must meet the total neighborhood cooling demand ($Cool^h$):

$$Cool^h \leq \sum_{\psi} Q^h_{SA,\psi} + \sum_{\omega} Q^h_{EC,\omega} \quad \forall h \in H \tag{3.47}$$

3.6.2 Overall Objective Function

The overall objective of the simultaneous design and operational optimization, is to minimize the cost of the plant. The four sources of expenditures are:

1. Capital from purchasing the equipment
2. Fuel
3. Maintenance fees from equipment operation
4. Transition penalties

There are only two pieces of equipment that require fuel, in the form of natural gas: the gas turbine and the boiler. Assuming that the cost of natural gas, NG_{cost}, remains constant for the lifetime of the plant, the daily fuel cost ($Fuel_d$) is calculated as follows:

$$Fuel_d = NG_{cost} \times \sum_{h=1,\ldots,24} \left(\sum_{\upsilon} W^h_{f,GT,\upsilon} + \sum_{\chi} W^h_{f,BR,\chi} \right) \tag{3.48}$$

The total daily transition penalties ($Trans.Pen._d$) are computed as:

$$Trans.Pen._d = \sum_{e} \sum_{s} \sum_{h=24(d-1)+1,\ldots,24*d} startcost^h_{e,s} \tag{3.49}$$

The overall objective function is:

$$\begin{aligned} \text{Max} \quad & -(Capital + Y \times Main_1) \\ & - Y \sum_{d=1,\ldots,D} (\tau_d \times (Fuel_d + Main_{2,d} + Trans.Pen._d)) \end{aligned} \tag{3.50}$$

where Y is the lifetime of the plant and τ_d is a parameter used to scale up each daily operational costs to simulate a year of operation.

3.6.3 Residential Neighborhood Utility Demand Model

Residential utility demand data were obtained from the Mueller neighborhood in Austin, TX. The neighborhood contains a collection of yard, row, garden court houses, and condominiums, designed to promote energy and water efficiency [112]. Pecan Street Inc. collects [8] data from over 700 of these homes, including but not limited to electricity, water, and natural gas data. Of the homes in the neighborhood, 277 have PV panels installed on the rooftop,

totaling a installed capacity of 1.51 MW [113], and data on the PV panels generation are also recorded.

For the purpose of this study, we collected a one-year set of hourly electricity, heating, and cooling demand data as well as the PV generation data from the PV panels located in the neighborhood. The data were then aggregated and scaled up to represent demand and generation for a neighborhood of approximately 5,600 homes:

Electricity Load: 88 homes $\times$ **64** = 5632 homes

Cooling Load: 88 homes $\times$ **64** = 5632 homes

Heating Load: 19 homes $\times$ **296** = 5624 homes

PV Generation: 25 homes $\times$ **225** = 5625 homes

The cooling load, which was disaggregated from the electricity demand [64], were calculated assuming that all homes have efficient air conditioning units with a seasonal energy efficiency ratio (SEER) of 18. The furnace efficiency for all homes was assumed to be 75% when back-calculating the heating demand. Lastly, it is assumed that almost all homes have PV panels on their rooftops. With these assumptions, the hourly utility demand and PV generation was created for a residential neighborhood.

One aspect that distinguishes the residential neighborhood utility from other sectors' energy demand, in addition to the peaks and valleys as introduced in Section 5.1 and seen in Figure 3.4, is demand variability. Selecting 8

days of utility demand and PV generation from the year of available data as an example, it is clear that the utility demands and PV generation fluctuate both between the four seasons and between the days in a season. Taking the electricity demand as an example (3.4a), the demand peak fluctuates from season to season, with the most electricity needed in the summer around 5 pm, while in the winter, the most electricity is needed between 7 and 8 pm. In the summer, the peak electricity demand varies from day-to-day, with the lowest summer daily peak being 50% less than the respective highest value.

With such extreme variation in seasonal and daily energy demands and PV generation, an average day of demand for each season (4 days total) will not be suitable to accurately represent the operation costs of the plant. Additional days will need to be included in the optimization to capture the uncertainty in utility demand and PV generation. Thus, in addition to average days of utility demand and PV generation for each season (calculated by averaging all days together in the perspective seasons), the days with the maximum and minimum total energy demand and days with the maximum utility demands (heating, electricity, and cooling) were included in the optimization to encompass the unpredictability in weather. To properly incorporate the minimum and maximum demand days into the operational costs, the minimum and maximum demand days carried less weight with the day-to-day operational costs (i.e., fuel, transitional penalties, maintenance), while the average days of seasonal demand were weighted more heavily.

While incorporating more days of data will help capture the uncertainty

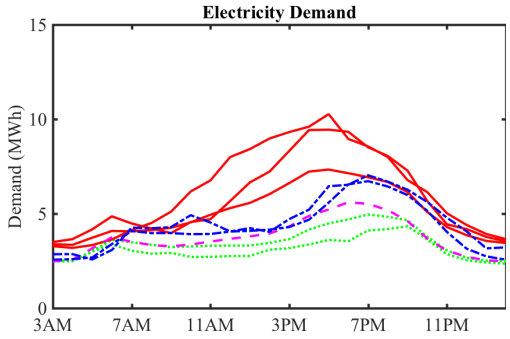

(a) Variability in residential electricity demand.

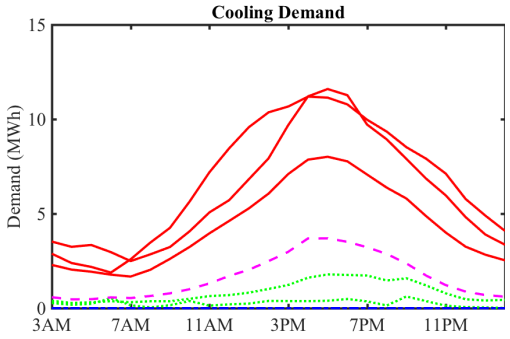

(b) Variability in residential cooling demand.

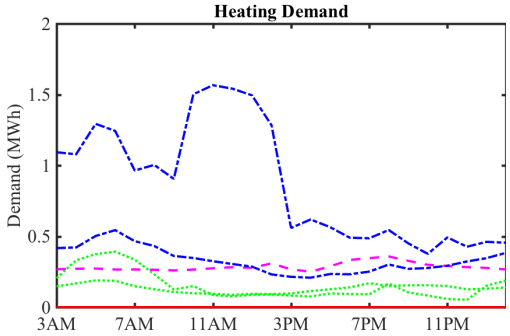

(c) Variability in residential heating demand.

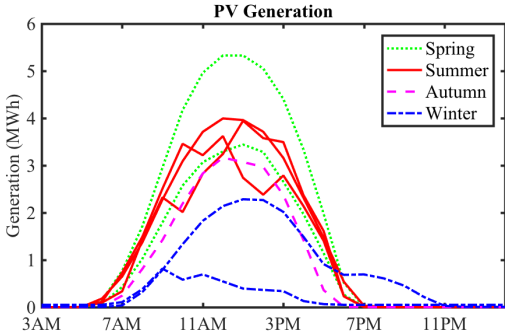

(d) Variability in rooftop PV generation.

Figure 3.4: In the residential sector, there is extreme variability between seasons and between days in the seasons for electricity (3.4a), cooling (3.4b), and heating demand (3.4c)and PV generation (3.4d).

in utility demand while improving the accuracy of the long-term operational costs, including more hours in the optimization greatly increases the number of variables and equations to be optimized, preventing the problem from being solved in a reasonable amount of time without involving a supercomputer. Thus, a decomposition method was created to quickly solve the optimization of the design and operation strategy problem, incorporating demand and PV generation variation. One scheduling feature observed in our previous work on CHP plants [16], was the lack of equipment dynamics (i.e., equipment turning on/off) in the early morning hours when scheduling a CHP plant to meet the utility demands of a residential neighborhood for a summer week. Because the energy demand profiles did not vary drastically between 2:00 AM and 5:00 AM, there was no need to turn any equipment on or off. This presented a natural break in plant operation, that could be used to separate the days of demand and optimize the daily equipment operation individually through a decomposition method.

3.7 Solution Algorithm: Temporal Lagrangean Decomposition

Due to the large amount of data that must be optimized in order to accurately depict the operational cost over the lifetime of the plant, the optimization needed to be decomposed to allow the problem to be solved in a reasonable amount of time. With eight days of demand data, the aforementioned optimization created a problem with over 61,000 equations and 40,500

variables, of which 4,800 were binary. The use of a traditional optimization solver could not solve the problem in five days. Thus, an iterative algorithm was created to solve the optimization of the design and operational strategies for the CHP plant, which uses a Lagrangian decomposition to determine a lower bound, a feasible full-space upper bound, and a hybrid Lagrange multiplier updater strategy.

3.7.1 Lower bound

As mentioned in Section 3.6.3, there is a break in equipment dynamics in the early morning hours, creating a natural daily separation feature for the decomposition. However, the variable $U_{e,s}$, which determines the equipment included in the CHP plant design, prevents the easy separation and individual optimization of the demand days. In Section 3.5.3, Equation (3.41) links $U_{e,s}$ to the hourly status of every piece of equipment e of size s for all optimized days. This prevents the division of the capital cost of the equipment as well as the maintenance costs for the electric chillers, steam absorption chillers, and steam turbines, because they are linked to every day via the variable $U_{e,s}$. On the other hand, the hour-to-hour operational aspects of the plant (fuel, maintenance for the gas turbines and boilers, and transition penalties) can be easily separated into days. Thus, we use the natural daily division of the operation to create a lower bound for the original optimization problem, artificially separating the long-term variables (i.e., the design), so $U_{e,s}$ can be optimized daily. Any difference in the artificially separated variables will be

penalized, with a penalty function that is iteratively updated to drive all days to use the same types and sizes of equipment.

Rewriting the objective function in a simplified form subject to some constraints, yields the following formulation:

$$\begin{aligned} Z = \text{Min } & L + \sum_{d=1,...,D} \tau_d R_d \\ & \text{st } U_{e,s} \geq j_d - g_d \quad i = 1, ..., D \\ & R_d \geq 0, L \geq 0, U_{e,s} \geq 0, d = 1, ...D \end{aligned} \tag{3.51}$$

where j_d and g_d are variables that can be optimized daily, L is a variable that is a function of $U_{e,s}$ (i.e., *Capital* and $Main_1$), and R_d is a variable that can be divided into days (i.e., $Fuel_d$, $Main_{2,d}$, and $Trans.Pen._d$).

$U_{e,s}$, which determines the design of the plant, can be divided into d components ($U^d_{e,s}$), creating scenario subproblems with an artificial linking of the newly separated variables ($U^1_{e,s} = U^d_{e,s}$). An asymmetric linking constraint structure was chosen, as it has been shown to converge quicker in less iterations compared to a symmetric structure (i.e., $U^1_{e,s} = U^2_{e,s} = ... = U^d_{e,s}$) [90]:

$$\begin{aligned} Z = \text{Min } & \sum_{d=1,...,D} \left(\frac{1}{D} L_d + \tau_d R_d \right) \\ & \text{st } U^d_{e,s} \geq j_d - g_d \quad d = 1, ..., D \\ & U^1_{e,s} = U^d_{e,s} \quad d = 2, ...D \\ & R_d \geq 0, L_d \geq 0, U^d_{e,s} \geq 0, d = i, ...D \end{aligned} \tag{3.52}$$

Relaxing the linking constraint with a Lagrangean relaxation, produces the following:

$$\begin{aligned} Z(\lambda) = \text{Min} \sum_{d=1,...,D} \left(\frac{1}{D} L_d + \tau_d R_d \right) + \sum_{d=1,...,D-1} \lambda_d \left(U^1_{e,s} - U^{d+1}_{e,s} \right) \\ \text{st } U^d_{e,s} \geq j_d - g_d \quad d = 1, ..., D \\ R_d \geq 0, L_d \geq 0, U^d_{e,s} \geq 0, \lambda^d = (-\inf, \inf), d = i, ...D \end{aligned} \tag{3.53}$$

where λ_d is the Lagrange multiplier used to penalize any variation between two variables. Formulation (3.53) can be decomposed into separate problems (i.e., one for each day) that can be solved individually:

$$\begin{aligned} Z_d(\lambda) = \text{Min } \left(\frac{1}{D} L_d + \tau_d R_d + f_d(\lambda) \right) \\ \text{st } U^d_{e,s} \geq j_d - g_d \\ R_d \geq 0, L_d \geq 0, U^d_{e,s} \geq 0, d = i, ...D \end{aligned} \tag{3.54}$$

where $Z^{LB} = Z(\lambda) = \sum_{d=1,...,D} Z_d(\lambda)$ and

$$f_d(\lambda) = \begin{cases} \sum_{d=1}^{D} \left(\lambda_d U^d_{e,s} \right) & \text{if } d = 1 \\ -\lambda_d U^d_{e,s}, & \text{otherwise} \end{cases} \tag{3.55}$$

This final formulation (3.54) gives an approximate solution to the original optimization, generating a lower bound for the algorithm. Physically, each day will operate with its most economic pieces of equipment, purchased at a fraction of the total capital cost. Although a cheaper solution, all equipment must be purchased at its full value, making this solution impractical.

3.7.2 Upper bound

While the Lagrangean decomposition gives a good approximate lower bound solution to the original optimization, it is not a feasible solution to the original problem because the long term variables, $U^d_{e,s}$, do no have to be equal, leading to incomplete capital and maintenance costs. To calculate a solution that exists in the full-space optimization using the solution from the Lagrangean decomposition, each piece of equipment that was used on any day d in the Lagrangean decomposition solution ($U^d_{e,s,LB}$) is set to be used on every day in order to compute an upper bound for the solution of the original problem ($U^d_{e,s,UB}$). Any equipment not used in the Lagrangean decomposition lower bound solution is not used in the optimization for the upper bound.

$$U^{tot}_{e,s} = \sum_{d=1,\ldots,D} U^d_{e,s,LB} \tag{3.56}$$

$$U^d_{e,s,UB} = \begin{cases} 1 & \text{if } U^{tot}_{e,s} > 0 \\ 0 & \text{otherwise} \end{cases} \tag{3.57}$$

$U^d_{e,s,LB}$ are the final values for $U^d_{e,s}$ from the Lagrangean decomposition and $U^d_{e,s,UB}$ are the fixed values for $U^d_{e,s,}$ in the upper bound optimization.

Unlike the Lagrangean decomposition solution, which allows for "partial" capital costs depending on how many days the equipment was used, this arrangement forces the total capital cost and maintenance cost to be included in the optimization creating an upper bound solution that exists in the full-space optimization. Formulation (3.54), employed to obtain the lower bound

solution, is solved again with fixed $U_{e,s}^{d} = U_{e,s,UB}^{d}$, to obtain the upper bound solutions, where $Z^{UB} = Z(\lambda) = \sum_{d=1,...,D} Z_d(\lambda)$.

3.7.3 Updating Lagrange multipliers

While the Lagrangean decomposition (Formulation 3.54) will decrease the computation intensity of the optimization, the lower bound solution, Z^{LB}, does not yield a solution to the original problem. By adjusting the Lagrange multipliers, it is possible to get a tight relaxation, as close as possible to the original problem solution. To update the Lagrange multipliers, a hybrid of the common subgradient method and cutting-plane method was used [90]. This method was selected because of its ability to improve convergence, through the cutting-planes method, with bounds that allow better multiplier selection in the early iterations, using the subgradient method.

The hybrid method for updating Lagrange multipliers proceeds as follows [90]:

$$
\begin{aligned}
&\max_{\lambda_d} \quad \zeta \\
&\text{s.t.:} \\
&\zeta \leq \sum_{d=1,...,D} \tau_d (L_d + R_d) + \sum_{d=1,...,D-1} \left(\lambda_d \Delta_d^k\right) \quad \forall k = 1, ..., K \\
&\lambda_d^{K-1} - \theta^K \frac{Z^{UB} - Z^{LB,K}}{\sum_d \left(\Delta_d^K\right)^2} \mid \Delta_d^K \mid \leq \lambda_d \leq \lambda_d^{K-1} + \theta^K \frac{Z^{UB} - Z^{LB,K}}{\sum_d \left(\Delta_d^K\right)^2} \mid \Delta_d^K \mid
\end{aligned}
\tag{3.58}
$$

where θ^k is the step length parameter and Δ_d^k is the difference between $U_{e,s}^{d}$

for the kth iteration:

$$\Delta_d^k = U_{e,s}^1 - U_{e,s}^{d+1} \quad \forall d < D, \tag{3.59}$$

The step length parameter, with an initial value between (0,2], is updated every iteration based on the dual solution obtained from the lower bound optimization [90, 114], using the following algorithm:

1. If $Z(\lambda_K) < Z(\lambda_{K-1})$, then $\theta^K = \beta^- \theta^{K-1}$
2. Otherwise, solve $c^k = \Delta^{K-1} \cdot \Delta^K$
   - If $c^K < 0$, then $\theta^K = \beta^o \theta^{K-1}$
   - Else $\theta^K = \beta^+ \theta^{K-1}$

where β^-, β^o, and β^+ are parameters used to adjust the step size based on the direction of the Lagrangian decomposition solution, such that $0 < \beta^- < \beta^o < 1 < \beta^+$.

3.7.4 Algorithm overview

Using the algorithm depicted in Figure 3.5, the large-scale optimization of the design and operational strategies for a CHP plant for a residential neighborhood can solved to a specific gap, ε. First, the Lagrange multipliers and iteration counter, k, are initialized. Next, the temporal Lagrangean decomposition is solved in pieces, and the solutions summed to obtain a lower

bound solution (Z^{LB}). If the solution is greater than the global lower bound solution (G^{LB}), the current solution is saved as the global lower bound solution, G^{LB}. Based on the results from the lower bound solutions, the variables, $U^d_{e,s}$ are fixed for all D subsections of the optimization, and the decomposition is solved again, summing the final solutions to obtain an upper bound to the optimization problem. If the current upper bound solution is less than the global upper bound solution (G^{UB}), the new solution is saved as the global upper bound. Then the difference between the upper and lower bound solutions is checked to determine if it is less than the tolerance. If it is less, the decomposition is done, with the final solution being the global upper bound solution, else the Lagrange multipliers are updated using the hybrid method, and the solver continues onto the next iteration.

3.8 Case Study

The algorithm to solve the optimization of design and operational strategies was applied to a case study, with the goal to determine the size and operation of a CHP plant using energy demand and PV generation data from the Mueller neighborhood in Austin, Texas (as described earlier in Section 3.6.3).

To accurately capture the operational costs of the plant over a year, eight days of data were selected to be optimized, including average days from every season, and minimum and maximum demands for each utility (Figure 3.6).

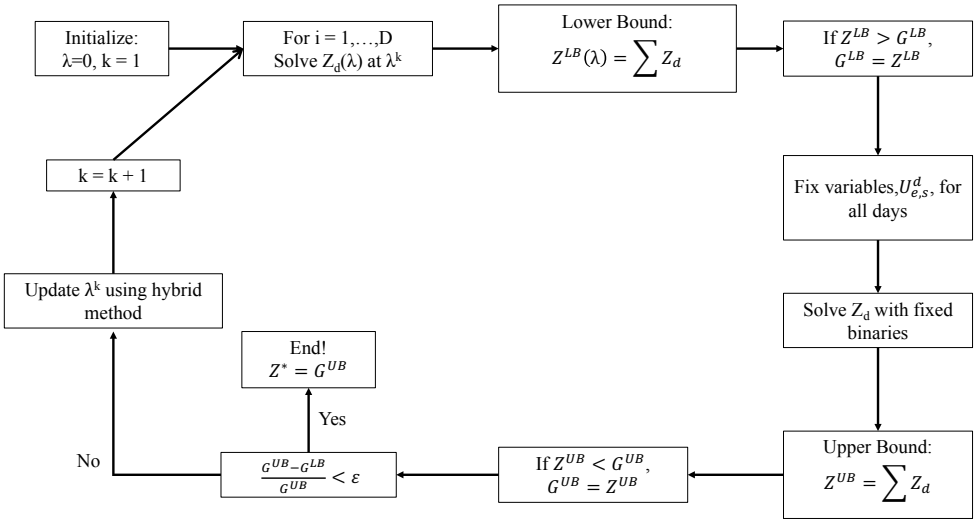

Figure 3.5: Schematic of the algorithm used to solve the simultaneous optimization of design and operational strategies.

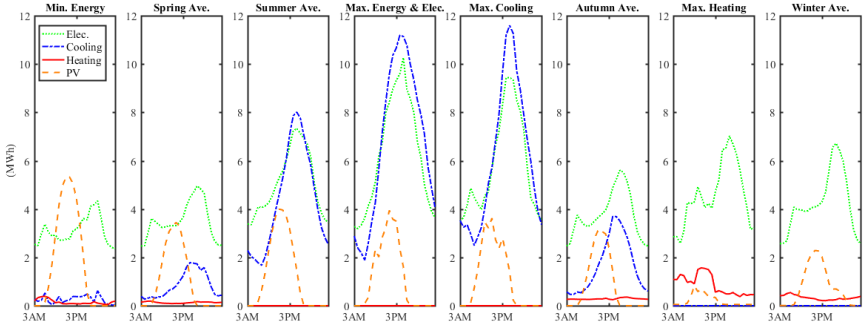

Figure 3.6: The eight days of demand and PV generation data optimized to determine the optimal CHP plant design and operation includes average seasonal utility demand and minimum and maximum days of utility demand.

The most extreme electricity and air conditioning demand is found in the summer months due to the large amount of electricity and cooling that

comes with a high temperature of 105^{o}F on June 26th, 2012, with an average temperature of 97^{o}F for the month of August [115]. The spring and autumn have significantly less cooling demand, and no cooling demand is present in the winter. Heating is present in the spring, autumn, and winter, with the most heating in the winter, but the amount of heating is much lower compared to heating and cooling. Lastly, PV generation in Austin, TX is seasonal, with the most generation seen in the spring and summer, and less generation in the winter.

With the days of data selected, the next step was to dissect the data in a manner that would allow quick solutions to the smaller problems, while avoiding interruptions of equipment dynamics (i.e., the equipment does not switch modes). While dividing the data into seasons would avoid more dynamic interruptions, the optimization still took too long to run. From previous work of scheduling a CHP plant for a residential neighborhood, it was observed that the equipment did not switch modes between 2 am and 5 am. During this time period, all demands are at their lowest levels, and PV generation is not present. Thus, it was decided to break the demand data into eight pieces, using the natural break in equipment dynamics at 3 am as a separation point (which is why the demand in Figure 3.6 is graphed from 3 am - 2am.) The scaling parameters for the daily costs (i.e., fuel, maintenance, and transition penalties), τ_d,were given the values of 112 for the summer, 83 for the spring, autumn, and winter, and 1 for the minimum and maximum utility demand days, totaling 365 days, or one year. These numbers were selected to repre-

sent the length of the different seasons, with summer being the predominant season in Austin.

The algorithm was run, with θ^k being set to an initial value of 1.5, and $\beta^- = 0.8$, $\beta^o = 0.99$, and $\beta^+ = 1.2$. Each subproblem, having 7,567 equations and 5,095 variables of which 600 are discrete, was solved with GAMS 24.4.6 using the commercial solver CPLEX (12.6.2.0) on a PC Intel Core i7, 3.40 GHz, 16 GB RAM, 64 bit and Windows 10.

3.8.1 Optimal CHP plant design

Utilizing the temporal Lagrangean decomposition method, a final solution with a 2% gap was reached in 6 hours (84 iterations). The optimal plant equipment selected by the optimization included two gas turbines (5 MW and 15 MW) with two heat recovery steam generators to generate electricity and steam, an auxiliary boiler (22,700 kg/hr) to generate extra steam, and two each of the steam absorption chillers (480 ton and 700 ton) and electric chillers (4,777 ton and 14,330 ton) to provide cooling for the neighborhood (Figure 3.7). A steam turbine was found to be uneconomical, due to the large amount of steam that is needed to power the turbine, and the inefficiency of the boiler to produce the large amount of steam. Overall, the capital cost of the equipment totals $48,832,800.

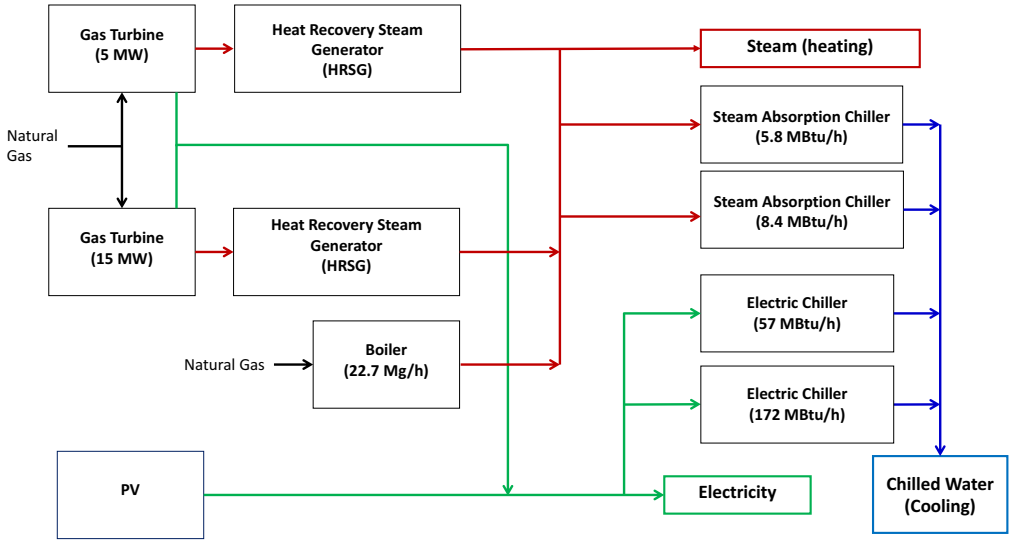

Figure 3.7: Optimal equipment to be included in a CHP plant to meet the utility demands for a residential neighborhood has a total capital cost of $48,832,800.

3.8.2 CHP plant operation

In addition to determining the optimal equipment and sizes of the equipment, the optimization determined the optimal operational strategy of the equipment to meet the heating, cooling, and electricity of the residential neighborhood, taking into consideration the maintenance fees, fuel costs, and start-up time, and transition penalties from turning the equipment off to on. Over a period of twenty years, the expected lifetime of the plant, the plant would pay $41,223,820 for natural gas to power the gas turbines and boiler, $14,014,830 for the maintenance on all equipment, and $5,076,000 for turning the equipment on.

3.8.2.1 Electricity generation

The results of the electricity-related equipment operation is shown in Figure 3.8, where Spr(1) is the Minimum Energy day, Spr(2) is the day that represents the average spring demand, Sum(1) is the day that represents the average summer demand, Sum(2) is the Maximum Energy and Maximum Electricity day, Sum(3) is the Maximum Cooling day, Aut(1) is the day that represents the average autumn demand, Win(1) is the Maximum Heating day, and Win(2) is the day that represents the average winter demand. The optimization found it economical to turn the gas turbines on and off depending on the demand. This kind of plant operation is unexpected, since most electricity generation plants are often turned on and left running at maximum capacity. However, the optimization found it economical to turn the CHP plant gas turbines on an off and run them at partial to maximum capacity to meet the neighborhood electricity and electric chiller demands. One advantage of including two gas turbines in the CHP plant, which aided in improving the plant economics, is the increased generation flexibility, demonstrated by the different seasonal operating profiles for the gas turbines. On one spring day, the plant was able to run on just PV generation from the rooftop PV panels in the neighborhood. In the autumn and winter, the larger gas turbine was used to meet peak demand, while in the summer, both gas turbines were needed to meet the peak demand around 5 PM. While this plant might seem to be oversized in terms of electricity generation, all extra electricity is being used to power the electric chillers.

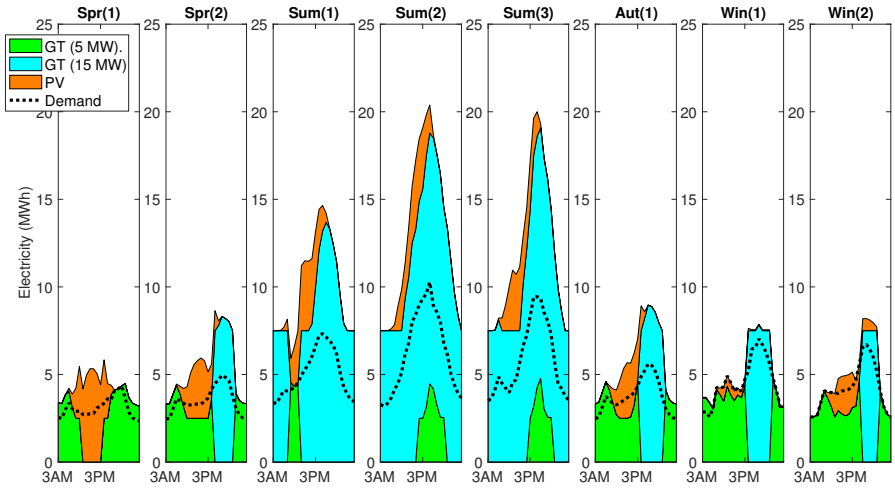

Figure 3.8: Most electricity demand can be met with just one gas turbine and PV generation, but the summer requires both gas turbines in combination with PV generation.

3.8.2.2 Cooling generation

While two steam absorption chillers are present in the CHP plant design, their chilled water production is minimal compared to the electric chillers, which are used to meet a majority of the neighborhood cooling demand (Figure 3.9). In the spring and fall, the smaller electric chiller is used to meet almost all of the neighborhood cooling demand, with the larger electric chiller turned on at partial capacity in the fall to help meet the peak in cooling. In the summer, the both electric chillers as well as both steam adsorption chillers are needed to help meet the high cooling demand present on the maximum electricity and cooling days. On an average summer day, only the larger electric chiller is needed to meet the peak cooling demand, with the smaller electric

chiller meeting the morning cooling demand.

Due to the equality constraint for electricity production in the optimization (Equation (3.45)), the electric chillers are used to dissipate extra electricity generation in the form of chilled water. This dissipation of energy is more noticeable in the spring, when the PV generation exceeds the electricity demand of the neighborhood, and in the winter, when the electric chiller is running but there is no cooling demand. However, it is also present in the summer during the morning hours.

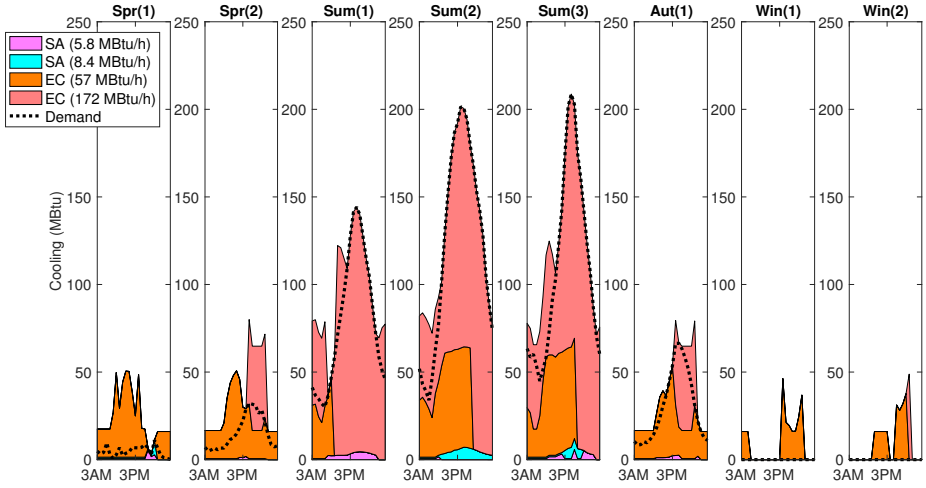

Figure 3.9: A majority of the cooling is met by the electric chillers. The largest contribution of to the chilled water generation by the steam adsorption chillers is seen in the summer, when both gas turbines and HRSGs are running, generating more steam.

3.8.2.3 Heating generation

Due to the warmer temperatures experienced in Austin, the steam generation is driven by mostly the cooling and electricity demands in all seasons except the winter. On the Minimum Energy Day, shown in Figure 3.10, the boiler allows the neighborhood to run off of PV generation only in the afternoon and the smaller gas turbine in the evening, using the steam adsorption chillers to help provide the needed chilled water. When the maximum cooling is needed in the summer, the boiler is used during peak cooling hours to allow both steam adsorption chillers to run at the same time to help meet the peak cooling demand. On all other days in the spring, summer, and autumn, the steam generation is defined by the gas turbine/HRSG schedule, which are driven by the electricity and cooling demands.

3.8.3 Summary of case study

Over the lifetime of the plant, with a constant cost of natural gas and the predicted energy demands, the total cost of the plant would be \$109,147,450, with about 50% of this cost coming from the capital cost of the equipment. The large electricity and cooling demands and the minimal heating demand, reducing the need for steam, make it uneconomical to include steam turbines in the plant design. The large changes in residential energy demand, from low demand in the early morning to peak demand in the late afternoon, and PV generation in the afternoon, improve the economics of turning on and off the equipment, using the smaller equipment in the morning

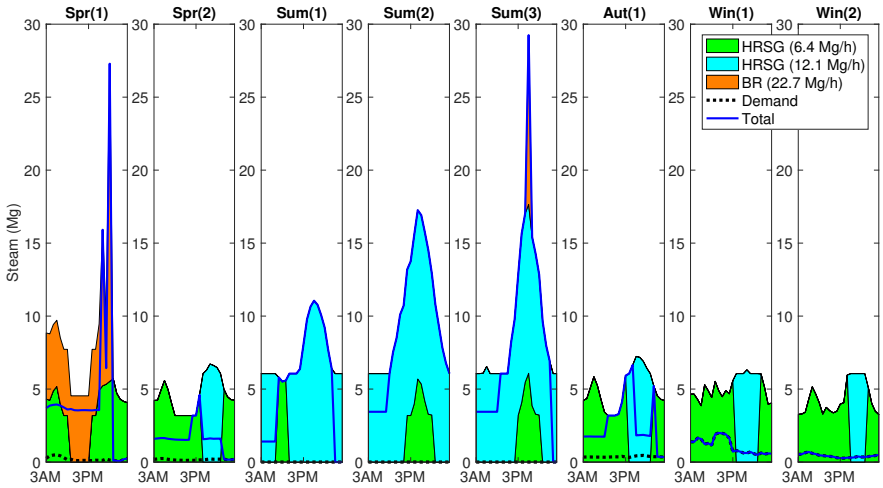

Figure 3.10: The steam generation is driven by electricity and cooling demands, and not heating demand.

and the larger equipment, or both pieces of equipment in some cases, in the evening.

3.9 Conclusions

In conclusion, we successfully optimized the design and operational strategy for a larger CHP system to meet the heating, cooling, and electricity demands of a residential neighborhood. Utilizing residential energy demand and PV generation data from Austin, Texas, we were able to determine the optimal design and operation, capturing the hourly and seasonal variability and uncertainty in the residential sector. With the new CHP plant design, the plant operation was able to better match the neighborhood demand in a

more efficient manner, and there was less over-generation of energy. Finding the extensive, multi-scale optimization problem "unsolvable" without the aid of a supercomputer, we solved the problem using a temporal Lagrangean decomposition with a hybrid Lagrange multiplier updating method, which cut the computation time down to 6 hours.

Chapter 4

The Effects of Rooftop Photovoltaics and Centralized Energy Storage on the Design and Operation of a Residential CHP System

4.1 Introduction

Over the past several years, PV generation in the United States has been increasing [116]. While PV generation decreases the need for carbon-based energy generation, it has created problems for the grid, such as over-generation, and complex scheduling of energy generation. In California, over-generation has caused a sharp decrease of electricity demand in the afternoon when PV generation is at its highest, but when the sun sets and PV generation diminishes in the evening, there is difficulty in turning on or ramping up electricity plants to be able to meet the high increase of electricity demand [75]. Also, with the decoupling of PV generation and utility demand in the residential sector, PV generation is highest in the afternoon when demand is low, and not present in the evening when residential demand is at its highest, causing complex energy scheduling of utility generation.

Electricity providers have tried to overcome these issues by incorporating grid-level energy storage, which has many different benefits, such as helping to integrate renewables by allowing shifting of excess generation to

peak hours, and helping to shave peak demand so that energy could be generated in the morning during low demand and be saved for use in the evening when energy demand is high. Previous research contained in this dissertation has shown that CHP can meet the heating, electricity, and cooling demands of a residential neighborhood when incorporating PV generation in a centralized manner. However, as demonstrated in Chapters 2 and 3, the demand of the neighborhood often leads to large peaks in electricity and cooling, and some periods of extra electricity, due to PV generation and minimum equipment capacities, both which could be addressed using energy storage. Thus, the question to be answered by this project, is *What are the economic benefits of incorporating PV and energy storage for a residential, neighborhood-level CHP plant?*

To determine the effect of PV generation and energy storage on the economics of a CHP plant for a residential neighborhood, two scenarios, each with a scheduling sub-problem, were optimized:

1. Design and operation of a CHP plant (without energy storage)
    - Schedule CHP plant operation (using plant design from Scenario 1) with PV generation
2. Design and operation of a CHP plant with energy storage
    - Schedule CHP plant with energy storage (using design from Scenario 2) with PV generation

To optimize the larger cases (Scenarios (1) and (2)), a bilevel decomposition is used to decrease the computational effort needed for the simultaneous optimization of the design and operation. By decreasing the solution nodes, an accurate solution can be calculated in a reasonable amount of time, allowing for a timely analysis of the economic advantages (or disadvantages) of energy storage and PV generation for a CHP plant for a residential neighborhood.

4.2 Background

Over the past several years, the number of studies on energy storage has increased due to the higher capacity of intermittent renewables and the drive to achieve more efficient and economic energy generation methods. These studies have analyzed the effects and interactions of energy storage on a wide range of energy scales, from the grid [117–121], to industrial plants [122,123], to mid-scale residential/commercial complexes [124–128], to individual residences [129, 130].

Concentrating on CHP plants (as an energy generation source) with energy storage, many papers concentrate on studying existing infrastructure with predetermined CHP equipment capacities. The researchers either fix the type and size of energy storage [126, 131–134], or determine the optimal type and size of the energy storage [125,130], both with the objective of maximizing the operational savings. On the other hand, Wang et al. did optimize the design and operation the CHP plant equipment, but fixed the size of the thermal energy storage [135]. Also, Streckienė et al. optimized the CHP

plant design and energy storage capacity, but she solved for the CHP plant design first, then optimized the thermal energy storage design and operation second [136].

A few researchers have investigated designing future CHP plants with energy storage, simultaneously optimizing design and operation of the CHP plant and energy storage. This approach can determine the effect of energy storage on both the design and operation, taking into consideration the capital cost of the equipment and the potential operational savings. While Steen et al. used a commercial energy software package, DER-CAM, to optimize the CHP plant with energy storage, Buoro et al. and Tveit et al. used general optimization software to solve their optimizations. However, Buoro et al. used simplified equipment models with constant efficiencies, to concentrate the study on the effects of allowing the transfer of electricity and heat between industrial sites [99]. Also, Tveit et al. problem was a large MINLP that had could not be solved with a global solver, and therefore had to initialized and solved twenty times, because the optimization was extremely sensitive to the initial points [137]. To help deal with the complexities of such problems and the difficulty in solving the multi-scale problems, Moradi et al. used a bilevel decomposition to iteratively solve the unit capacity of the plant and energy storage with particle swarm optimization, and then solve the dispatch of the plant with the selected capacities, using quadratic programming [86]. To our knowledge little work has been done in the simultaneous optimization of the design and operation of a CHP plant with energy storage for a residential

neighborhood, using complex turbine models and decomposition methods to solve the problem formulation to optimality.

4.3 Energy Storage Selection

Today there are many different types of energy storage methods available, as shown in Figure 4.1. The storage methods can be discharged in seconds, such as flywheels and high-power supercapacitors, to over periods of several hours, such as pumped hydro and thermal energy storage. With an hourly time step for the optimization, as well as high peaks in electricity and cooling demand and the potential to implement large amounts of rooftop solar generation, we have selected lithium ion batteries, flow batteries, and thermal energy storage as the possible energy storage methods to be implemented into the CHP plant. In addition to their high efficiencies, these energy storage devices are easily scaleable and do not require a large amount of additional construction to be implemented.

4.4 CHP Plant Model

In order to capture the initial design of the CHP plant with all possible equipment, a plant superstructure was created (Figure 4.2). In addition to the already modeled equipment (i.e., gas turbines/HRSGs, steam turbines, boilers, steam adsorption chillers, and electric chillers), which can be found in our previous work (Section 3.3), three additional pieces of equipment are modeled to store energy: thermal energy storage (TES) unit, lithium-ion (LI)

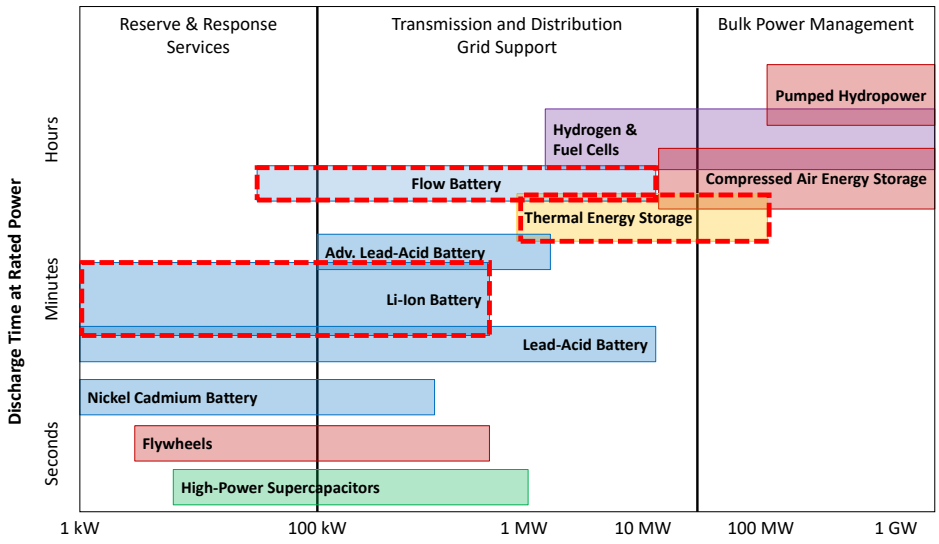

Figure 4.1: Availability of different energy storage technologies at the grid-level, where red indicates mechanical storage, blue indicates electrochemical storage, green indicates electrical storage, purple indicates hydrog-related storage, and yellow indicates thermal storage (figure adapted from [10]).

battery, and flow battery.

4.4.1 Energy Storage Model

All of the devices used to store energy use the same set of equations to model the operation of the storage. At every hour h for every day d, the energy stored (L_b^h) is calculated based on the energy in the device at the previous hour *h-1*, the efficiency of the device (η_b), the energy put into storage (in_b^{h-1}), and the energy removed from storage (out_b^{h-1}):

$$L_b^h = L_b^{h-1} + \eta_b in_b^h - out_b^h \quad \forall\, b \in B, h = 24(d-1)+1, ..., 24d, d \in D \quad (4.1)$$

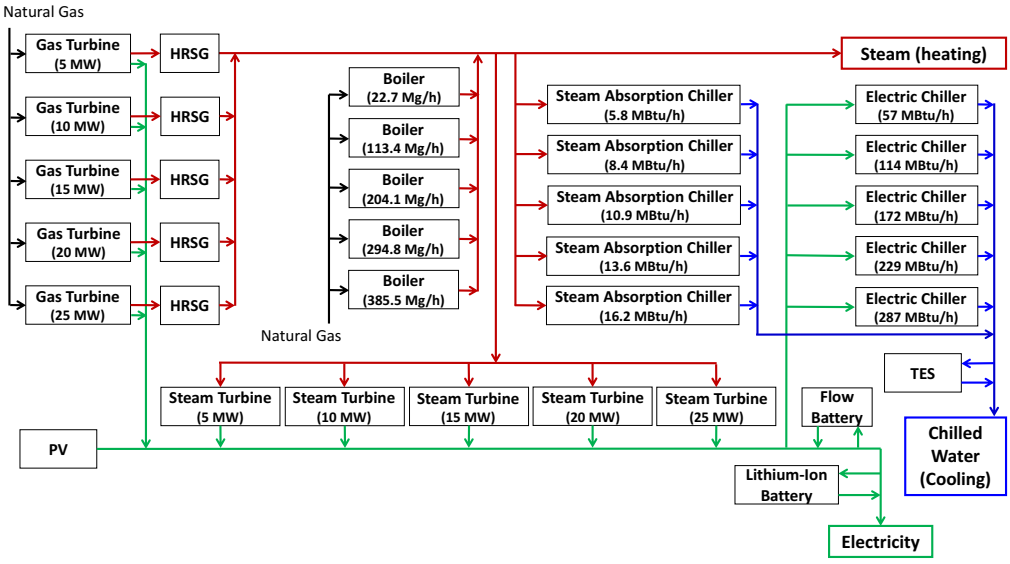

Figure 4.2: The CHP plant superstructure, including energy storage.

where b is the type of energy storage device, B is the set of all energy storage devices, and D is the total number of days optimized. The efficiencies of the selected storage methods are assumed to be constant and not dependent on the sizes of the devices, with the lithium-ion battery having an efficiency of 95% ($\eta_{LI} = 0.95$) [138], the flow battery having an efficiency of 85% ($\eta_{FL} = 0.85$) [139], and the thermal energy storage system having an efficiency of 92% ($eta_{TH} = 0.92$) [140].

The energy stored in the battery at each hour is limited by the size of the storage device, L_b^{max}, and the minimum capacity:

$$m_b L_b^{max} \leq L_b^h \leq L_b^{max} \quad \forall\, b \in B, h \in H \tag{4.2}$$

where m_b is a parameter used to dictate the minimum capacity as a function

of the maximum capacity. For the energy storage models, the maximum sizes of the devices are positive continuous variables, and are not a pre-selected discrete size. This is why in the CHP plant superstructure (Figure 4.2), there is only one possible piece of equipment per type of energy storage, and five pre-selected sizes for all of the other equipment.

The amount of energy put into storage and removed from storage is constrained as follows:

$$in_b^h \leq f_b^{in} L_b^{max} \quad \forall\, b \in B, h \in H \tag{4.3}$$

$$out_b^h \leq f_b^{out} L_b^{max} \quad \forall\, b \in B, h \in H \tag{4.4}$$

where f_b^{in} and f_b^{out} are parameters representing the percentage of the maximum capacity limiting the flow of energy in and out, respectively.

Lastly, in order to avoid the exploitation of the energy storage in the scheduling, the amount of energy stored at the first hour of every day optimized must equal the amount of energy stored at the last hour of each day:

$$L_b^{24(d-1)+1} = L_b^{24d} \quad \forall\, b \in B \tag{4.5}$$

This constraint prevents the scheduling from filling the energy storage device in the first hour and emptying it by the end of the optimization horizon.

4.5 Operation Scheduling

To accurately capture the dynamics and operating cost of the CHP plant with energy storage, the optimization considers both the capital cost,

associated with the design, and the operational costs, associated with the scheduling. While the original CHP plant equipment (gas turbines/HRSGs, steam turbines, boilers, electric chillers, and steam adsorption chillers) are scheduled with four possible equipment modes (on, off, cold startup and warm startup) (Section 3.4.1), the energy storage devices will be scheduled without operating modes. This means binary variables to track their current modes are not necessary, and there will not be any associated startup penalties from the energy storage equipment.

4.6 Capital Investment and Maintenance Costs

While energy storage devices do not have an associated fuel cost, the capital and maintenance cost need to be considered in the optimization. This will determine if the money saved from shifting energy generation or storing extra energy, outweighs the total cost of the energy storage devices. In addition to the already created capital investment (Section 3.5.1) and maintenance cost models (Section 3.5.2) for the original CHP plant superstructure, additional economic models were created for the energy storage devices.

4.6.1 Capital Cost Models

The capital costs of the lithium-ion battery (C_{LI}) and flow battery (C_{FL}) are functions of their sizes:

$$C_{LI} = Cost_{LI} \times L_{LI}^{max} \tag{4.6}$$

$$C_{FL} = Cost_{FL} \times L_{FL}^{max} \tag{4.7}$$

where $Cost_{LI}$ and $Cost_{FL}$ are the is average costs of the batteries per MWh obtained from Lazard's Levelized Cost of Storage Analysis [141].

The capital cost of the thermal energy storage is a function of the size of the thermal energy storage tank:

$$C_{TH} = Cost_{TH} \times L_{TH}^{max} \tag{4.8}$$

where $Cost_{TH}$ is the average cost of the tank per million gallons [142].

4.6.2 Maintenance Cost Models

For all three energy storage methods, the yearly constant maintenance costs (M_b) are linearly proportional to the size of the device:

$$M_b = MC_b \times L_b^{max} \quad \forall\, b \in B \tag{4.9}$$

where MC_b is the cost per energy unit [141, 142]

4.6.3 Capital and Maintenance Costs

The total capital cost for all pieces of equipment used, including energy storage ($Capital$), is calculated using the following equation:

$$Capital = \sum_{e} \sum_{s} (U_{e,s} \times C_{e,s}) + \sum_{b} C_b \tag{4.10}$$

where the first half of the right side is the cost of the discrete-sized CHP plant equipment (i.e., gas turbines, steam turbines, etc.) and the second half is the cost of the energy storage. For the variables with discrete equipment sizes, the

capital cost of the equipment is multiplied by the binary variable, $U_{e,s}$, which determines if a piece of equipment is included in the plant design. This assures that the total capital cost only includes equipment in the plant design.

As seen in Sections 3.5.2 and 4.6.2, the maintenance cost is either a constant fee each year (steam turbine, electric chiller, steam absorption chiller, and energy storage) or can change based on hourly equipment use (gas turbine/HRSG and boiler). The equipment with a constant maintenance fee ($Main_1$) includes both equipment with discrete equipment sizes and positive continuous sizes. For the equipment with discrete equipment sizes, the binary variable $U_{e,s}$ is incorporated so only maintenance costs are included for equipment used in the plant design. Equipment with positive continuous sizes (i.e., the energy storage devices) do no require any additional variables, because if the equipment is not used, the size and consequently the maintenance cost will both be zero:

$$Main_1 = \sum_{e} \sum_{s} (U_{e,s} \times M_{e,s}) + \sum_{b} M_b \quad \forall \quad e \neq \{GT, BR\} \tag{4.11}$$

The total maintenance cost for equipment whose maintenance cost is based on hourly generation ($Main_{2,d}$) is calculated as follows:

$$Main_{2,d} = \sum_{h=24(d-1)+1,\ldots,24*d} \left(\sum_{\upsilon} M^{h}_{GT,\upsilon} + \sum_{\chi} M^{h}_{BR,\chi} \right) \quad \forall \quad s \in S, d \in D \tag{4.12}$$

4.7 Simultaneous Design and Operational Optimization

4.7.1 Meeting Neighborhood Utility Demand

All electricity, heating, and cooling demands of the neighborhood must be met by the CHP plant at all hours. The following constraints on electricity, steam and chilled water are used to guarantee all utility requirements are met:

$$Elec^h + \sum_{\omega} P^h_{EC,\omega} + in^h_{LI} + in^h_{FL} = \sum_{\upsilon} P^h_{GT,\upsilon} + \sum_{\phi} P^h_{ST,\phi} + out^h_{LI} + out^h_{FL} \quad \forall h \in H \quad (4.13)$$

$$Heat^h + \sum_{\phi} W^h_{ST,\phi} + \sum_{\psi} W^h_{SA,\psi} \leq \sum_{\upsilon} W^h_{HRSG,\upsilon} + \sum_{\chi} W^h_{BR,\chi} \quad \forall h \in H \quad (4.14)$$

$$Cool^h + in^h_{TH} \leq \sum_{\psi} Q^h_{SA,\psi} + \sum_{\omega} Q^h_{EC,\omega} + out^h_{TH} \quad \forall h \in H \quad (4.15)$$

where $Elec^h$ is the electricity demand, $Heat^h$ is the heating demand, and $Cool^h$ is the cooling demand. In the electricity (Equation (4.13)) and cooling (Equation (4.15)) balances, energy storage is available to help meet the demands. Also, in order to account for the possibility that PV generation is not present, i.e., a cloudy day, the simultaneous optimization of the design and operational strategy is solved without PV generation.

4.7.2 Overall Objective Function

The overall objective of the simultaneous design and operational optimization, is to minimize the cost of the plant. The four sources of expenditures

are:

1. Capital from purchasing the CHP plant equipment and energy storage
2. Fuel
3. Maintenance fees from CHP plant equipment and energy storage operation
4. Transition penalties

The two types of equipment that require fuel, in the form of natural gas, are the gas turbines and the boilers. Assuming that the cost of natural gas, NG_{cost}, remains constant for the lifetime of the plant, the daily fuel cost ($Fuel_d$) is calculated as follows:

$$Fuel_d = NG_{cost} \times \sum_{h=1,\ldots,24} \left(\sum_{\upsilon} W^h_{f,GT,\upsilon} + \sum_{\chi} W^h_{f,BR,\chi} \right) \tag{4.16}$$

The total daily transition penalties ($Trans.Pen._d$) are computed as:

$$Trans.Pen._d = \sum_{e} \sum_{s} \sum_{h=24(d-1)+1,\ldots,24*d} startcost^h_{e,s} \tag{4.17}$$

where $startcost^h_{e,s}$ is the cost from transitioning equipment from one mode to the next. For more information on how this value is calculated, see Sections 3.4.2 and 3.4.3.

The overall objective function is:

$$\begin{aligned} \min \quad & Capital + Y \times Main_1 \\ & + Y \sum_{d=1,\ldots,D} (\tau_d \times (Fuel_d + Main_{2,d} + Trans.Pen._d)) \end{aligned} \tag{4.18}$$

where Y is the lifetime of the plant and τ_d is a parameter used to scale up each daily operational costs to simulate a year of operation.

4.7.3 Residential Neighborhood Utility Demand Model

To create a residential neighborhood utility demand model, residential utility demand data were obtained from the Mueller neighborhood in Austin, TX, which is designed to promote energy and water efficiency [112]. Pecan Street Inc. collects [8] data from over 700 of these homes, including but not limited to electricity, water and natural gas use, and rooftop PV generation data. After disaggregating the cooling demand [64], the hourly data for electricity, heating, cooling, and PV generation were scaled up to represent neighborhood of approximately 5,600 homes. As noted in Section 3.6.3, residential utility demand exhibits extreme variability and uncertainty. Thus, eight days of data were used to capture a combination of the average seasonal demand and the extreme utility demands (based on historical data). In order to solve the optimization using a decomposition method, which was found to be necessary due to the type of problem (MILP) and the problem size, the eight days were separated using a natural break in plant dynamics at 3:00 AM, when energy demand is at its lowest. [72].

4.8 Solution Algorithm: Bilevel Decomposition

In the previous chapter, a temporal Lagrangean decomposition method was used to solve the optimization when vast amounts of residential energy

demand data were incorporated to account for demand variability and uncertainty. While this method worked well for the one scenario, once rooftop PV generation was removed from the electricity balance and energy storage was added, the temporal Lagrangean decomposition was unable to solve the optimization in a relatively short amount of time (three iterations took approximately 24 computational hours). Thus, a new decomposition method needed to be investigated as a possible fix to quickly the solve the simultaneous design and operational optimization of the CHP plant with energy storage. Due to the multi-purpose nature of the problem, with the intention of determining both the *design* and *operation* of the plant, a bilevel decomposition approach was selected. This approach iterates through an upper level problem that selects the optimal equipment utilizing a relaxed version of the full problem, a lower level problem that solves the full scheduling problem to determine the true cost, and integer cuts to eliminate uneconomical and/or infeasible solutions.

4.8.1 Upper Level Problem

In the simultaneous optimization of the design and operation of a CHP plant with energy storage devices, the most complex part of the optimization model is the CHP plant equipment with binary variables to determine the hourly status of the equipment (on/off). Since the goal of the upper level of the decomposition is to to determine the type and size of equipment (including energy storage) to be used in the CHP plant, and not the exact scheduling of the equipment, a relaxed version of the full problem is developed. This entails

1) removing lower bounds on the equipment operation, and 2) removing the hourly "on" and "off" modes of the equipment ($y^h_{e,s}$), so the upper bound constraints are a function of the binary design variable $U_{e,s}$. The new relaxed upper level problem (UL) will results in fewer, less complex combinations of solutions, creating an easier to solve lower bound solution for the equipment selection with the operation being a function of the binary design variable, $U_{e,s}$, and not the binary scheduling variables, $y^h_{e,s}$.

Using this relaxation, the UL optimization problem for the simultaneous optimization of the design and operation of a CHP plant with energy storage has the following format:

$$Z^{UL} = min \quad Capital + Y * Main_1 + Y \times (\tau_d \, (Fuel_d + Main_{2,d})) \tag{4.19}$$

s.t.

$$P^h_{GT,\upsilon} = \alpha_{GT} \times \eta^h_{GT,T,\upsilon} \times W^h_{f,GT,\upsilon} \quad \forall \, \upsilon \in N_{GT}, h \in H \tag{4.20}$$

$$0 \leq W^h_{f,GT,\upsilon} \leq U_{GT,\upsilon} \times W^{max}_{f,GT} \quad \forall \, \upsilon \in N_{GT}, h \in H \tag{4.21}$$

$$0 \leq P^h_{GT,\upsilon} \leq U_{GT,\upsilon} \times 10000 \times P^{max}_{GT,\upsilon} \quad \forall \, \upsilon \in N_{GT}, h \in H \tag{4.22}$$

$$W^h_{HRSG,\upsilon} = W^{nom}_{HRSG,\upsilon} \times \left(\frac{P^h_{GT,\upsilon}}{1000 P^{max}_{GT,\upsilon}} \right) \quad \forall \, \upsilon \in N_{GT}, h \in H \tag{4.23}$$

$$P^h_{ST,\phi} = n_\phi \times W^h_{ST,\phi} - (W_{int,\phi} \times U_{ST,phi}) \quad \forall \, \phi \in N_{ST}, h \in H \tag{4.24}$$

$$0 \leq W^h_{ST,\phi} \leq U_{ST,\phi} \times W^{max}_{ST,\phi} \forall \, \phi \in N_{ST}, h \in H \tag{4.25}$$

$$0 \leq P^h_{ST,\phi} \leq U_{ST,\phi} \times P^{max}_{ST,\phi} \forall \, \phi \in N_{ST}, h \in H \tag{4.26}$$

$$W^h_{BR,\chi} = \frac{\eta_{BR} \times LHV \times W^h_{f,BR,\chi}}{H_{BR,out} - H_{BR,in}} \quad \forall\, \chi \in N_{BR}, h \in H \tag{4.27}$$

$$0 \leq W^h_{f,BR,\chi} \leq U_{BR,\chi} \times W^{max}_{f,BR,\chi} \quad \forall\, \chi \in N_{BR}, h \in H \tag{4.28}$$

$$Q^h_{SA,\psi} = COP_{SA}\,(H_{s,in} - H_{s,out}) \times W^h_{SA,\psi} \quad \forall\, \psi \in N_{SA}, h \in H \tag{4.29}$$

$$0 \leq W^h_{SA,\psi} \leq U_{SA,\psi} \times W^{max}_{SA,psi} \quad \forall\, \psi \in N_{SA}, h \in H \tag{4.30}$$

$$Q^h_{EC,\omega} = P^h_{EC,\omega} \times COP_{EC} \times 3412 \quad \forall\, \omega \in N_{EC}, h \in H \tag{4.31}$$

$$0 \leq P^h_{EC,\omega} \leq U_{EC,\omega} \times P^{max}_{EC,\omega} \quad \forall\, \omega \in N_{EC}, h \in H \tag{4.32}$$

and Eqs. (4.1 - 4.5, 4.10 - 4.16)

where the HRSG model is represented by Eq. (4.23), the steam turbine model is represented by Eqs. (4.24), (4.25), and (4.26), the boiler model is represented by Eqs. (4.27) and (4.28), the steam adsorption chiller model is represented by Eqs. (4.29) and (4.30), and the electric chiller model is represented by Eqs. (4.31) and (4.32). The gas turbine model (Eqs. (4.20), (4.21), and (4.22)) was simplified from the original model (Section 3.3.1) by assuming a constant efficiency, ignoring the effect of running the gas turbine at partial load on the efficiency. The simplification made a McCormick relaxation to linearize the model unnecessary, allowing the lower bound of the fuel consumption to be zero. By assuming the constant efficiency equal to the maximum efficiency based on the outdoor temperature, the gas turbine would always be running with the minimal amount of fuel necessary to meet a certain power output, maintaining a lower bound solution from the upper level optimization.

With this upper level formulation, a lower bound solution, Z^{UL}, can be found that minimizes the design with a relaxed scheduling of the equipment. The solutions to the CHP plant equipment in the plant design, $\overline{U}_{e,s}$, and the sizes of the energy storage devices, $\overline{L}_b^{max}$, can then be passed on to the lower level to capture a more accurate representation of the plant dynamics and operational cost.

4.8.2 Lower Level Problem

The goal of the lower level (LL) problem is to accurately capture the operational dynamics and costs (i.e., fuel, startup penalties, etc.) of the CHP plant using more complex models of the equipment with discrete operating modes. To obtain this objective, the full models of the CHP plant equipment and energy storage as well as their operating constraints are included in the optimization, which is limited to the "preselected" equipment determined in the upper level problem ($\overline{U}_{e,s}$ and $\overline{L}_b^{max}$), resulting in fewer possible combinations of equipment operation. With the equipment already selected and sized, the natural break in utility demand dynamics in the early morning can be utilized so each day of residential energy demand can be scheduled individually, decreasing the lower level computation time.

To solve the lower level optimization, each day is solved individually to

obtain an upper bound solution (Z_d^{LL}):

$$Z_d^{LL} = \min \quad \frac{1}{D}\left(Capital + Y \times Main_1\right) + Y\left(\tau_d \times \left(Fuel_d + Main_{2,d} + Trans.Pen._d\right)\right) \quad (4.33)$$

subject to cost calculations (Sections 4.6.3 and 5.5.2), non-relaxed CHP plant equipment models (Section 3.3), energy storage models (Section 4.4.1), equipment operating constraints (Section 3.4.2), and energy demand balances (Section 4.7.1). Summing all of the days optimized will give the final upper bound solution, Z^{LL}:

$$Z^{LL} = \sum_{d=1,\ldots,D} Z_d^{LL} \quad (4.34)$$

4.8.3 Integer Cuts

To help direct the upper level problem to select the optimal equipment design based on the lower level scheduling, integer cuts are added to the upper level for each iteration, until a certain tolerance, η, between the global upper and lower level solutions is reached. One of the simpler, weaker integer cuts that has been used to remove one solution from the upper level [143–145] is:

$$\sum_{e,s \in Y_1^i} U_{e,s} - \sum_{e,s \in Y_0^i} U_{e,s} \leq |Y_1^i| - 1 \quad (4.35)$$

where i is the iteration, $Y_0^i = \{e, s | \overline{U}_{e,s}^i = 0\}$, and $Y_1^i = \{e, s | \overline{U}_{e,s}^i = 1\}$. The sets pertaining to $\overline{U}_{e,s}$ are obtained from the upper level solution, where the binary design variables are selected. While this integer cut is safe and can be applied if the lower level solution is feasible or infeasible, the number of

iterations needed to solve the total problem can be large, because Equation (4.35) only removes one possible equipment combination from the upper level problem.

One possible way to decrease the number of equipment combinations and thus decrease the number of iterations, is to apply a cover cut [146, 147] to the upper level formulation:

$$\sum_{e,s \in Y_1^i} U_{e,s} \leq |Y_1^i| - 1 \tag{4.36}$$

This cut removes the upper level equipment selection of iteration i, as well as any supersets (i.e., any additional equipment to the equipment already selected). The downside of using this tight cut is the possibility of missing a better solution, especially if the cut is applied to a plant design that is infeasible and unable to meet all utility demands.

While both of these cuts have their weaknesses, their strengths can be used in combination to create a hybrid cut method for the bilevel decomposition, that utilizes the weak cut's ability to remove only one exact solution and the cover cut's ability to remove any supersets. If an upper level equipment selection leads to an infeasible solution where all the utility demand is not met, the integer cut (Equation (4.35)) is used to prevent the same exact design from happening again, but allows for additional equipment to be added to the original design so the demand can be met. On the other hand, if the upper level equipment selection leads to a feasible solution, adding another piece of equipment would only increase the total cost of the plant, since the

capital cost is greater than the fuel cost. Thus, a cover cut (Equation (4.36)) can be used to remove the plant design and and any supersets from the upper level problem.

4.8.4 Algorithm overview

Using the algorithm depicted in Figure 4.3, the simultaneous optimization of the design and operation strategies can be solved to a specific tolerance, ε. First, the iteration is initialized, and the upper level problem is solved to obtain a lower bound solution, Z^{UL}. If the current upper level solution at iteration k is greater than the global upper level solution, G^{UL}, the global upper level solution is updated. Next, using the selected CHP plant equipment, when $U_{e,s} = 1$, and the selected sizes of the energy storage devices (L_b^{max}), the lower level scheduling problem is solved for each day individually, and the individual day results are summed together to obtain the total lower level solution, Z^{LL}. If Z^{LL} is infeasible, then an integer cut is added to the upper level problem, and the algorithm continues onto the next iteration. If Z^{LL} is feasible and the current lower level solution is less than the global lower level solution, G^{LL}, then $G^{LL} = Z^{LL}$. Next, the difference between the global upper bound solution (G^{LL}) and the global lower bound solution (G^{UL}) is taken, and if it is less than the tolerance, the bilevel decomposition is done. Else, a cover cut is added to the upper level formulation, and the algorithm continues onto the next iteration.

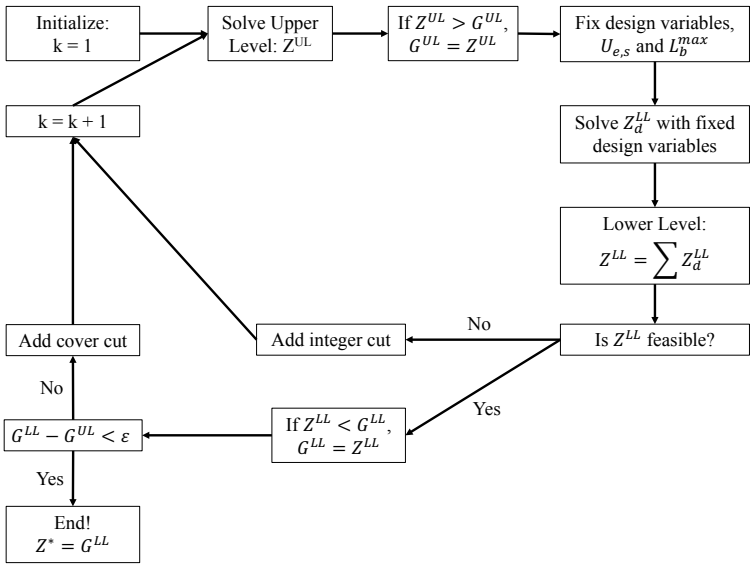

Figure 4.3: Schematic of the algorithm used to solve the simultaneous optimization of design and operational strategies.

4.9 Case Study

To determine the economic effect of rooftop PV generation and energy storage on the design and operation of a residential CHP plant, the bilevel decomposition algorithm to solve the simultaneous optimization of design and operational strategies was implemented. This consisted of running two scenarios: 1) Design and operation of a CHP plant (without energy storage), and 2) Design and operation of a CHP plant with energy storage. Each of the scenarios was analyzed for differences in cost, design, and operation, and rooftop PV generation was added to a separate scheduling of the plant design to determine if/when it would become economical.

Using energy demand and PV generation data from the Mueller neigh-

Optimized Day	τ_d
Minimum Energy	1
Spring Average	83
Summer Average	112
Maximum Energy & Electricity	1
Maximum Cooling	1
Autumn Average	83
Maximum Heating	1
Winter Average	83

Table 4.1: Scaling parameter used for each day d optimized.

borhood in Austin, Texas (as described earlier in Section 4.7.3), eight days were selected to capture the uncertainty in residential energy demand, and to determine the yearly operational cost of the plant.

With the days of data selected, the data were separated to allow easier scheduling in the lower level optimization, without interrupting the equipment dynamics (i.e., the equipment does not switch modes). From previous work of scheduling a CHP plant for a residential neighborhood, it was observed that the equipment did not switch modes between 2 am and 5 am [16, 72]. Thus, it was decided to break the demand data into eight pieces, using the natural break in equipment dynamics at 3 am as a separation point (which is why the demand in Figure 3.6 is graphed from 3 am - 2am). The scaling parameters for the daily costs, τ_d,are shown in Table 4.1.

The algorithm was run with $\varepsilon = 10,000$ and solved with GAMS 24.4.6 using the commercial solver CPLEX (12.6.2.0) on a PC Intel Core i7, 3.40 GHz, 16 GB RAM, 64 bit and Windows 10.

4.9.1 Scenario 1: CHP plant (no energy storage)

4.9.1.1 Optimal CHP plant design

Utilizing the bilevel decomposition method, a final solution with approximately 1% gap was reached in 8 hours (2,700 iterations). The optimal plant equipment selected by the optimization included two gas turbines (10 MW and 15 MW) with two heat recovery steam generators to generate electricity and steam, and two electric chillers (57 MBtu/h and 172 MBtu/h) to provide cooling for the neighborhood (Figure 4.4). Overall, the capital cost of the equipment totals $52,418,998.

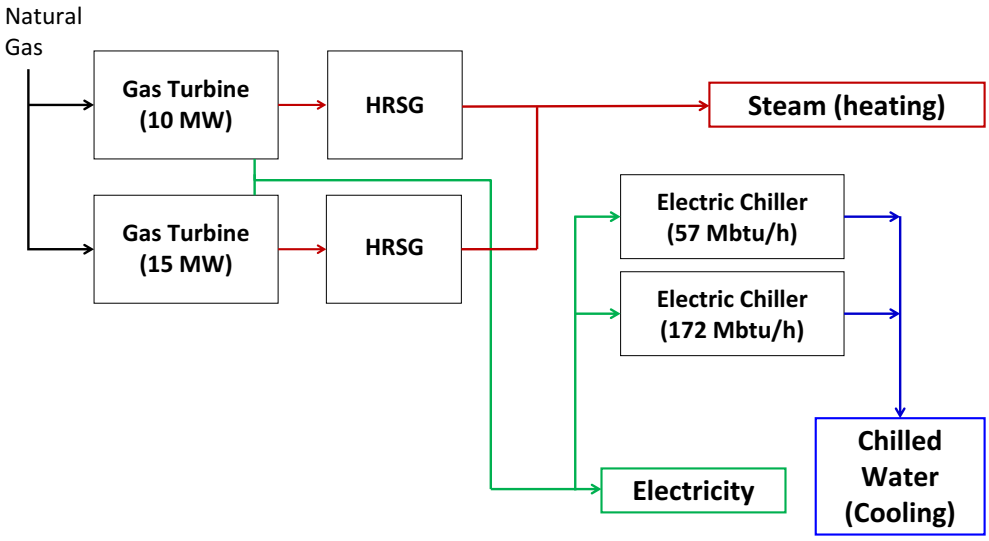

Figure 4.4: The optimal equipment to be included in a CHP plant to meet the utility demands for a residential neighborhood.

4.9.1.2 CHP plant operation

In addition to determining the optimal equipment and sizes of the equipment, the optimization determined the optimal operational strategy of the equipment to meet the heating, cooling, and electricity of the residential neighborhood, taking into consideration the maintenance fees, fuel costs, and start-up time, and transition penalties from turning on the equipment. Over a period of twenty years, the expected lifetime of the plant, the plant would pay $48,336,109 for natural gas to power the gas turbines, $14,904,333 for the maintenance on all equipment, and $1,697,000 for turning on the equipment.

Concentrating on electricity generation shown in Figure 4.5 (where Spr(1): Minimum anergy, Spr(2): Spring average, Sum(1): Summer average, Sum(2): Maximum energy and electricity, Sum(3): Maximum cooling, Aut(1): Autumn average, Win(1): Maximum heating, and Win(2): Winter average), the optimization found it economical to turn the larger 15 MW gas turbine only in the summer. While two of these summer days are used to account for uncertainty (Sum(2) and Sum(3)), the average summer day (Sum(1)) still needs the two gas turbines and thus will be used for many days, considering how long the Texas summer season can be. While the electricity generation is still greater than the demand, the extra electricity in the spring, summer, and autumn is being used to power the electric chillers to meet the cooling demand.

In terms of cooling equipment, only the electric chillers were found to be economical to generation cooling for the residential neighborhood. This is

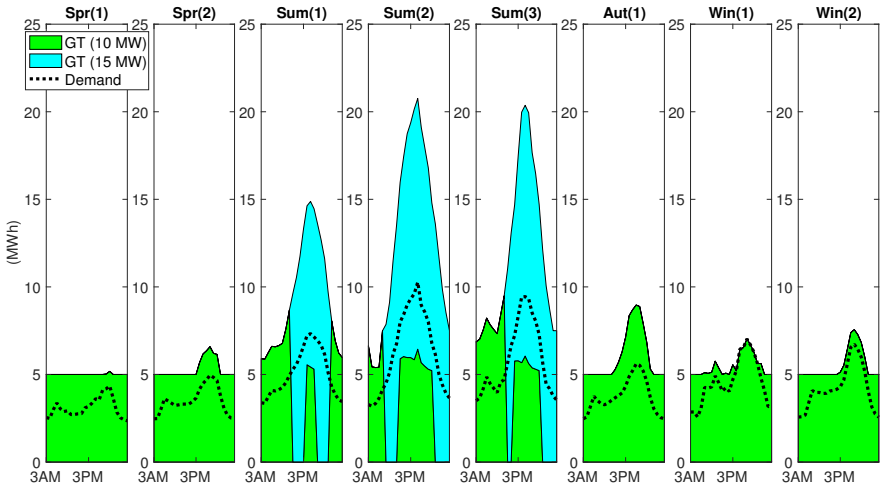

Figure 4.5: While all electricity demands (neighborhood and electric chillers) can be met in the spring, autumn, and winter with just one gas turbine, two gas turbines are needed in the summer to meet the electricity demand during peak hours.

not a big surprise, considering the electric chillers are over two times more efficient compared to the steam adsorption chillers. Similar to the gas turbine selection, two electric chillers (EC(1) - 57 MBtu/h and EC(2) - 172 MBtu/h) were selected to meet the cooling demand (Figure 4.6). In the summer months, the larger electric chiller is used at almost all hours, and both chillers are needed to meet the cooling demand when the electricity generation and total energy demand is at its highest for the year (Sum(2)) and on the day with the maximum amount of cooling (Sum(3)). On the other hand, in the spring when cooling demand is low, only the smaller electric chiller was used. Lastly, due to the equality constraint in the electricity balance (i.e., the electricity generated must be consumed), the only way to "consume" extra electricity generation is

to power the electric chiller so the generated cooling can either be consumed by the residential neighborhood, or be dissipated into the environment. In the spring and winter months, the electricity demand is less than the minimum capacity of the small gas turbine, so the extra electricity is sent to the electric chillers. In the spring, part of the chilled water is consumed by the residential neighborhood, with the rest being released into the air. However, in the winter, there is no cooling, so all of the excess energy is lost, leading to a loss in overall plant efficiency.

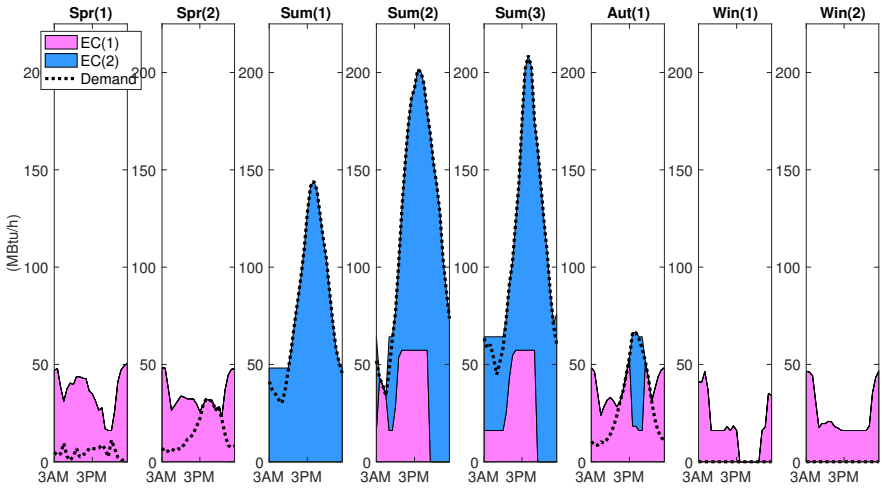

Figure 4.6: All of the cooling demand is met by the electric chillers, where EC(1) is the 57 MBtu/h chiller and EC(2) is the 172 MBtu/h chiller.

With the warmer weather in Austin, Texas, the heating demand is much less, compared to the cooling and electricity demand (Figure 4.7). The steam generated from the gas turbines' exhaust via the HRSGs by far exceeds the the heating demands of the residential neighborhood, even on the day with the

most heating (Win(1)). Thus, no additional pieces of equipment are needed in the plant to help meet the residential heating demand.

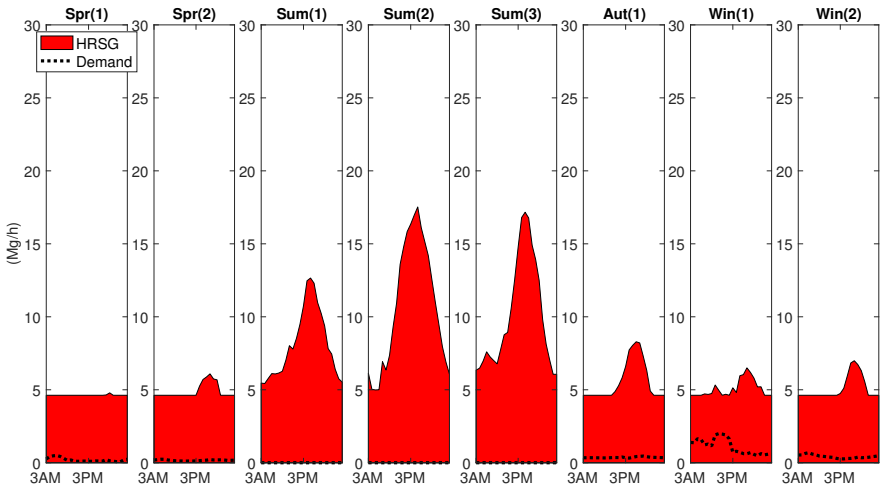

Figure 4.7: The steam generation produced by the HRSGs is much greater than the demand.

4.9.1.3 CHP plant operation with PV generation

Once the optimal design and operation of the CHP plant without energy storage had been determined, PV generation was added to the electricity balance (Equation (4.13)) as a source of energy for the neighborhood. By optimizing the operation of the CHP plant with PV generation, the operational savings could be compared to the price of rooftop PV generation to determine if/when this technology will be economical. Using the equipment shown in Figure 4.4, the lower level problem (Section 4.8.2) was solved. In a twenty year life-span, the plant would pay $45,892,564 for natural gas, $14,099,433

for maintenance, and $1,196,000 for turning on the equipment. Overall, the operational savings from investing in rooftop PV panels for the whole neighborhood would be around 4.5 million dollars.

All of the operational savings from adding PV generation come from the decreased amount of electricity that needed to be generated by the gas turbines (Figure 4.8). This is easier to notice in the three summer days (Sum(1), Sum(2), and Sum(3)), where the latter half of the PV generation coincides with the early half of the electricity demand peak. There would be more value to the PV generation and less use of the gas turbines if the PV peak aligned better with the electricity demand, especially in the spring and autumn when there is more solar generation. This highlights the need for some sort of energy storage for the extra PV generation in the off-peak hours.

The cooling generation, shown in Figure 4.9, was greatly affected by the addition of PV generation. In the summer months, the chilled water is generated by the electric chillers to exactly match the cooling demand. However, the PV generation added an additional peak of extra electricity in the spring, autumn, and winter. This extra electricity had to be used somehow so that the amount of electricity generated equaled the amount of electricity used. Thus, during peak PV generation hours, the electric chillers had to be run to dispense of the extra energy.

Since the HRSG steam production is tied to the gas turbine operation, whenever there was a reduction in gas turbine power due to PV generation, the HRSG steam production also decreased (Figure 4.10). However, because the

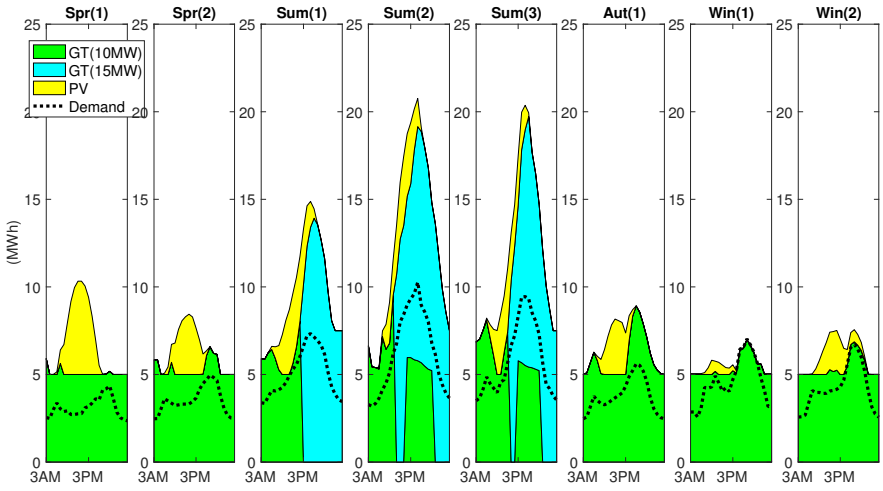

Figure 4.8: Most electricity demand can be met with just one gas turbine and PV generation, but the summer requires both gas turbines in combination with PV generation.

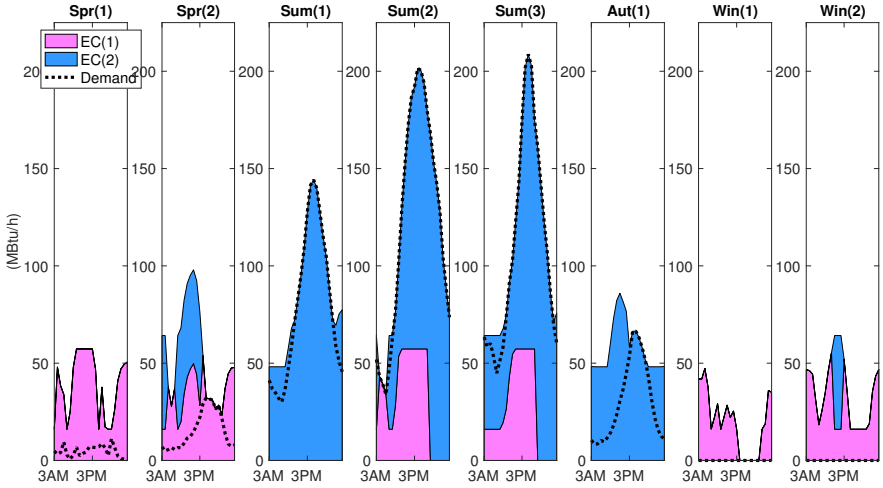

Figure 4.9: All of the cooling demand is met by the electric chillers operating, but extra electricity when PV generation is present led to over generation of chilled water.

steam production is still much higher than the neighborhood steam demand, the effect of PV generation on heat demand is nonexistent.

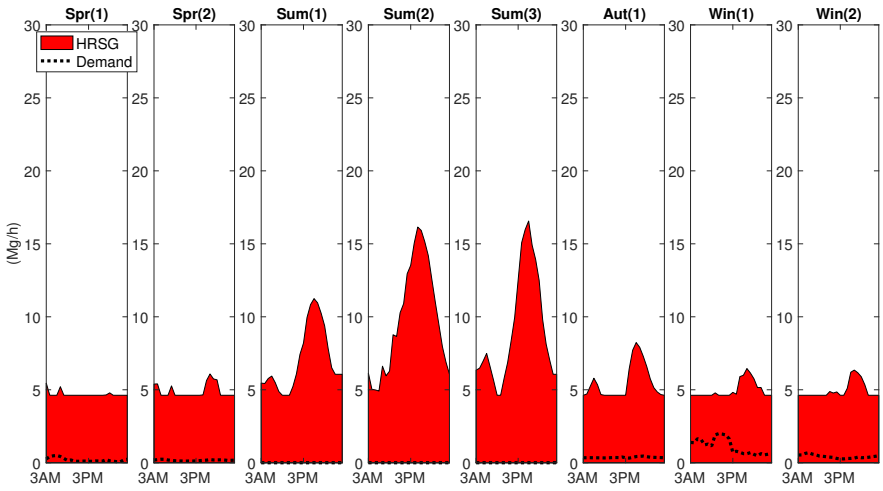

Figure 4.10: The steam generation produced by the HRSGs, when the CHP plant is scheduled with PV generation, is greater than the demand.

With the slight changes to the operation of the CHP plant equipment, as shown previously, the plant can be expected to save around $3,750,000 in operation costs over a period of 20 years. Comparing this to the predicted cost of $33,000,000 for the rooftop PV panels for the neighborhood (assuming a future price of $1.00/watt [148] with a 6 kW per house [149]), PV panels are currently not economic. However, the PV panel economics could improve if there were some way to store the extra PV generation that is not generated during peak utility hours.

4.9.2 Scenario 2: CHP plant with energy storage

4.9.2.1 Optimal CHP plant design with energy storage

The next step in the case study was to determine the most economic method of energy storage considering the uncertainty and variability in residential utility demand as well as determine the effect of energy storage on the CHP plant design and operation. The addition of energy storage has the potential to decrease the peak in utility generation in the evening as well as store the extra PV generation in the afternoon, seen in the scheduling of the electricity generation in Figure 4.8.

The bilevel decomposition method was used to simultaneously determine the optimal plant design, the type and size of energy storage (lithium-ion battery, flow battery, and thermal energy storage), and the operation of the plant with the selected energy storage devices. In 12,675 iterations taking approximately 75 hours, a solution with a tolerance of 5% was obtained. The optimal equipment, shown in Figure 4.11, includes two gas turbines to generate electricity, two electric chillers to generate chilled water, and a 2.2 million gallon TES tank to store the chilled water. The total capital cost for the equipment and TES tank is $44,274,440.

4.9.2.2 CHP plant operation with energy storage

Using the scheduling solution from lower level of the bilevel decomposition, the minimum operational cost for the plant to meet the neighborhood utilities was calculated. Over a period of twenty years, the plant would pay

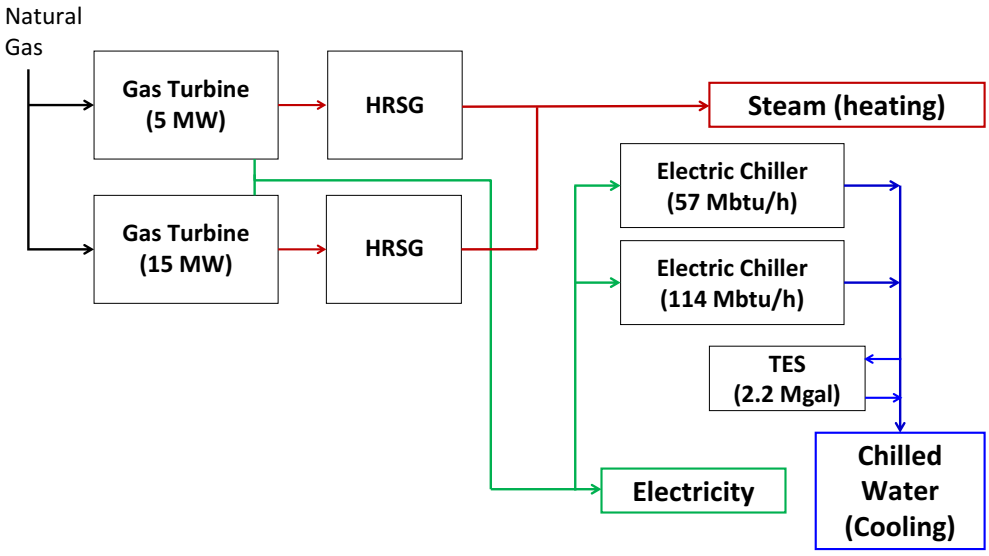

Figure 4.11: The optimal equipment, with thermal energy storage, to be included in a CHP plant to meet the utility demands for a residential neighborhood.

$42,423,539 for natural gas to power the gas turbines, $13,357,467 for the maintenance on all equipment, and $4,563,000 for turning on the equipment.

As shown in Figure 4.12, due to the smaller size of the 5 MW gas turbine, the larger 15 MW gas turbine is needed on all but one day to meet the peak in electricity demand from the neighborhood and electric chillers. The need for both gas turbines has led to an increase in turning on and off the equipment, preventing decreased gas turbine efficiency and over-production of electricity. This caused a high penalty for turning on the equipment, which is over $2 million for the lifetime of the plant for this scenario. However, with the 5 MW gas turbine, the electricity generation profile does better match the utility demand, and there is less time when the gas turbines are running flat

at their minimum capacity, possibly wasting fuel and electricity. Also of importance in the electricity generation results is the decrease in peak electricity generation. Comparing these results to those when the plant is designed without energy storage (Figure 4.5), the peak electricity generation has decreased by several MW in the summer. This can be attributed to the TES, which has decreased the electric chiller loads during peak electricity demand hours.

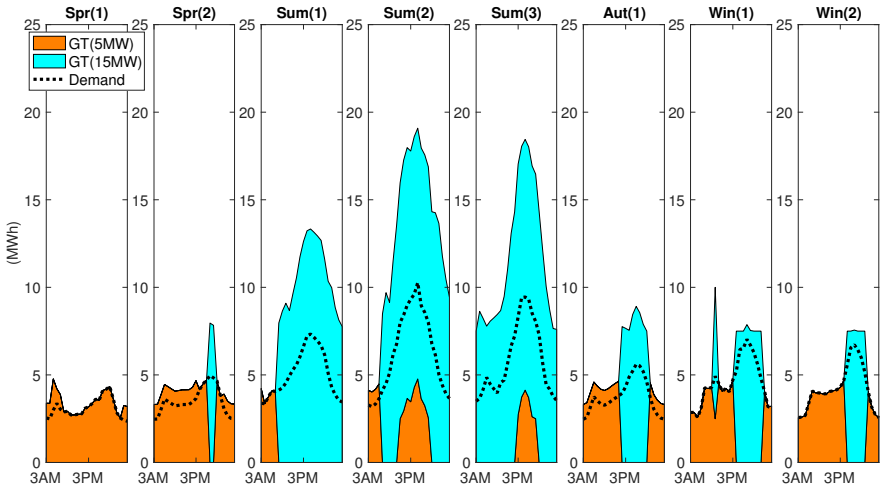

Figure 4.12: Most electricity demand can be met with just one gas turbine, but the summer electricity and cooling peak demands require both gas turbines to generate electricity for the neighborhood electricity demand and electric chillers.

The effects of the 2.2 million gallon TES are more apparent in the scheduling of the chilled water generation (Figure 4.13). Both gas turbines are needed only in the summer on the extreme demand days (Sum(2): Maximum energy and electricity, and Sum(3): Maximum cooling) when the cooling demand high, while one gas turbine is able to meet the cooling demand for all

other days. The TES tank level follows a similar path on all days, where it loads in the morning when electricity and cooling demand are low. The storage is then used in the afternoon/evening when electricity demand and cooling are both high. By operating in this manner, the electricity generated during peak hours is less, which was seen in Figure 4.12. At one point, on the minimum energy day (Spr(1)), the thermal energy storage is able to meet all of the cooling demand during the day so the only electricity needed by the electric chiller is in the early morning when the TES tank is being loaded. With TES, part of the peak in cooling generation can be shifted to the morning, allowing part of the electricity generation for the electric chillers to be shifted to the morning during non-peak electricity hours. This corresponds to economic savings from purchasing smaller capacity equipment and generating less "un-used" energy.

Unfortunately, even with the TES unit, there is still a loss of overall plant efficiency in the winter. Due to the equality constraint on power generation, all excess electricity is sent to the electric chillers to be dispensed as thermal energy in the form of cooling. This cooling, which is used to help meet the cooling demand in the spring, summer, and autumn, can only be released into the environment in the winter when there is no cooling demand. Due to the high capital cost of the battery storage units, the optimization found it more economic to suffer a loss of efficiency, over purchasing a battery unit.

Due to the smoother generation of electricity by the gas turbines through the day, the HRSG steam generation has also become more level. The peaks in steam generation in the summer are far less severe, and the spring steam

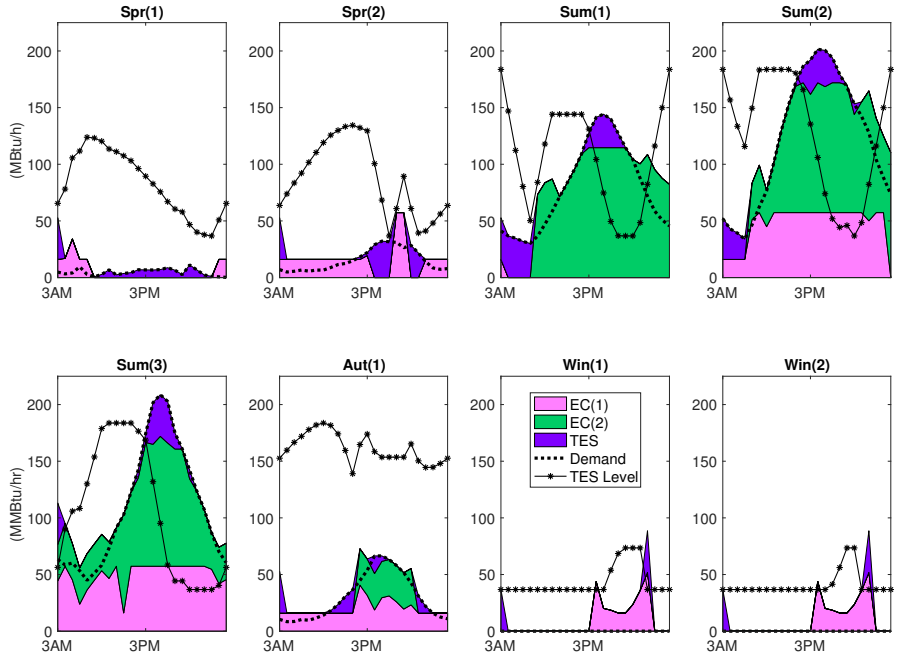

Figure 4.13: The thermal energy storage, loaded in the morning and early afternoon when electricity and cooling demands are low, is used to minimize the electric chiller generation in the evening during peak electricity and cooling hours. EC(1) is the 57 MBtu/h chiller and EC(2) is the 114 MBtu/h chiller.

generation has decreased because the smaller gas turbine can now reach lower levels of electricity generation. Because the steam generation is greater than the steam demand from the neighborhood, the TES only effected the gas turbine/HRSG schedule through electricity and cooling generation, and not heat generation. Also, the smallest amount of steam generated by the HRSGs, when the smallest gas turbine is running at minimum power, is more then the maximum amount of heat needed by the neighborhood. The steam genera-

tion will only be greatly influenced if during some period, a gas turbine is not needed to provide electricity.

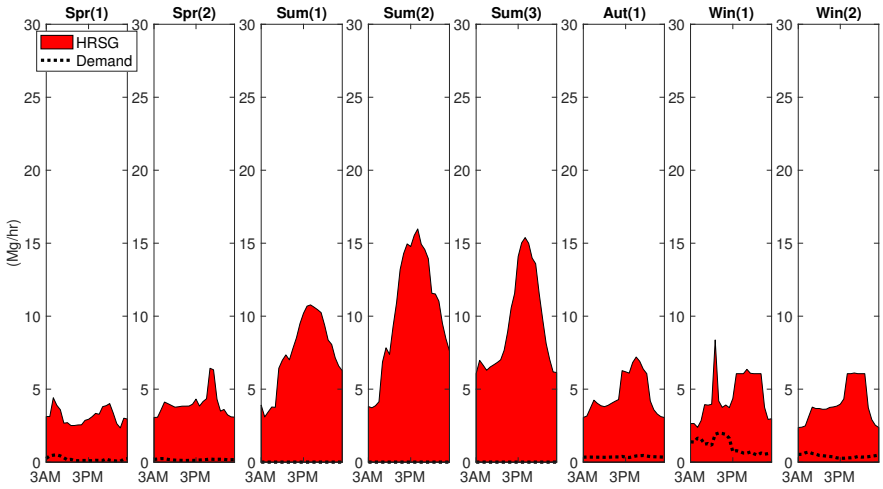

Figure 4.14: The steam generation produced by the HRSGs, when the CHP plant is optimized with energy storage, is greater than the demand.

4.9.2.3 CHP plant operation with PV generation

With the CHP plant design with energy storage determined by the bilevel decomposition, PV generation was added to the electricity balance (Equation (4.13)) as a source of energy for the neighborhood. The plant and energy storage were scheduled using the full-scale scheduling contained in the lower level of the bilevel decomposition. In a twenty year life-span, the plant would pay $37,194,251 for natural gas, $11,569,130 for maintenance, and $4,735,000 for turning on the equipment. Overall, the operational savings from investing in rooftop PV panels for the whole neighborhood would be around

seven million dollars.

Adding the PV generation the CHP plant with TES decreases the amount of electricity generated by the gas turbines in the afternoon and early evening, during peak electricity demand hours (Figure 4.15). The PV generation created larger amounts of excess electricity generation in the spring and winter, forcing the extra electricity to be sent to the electric chillers. However, most of this extra electricity, especially in the spring, is able to be incorporated into the cooling scheduling via the TES tank.

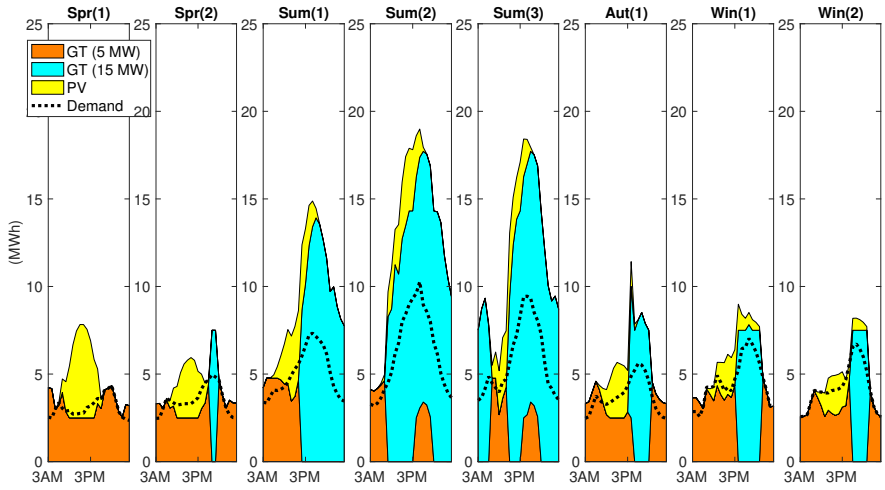

Figure 4.15: On almost all days, both turbines are needed during the day to meet the electricity demand for the neighborhood and electric chillers.

While there does seem to be extreme over generation of electricity in the spring due to the minimum capacity of the 5 MW gas turbine and the PV generation, a majority of this electricity is being used to load the TES

tank, as shown in Figure 4.16. In the spring and autumn, the PV generation peak in the afternoon does not overlap with the cooling demand peak in the evening. Having the extra electricity from the rooftop PV in the afternoon shifts the loading of the TES tank with chilled water from the early morning (in Figure 4.13) to the afternoon, when the PV generation is available. In the summer, when the maximum PV generation is closer to the peak electricity and cooling demands in the evening, the chilled water is used in the early afternoon when there will be more than enough electricity in the early evening (Sum(1) and Sum(2)), or is used in later evening when the cooling peak is still extremely high but rooftop PV generation is not available (Sum(2) and Sum(3)). Unfortunately, in the winter, the excess electricity generation is sent to the electric chillers so that the extra energy can be dispensed to the environment, leading to a loss of overall plant efficiency.

Lastly, because the gas turbine generation decreased when PV generation was added, the associated steam generation from the HRSG also decreased. However, the decrease in steam generation is always more then the heat demand of the neighborhood.

With the inclusion of TES to store extra electricity in the form of chilled water, the plant can be expected to save around $7,000,000 in operation costs over a period of 20 years. Comparing this to the predicted cost of $33,000,000 for the rooftop PV panels for the neighborhood, PV panels are currently not economic, but are more economic when energy storage is included in the CHP plant.

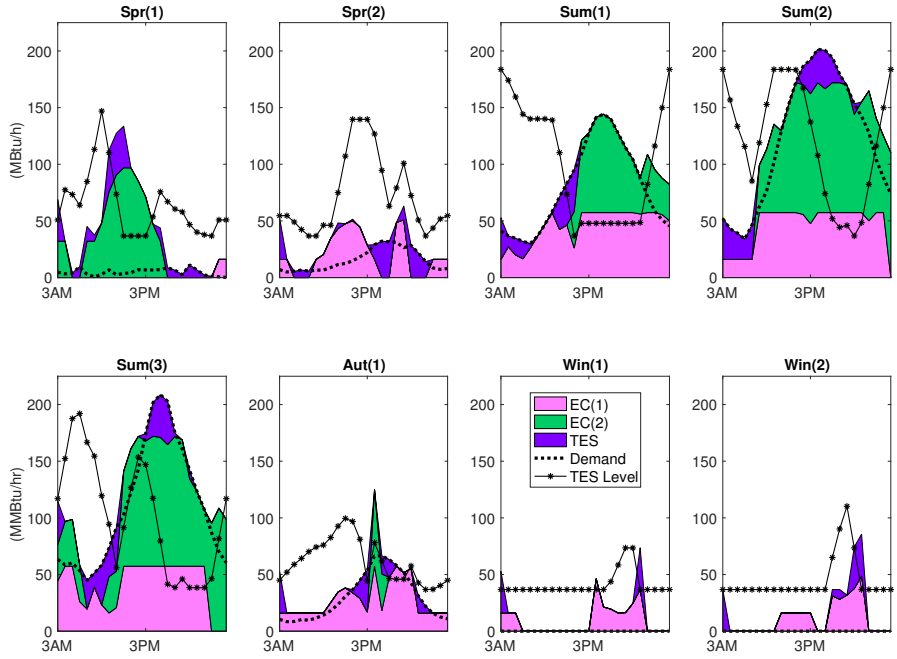

Figure 4.16: With the addition of PV generation to the CHP plant with TES, the TES is usually loaded in the afternoon when PV generation is present, so the chilled water can reduce the electric chiller loads in the evening.

4.9.3 Summary of case study

After analyzing the total costs for the different CHP design scenarios (Table 4.2), the most economic design and operation of a CHP plant to meet the heating, electricity, and cooling demands of a residential neighborhood was found to be when the CHP plant is optimized with energy storage and does not include PV generation. While the cheapest case in terms of operation is when PV generation is added to the CHP plant with TES, the capital cost of the rooftop PV panels for the entire neighborhood makes the case economically

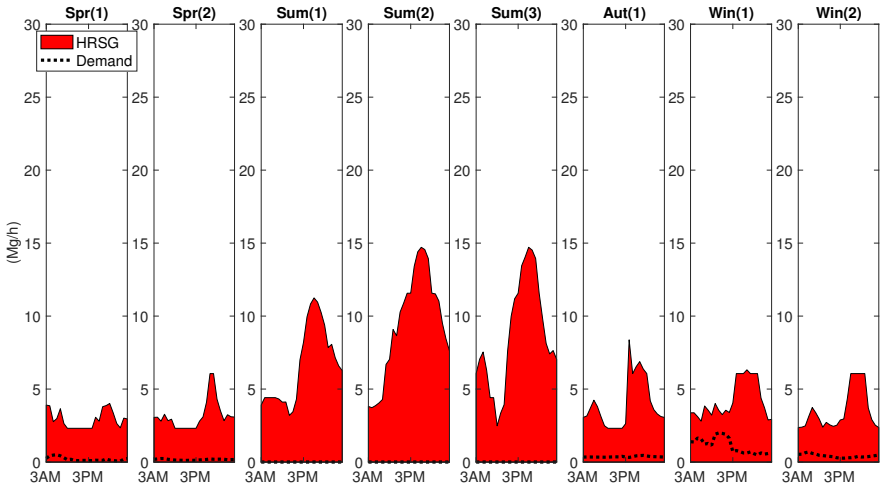

Figure 4.17: The steam generation produced by the HRSGs, when the CHP plant is optimized with energy storage and scheduled with PV generation, is greater than the demand.

disadvantageous. However, looking past the capital cost of the rooftop PV panels, the most value, in terms of operational savings, from PV generation comes when there is some sort of storage available to store electricity in the afternoon and use it later during peak demand hours.

	CHP		CHP and Energy Storage	
	No PV	With PV	No PV	With PV
Capital	$52,419,000	$85,418,998	$44,274,440	$77,274,440
Fuel Cost	$48,336,109	$45,892,564	$42,423,539	$36,791,370
Maintenance	$14,904,333	$14,099,433	$13,357,467	$9,900,600
Penalties	$1,697,000	$1,196,000	$4,563,000	$2,818,000
Total	$117,356,440	$147,606,995	$104,618,446	$130,772,821

Table 4.2: Summary of total plant costs with and without energy storage and PV generation.

4.9.4 Sensitivity Analysis

While the results of the case study study showed that energy storage, in the form of chilled water, is economical for a residential-level CHP plant with district cooling, the results also demonstrated the need to decrease the cost of battery storage. Even though lithium-ion batteries are more efficient than thermal energy storage, their capital cost per unit of energy stored is much greater, preventing the batteries from being selected as an energy storage method. However, with the research being conducted on batteries, the cost can be expected to decrease in the near future. Some researchers predict the cost of lithium-ion batteries to decrease to $217 per kWh by 2020 [150] and possibly as low as $150 per kWh by 2030 [151]. Thus, a sensitivity analysis was conducted to determine when lithium-ion batteries become economical in a natural gas fired CHP plant that provides utilities to a residential neighborhood.

Utilizing varying lithium-ion battery prices between the original quoted price of $622/kWh and $5/kWh, the bilevel decomposition used to solve the simultaneous optimization of the design and operation of a CHP plant with energy storage. Unfortunately, in all scenarios, TES was found to be a more economical than lithium-ion batteries, and the lithium-ion battery was never selected as an energy storage method.

So to help determine when batteries will become economical, TES was removed as an option of energy storage for the optimization. Again, the price of lithium-ion batteries was tested in a range of $5/kWh to $622/kWh, and it was found that a lithium-ion battery is economical at some point between

$5 - $10/kWh. For example, at a price of $5/kWh, the optimization chose to install a 5.45 MWh lithium-ion battery in the CHP plant. As shown in Figure 4.18, the lithium-ion battery (abbreviated as LI), is loaded in the morning when demand is lower, and the battery is drained to its minimum capacity in the evening during peak hours. Once PV generation was added to the electricity generation mix (Figure 4.19), the lithium-ion battery was loaded both in the morning and in the afternoon when PV generation was present. Incorporating electrical energy storage shifted electricity generation from peak hours to non-peak hours, and helped to synchronize PV generation with peak electrical demand.

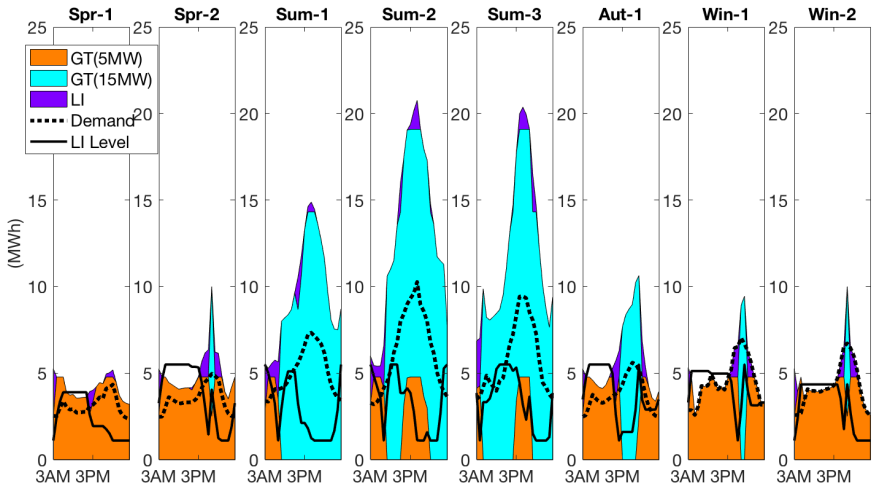

Figure 4.18: With the addition of a lithium-ion battery in the CHP plant, electricity that would normally be generated during peak hours can now be generated in the morning, when utility demands are low.

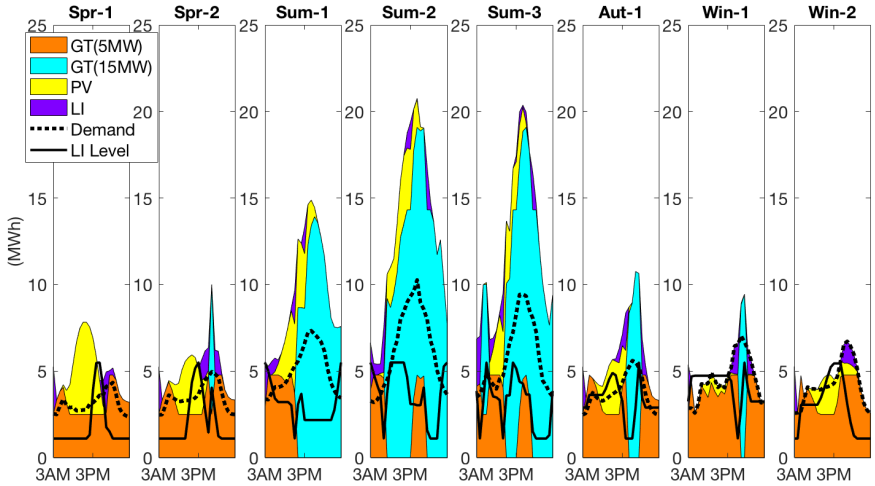

Figure 4.19: A lithium-ion battery can be used to store PV generation, so that it can be utilized later in the day during peak demand hours.

4.10 Validation of Integer Cuts

In order to verify the validity of the integer cuts, the simultaneous optimization of the design and operation strategy of the CHP plant was solved with both the Lagrangean and bilevel decompositions. If the bilevel decomposition solution is equal to or smaller than the Lagrangean decomposition, then the cuts in the bilevel decomposition are not too aggressive. Overly aggressive cuts would eliminate paths to the optimal solution, causing the solution to be sub-optimal.

Analyzing the two methods and their solutions, the bilevel decomposition converged to a better solution, $117,356,440, in a shorter amount of time, 7.25 hours, compared to the Lagrangean decomposition solution, which

converged to a value of $118,362,140 in 46 hours. This higher cost, created by the addition of another piece of equipment, is most likely due to the 2% tolerance for the Lagrangean decomposition, which prevented the problem from solving to a lower solution. If a smaller tolerance had been selected for the Lagrangean decomposition, the optimization would not have included the steam adsorption chiller in the CHP plant design, which is not necessary to meet the neighborhood cooling demand (Figure 4.20). However, a smaller tolerance for the Lagrangean decomposition would mean an even longer computation time, which already takes over 6 times longer to solve than the bilevel decomposition. With the bilevel decomposition, the upper level formulation vastly reduced the number of binary variables by eliminating equipment operating modes, and the lower level had a smaller number of scheduling nodes to solve because the equipment was pre-selected. This reduction in problem size and complexity helps the bilevel decomposition to solve quickly. On the other hand, even though the Lagrangean decomposition can optimize each day individually, each day still requires a design and scheduling solution, which increases the number of binary variables and possible solution nodes, causing the optimization to take longer. While both methods are able to obtain a valid solution to the design and operation optimization, the bilevel decomposition by far exceeds the Lagrangean decomposition for this case.

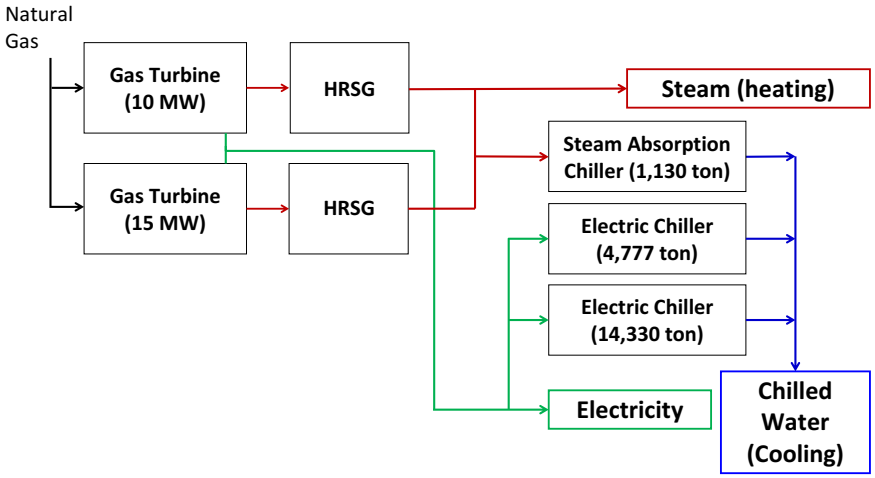

Figure 4.20: CHP plant design without energy storage, solved using the Lagrangean decomposition method from the previous chapter.

4.11 Conclusions

In conclusion, we have successfully implemented a bilevel decomposition to optimize the design and operational strategy for a CHP system with energy storage to meet the heating, cooling, and electricity demands of a residential neighborhood. Incorporating the variability and uncertainty of residential energy demand and PV generation data from Austin, Texas, we determined that the most valuable for this scenario is a 2.2 million gallon thermal energy storage tank. Rooftop PV panels in the whole neighborhood has the potential to save around $3,750,000 without energy storage, or $7,000,000 with thermal energy storage. However, the the current high cost for rooftop PV panels makes the panels economically disadvantageous.

Chapter 5

The Economic Impact of Integrating a Mid-sized CHP Plant into the Power Grid

5.1 Introduction

In the past two chapters, methodologies were developed to simultaneously optimize the design and operation of a CHP plant with PV generation to meet all of the energy demands of a residential neighborhood, as well as determine the best type and size of energy storage to be incorporated into the CHP plant. For these optimizations, the CHP plant was assumed to be operating in island mode at all hours, i.e., completely disconnected from the grid. This assumption greatly simplified the optimization by removing several factors of uncertainty (e.g., electricity prices), making the problem easier to solve. However, forcing the CHP plant to meet all neighborhood energy utilities may not be the best economic or logical decision for the CHP plant and the residents. In addition to possibly improving the utility generation economics, connecting the CHP plant to the grid can provide the plant and neighborhood with many additional benefits, such as increased reliability (the ability of the grid to be able to meet demand and withstand sudden planned/unplanned disturbances), increased flexibility (to diversify the fuel and energy generation sources), decreased energy costs, and increased competition [152].

While there are many benefits to having an expansive, interconnected grid, the potential value of a grid connection can vary based on the level of implementation in the grid (i.e., at the level of the NERC, ERCOT, load zones, resource nodes, individual generators, individual consumers, etc.). Because the natural-gas fired CHP plant with PV generation is an individual generator for the single residential neighborhood, and the optimizations used in the previous chapters were economic, this chapter will concentrate on determining the economic value of connecting the CHP plant to the grid. Thus, the question to be answered by this research is: *What is the economic impact of integrating a CHP plant with rooftop PV generation, a sole provider of energy to a residential neighborhood, into the power grid?*

Motivated by this this question, a moving horizon scheduling is developed and implemented to study the hourly impact of the ERCOT day ahead market on the plant operation. Using the optimal CHP plant design with rooftop PV generation and energy storage from Chapter 4, a data-based model for energy demand in a residential neighborhood, and day ahead market settlement price points from ERCOT, the CHP plant operation is scheduled daily to incorporate newly published electricity prices. With two weeks of electricity prices and energy demand models, one week from the winter and one week from the summer, the estimated energy savings from connecting the CHP plant to the grid can be calculated and compared to the results when the CHP plant is operated in island mode.

5.2 CHP Plant Model

The design for the CHP plant used in the moving horizon scheduling is shown in Figure 5.1. The plant includes two gas turbines (5 MW and 15 MW) to provide electricity, two heat recovery steam generators (HRSGs) to produce steam for heating, two electric chillers (4,777 ton and 9,500 ton) to generate chilled water to cool the homes, and a 2.2 million gallon thermal energy storage (TES) tank to store chilled water. PV generation, from the rooftop panels in the neighborhood, is available to the plant as a source of electricity that can either be used to help meet the neighborhood electricity demand, be used to power the electric chillers, or be sold to the grid. The plant design is taken from Chapter 4, when a bilevel decomposition was used to solve the simultaneous optimization of the design and operational strategy of the CHP plant with energy storage.

The models of the equipment in the plant are the same as described earlier in Sections 3.3.1,3.3.2, and 3.3.6 for the gas turbines, HRSGS, and electric chillers, and Section 4.4 for the TES tank.

5.3 Equipment Operation and Constraints

To accurately capture the dynamics and behavior of the equipment in the CHP plant, and their effects on the economic optimization, the operating modes of the gas turbines, HRSGs, and electric chillers are tracked and constrained. Because the HRSGs are run using the exhaust of the gas turbines, they are scheduled in conjunction with the gas turbines. The TES tank is not

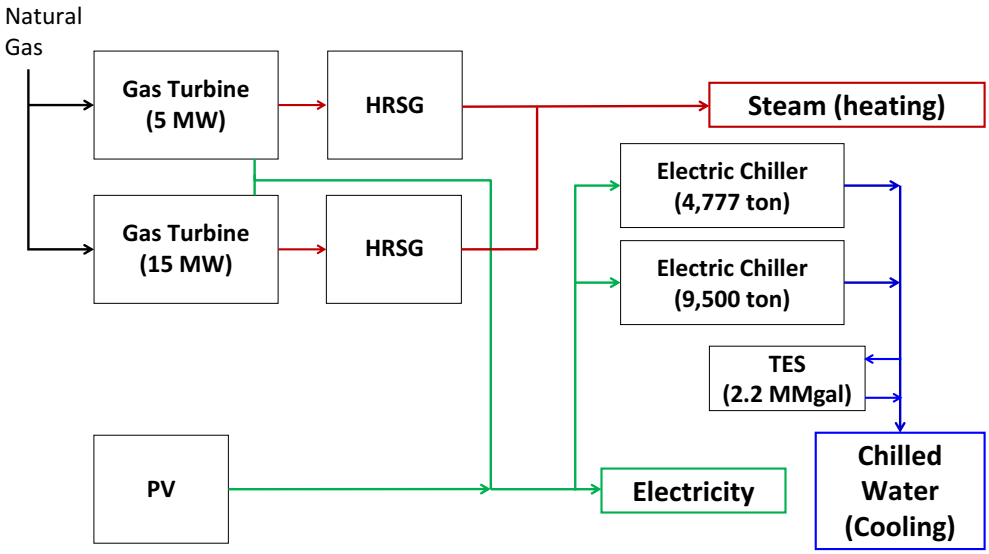

Figure 5.1: The optimal equipment, with thermal energy storage, to be included in a CHP plant to meet the utility demands for a residential neighborhood.

included, as its operation is not described well by a binary "on" and "off" state.

Each piece of equipment can operate in one of four modes: on, off, cold startup and warm startup. As described in previous chapters (Chapters 3 and 4), the binary variable $y^h_{e,s}$ is used to track the on/off operation of equipment e of size s at hour h, where one indicates that the component is on and zero indicates that the component is off. The following constraints, incorporating the on/off statuses ($y^h_{e,s}$), are used to determine if a warm ($warm^h_{e,s}$) or cold ($cold^h_{e,s}$) start is happening, were $warm^h_{e,s}$ and $cold^h_{e,s}$ are positive continuous variables:

$$y_{e,s}^{h} - y_{e,s}^{h-1} \leq warm_{e,s}^{h-1} + cold_{e,s}^{h-1} \quad \forall\, e \in E, s \in S, h > 1 \tag{5.1}$$

$$warm_{e,s}^{h} \leq \sum_{\theta=1}^{t_e^{ws}} y_{e,s}^{h-\theta} \quad \forall\, e \in E, s \in S, h > 5 \tag{5.2}$$

Equation (5.1) states that a warm or cold startup must happen if a piece of equipment has turned on at hour h, and Equation (5.2) says that piece of equipment can only turn on in a warm start up if it has been on at any hour in the past t_e^{ws} hours.

In order to allow time for a startup to occur, the gas turbines, HRSGs, and electric chillers must have an hour of startup time. They cannot alternate from on to off to on:

$$y_{e,s}^{h-2} + y_{e,s}^{h} - y_{e,s}^{h-1} \leq 1 \quad \forall\, e \in E, s \in S, h > 2 \tag{5.3}$$

5.3.1 Start-up penalties

Each time a gas turbine/HRSG or electric chiller turns on, there is an associated economic penalty to account for equipment wear and tear. The hourly startup penalty ($start_{e,s}^{h}$) is calculated by following:

$$startcost_{e,s}^{h} = \left(\kappa_e \times warm_{e,s}^{h}\right) + \left(\gamma_e \times cold_{e,s}^{h}\right) \quad \forall\, e \in E, s \in S, h \in H \tag{5.4}$$

where κ_e is the penalty associated with a warm startup and γ_e is the penalty associated with a cold startup for equipment e. The penalties, located in Table 3.1, are assumed to be constant for all equipment sizes. While $warm_{e,s}^{h}$ and

$cold^h_{e,s}$ are positive continuous, Equation (5.4) forces them to act as binaries if the overall cost of operating the plant is to be minimized.

5.4 Maintenance Cost

The maintenance costs for the moving-horizon scheduling are calculated using the maintenance models developed in Sections 3.5.2 and 4.6.2. For the equipment with a fixed yearly maintenance cost (i.e., the electric chillers and TES), the total maintenance cost ($Main_1$) is divided so that it is hourly and can be summed over the total number of hours optimized in each iteration (H):

$$Main_1 = \frac{H}{8760} \sum_e \sum_s M_{e,s} \quad \forall \quad e \in \{EC, TH\}, s \in S \tag{5.5}$$

The total maintenance cost for the gas turbines ($Main_2$), which is a function of equipment load, is summed over the number of hours optimized:

$$Main_2 = \sum_h \left(\sum_\upsilon M^h_{GT,\upsilon} \right) \quad \forall \quad \upsilon \in N_{GT}, h \in H \tag{5.6}$$

5.5 Optimal Operating Schedule

5.5.1 Meeting Neighborhood Utility Demand

A major requirement for the CHP plant is that all neighborhood electricity ($Elec^h$), heating ($Heat^h$), and cooling ($Cool^h$) demands must be met at all hours. To assure these requirements are met, the following balances (electricity (Equation (5.7)), heat (Equation (5.8)), and cooling (Equation (5.9)))

are included in the optimization:

$$E^h_{out} + Elec^h + \sum_{\omega} P^h_{EC,\omega} = \sum_{\upsilon} P^h_{GT,\upsilon} + PV^h + E^h_{in} \quad \forall h \in H \tag{5.7}$$

$$Heat^h \leq \sum_{\upsilon} W^h_{HRSG,\upsilon} \quad \forall h \in H \tag{5.8}$$

$$Cool^h + in^h_{TH} \leq \sum_{\omega} Q^h_{EC,\omega} + out^h_{TH} \quad \forall h \in H \tag{5.9}$$

where E^h_{out} is the electricity sold to the grid at hour h and E^h_{in} is the electricity purchased from the grid at hour h.

5.5.2 Overall Objective Function

The overall objective of the moving horizon scheduling is to minimize the operational cost of the plant. The four sources of expenditures are:

1. Fuel
2. Maintenance fees from equipment operation
3. Transition penalties
4. Purchasing electricity from the grid

and the one source of revenue is:

1. Selling electricity to the grid

The total cost for natural gas to power the gas turbines ($Fuel$), assuming that the cost of natural gas (NG_{cost}) remains constant for the optimization horizon, is calculated as follows:

$$Fuel = NG_{cost} \times \sum_{h} \left(\sum_{\upsilon} W^{h}_{f,GT,\upsilon} \right) \quad \forall \upsilon \in N_{GT}, h \in H \tag{5.10}$$

The total transition penalties ($Trans.Pen.$) are computed as:

$$Trans.Pen. = \sum_{e} \sum_{s} \sum_{h} startcost^{h}_{e,s} \quad \forall e \in E, s \in S, h \in H \tag{5.11}$$

The cost of purchasing electricity from the grid, C_{in}, and the revenue from selling electricity to the grid, C_{out}, are calculated as follows:

$$C_{in} = \sum_{h} \left(C^{h}_{DAM} \times E^{h}_{in} \right) \tag{5.12}$$

$$C_{out} = \sum_{h} \left(C^{h}_{DAM} \times E^{h}_{out} \right) \tag{5.13}$$

where C^{h}_{DAM} is the day ahead market settlement price point at hour h.

The overall objective function to minimize the operational costs is:

$$\min \quad (Main_1 + Fuel + Main_2 + Trans.Pen. + C_{in} - C_{out}) \tag{5.14}$$

5.6 Residential Neighborhood Utility Demand Model

As described in Sections 3.6.3 and 4.7.3, residential utility demand and PV generation data were attained from the Mueller neighborhood in Austin, TX. The data, collected by Pecan Street Inc. [8], included electricity and heating demand as well as PV generation from rooftop solar panels.

From the one-year set of hourly electricity, heating, and cooling [64] demand and PV generation data, ten days of data were selected from both March and July. The month of March was selected due to the availability of day-ahead market settlement point prices (see Section 5.7) and the presence of heating demand, as shown in Figure 5.2. On the other hand, to determine the operational behavior of the CHP plant with the grid when heating isn't present and cooling is in high demand, ten days of demand from July were selected (Figure 5.2).

As can be seen in Figure 5.2, the biggest difference between these two months is the different thermal demand, which is heating in March and cooling in July. While heating is present in March, it is minimal compared to the electricity demand, with the peak electricity demand steadily increasing over the ten day span. From March 10^{th} to the 16^{th}, the peaks in electricity demand are nominal compared to the peaks on the 18^{th} and 19^{th}. These sharp electricity peaks in the late afternoon and early evening are often characteristic of the summer electricity and cooling demand, as observed in the July utility demand. All days have large electricity demands, with equal or higher cooling demand peaks that coincide with the electricity peaks. While having extra electricity generation from the rooftop PV panels might help alleviate the electricity and cooling demands on the CHP plant, the PV generation only covers the early hours of peak generation in July, and is further offset from the larger peaks in electricity demand than in March.

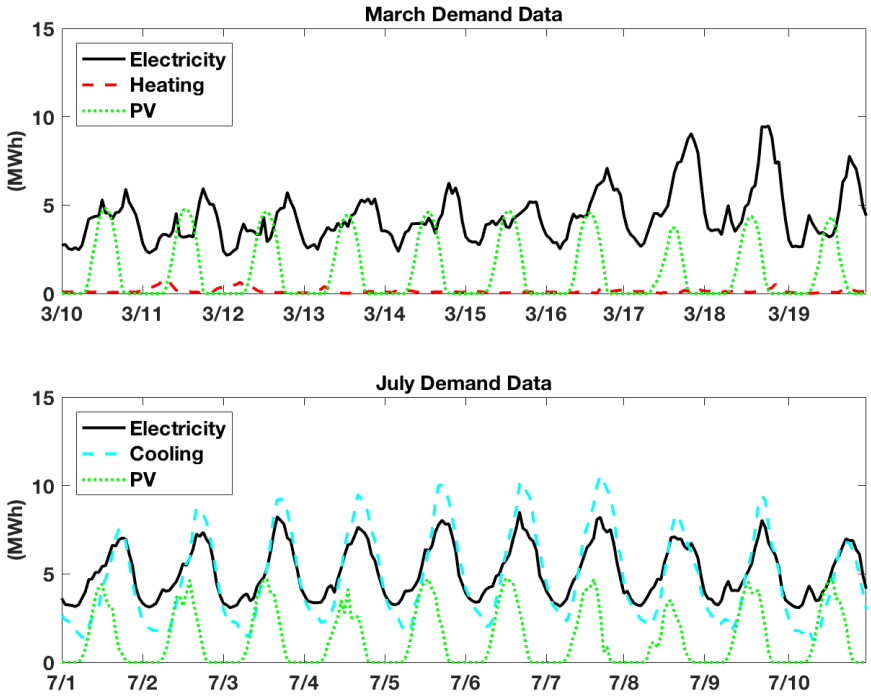

Figure 5.2: Residential utility demand data from March and July to be used in the moving horizon scheduling (data from [8]).

5.7 DAM Electricity Prices

In addition to the residential neighborhood utility demand data, the price of selling/purchasing electricity from the grid needed to be collected. In ERCOT, the Day-Ahead Market (DAM) is a voluntary financially-binding forward energy market [11]. Every morning at 6 AM, ERCOT releases information on energy obligations for the next operating day. Between 6 AM to 10 AM, companies have the option to submit hourly energy bids and offers, to either purchase or sell electricity at the DAM settlement price. By 1:30 PM,

ERCOT publishes the DAM settlement price points, i.e., the price that each generator will receive, or consumer will have to pay, for electricity the next day [153]. Information on next day DAM settlement price points as well as the current day, and 5 days previous are available online for public use [11]. For the purpose of this research, the DAM settlement price point (C^h_{dam}) is assumed to be equal to both the cost to purchase electricity from the grid and the price to sell electricity to the grid.

Using the ERCOT DAM website [11], data on the settlement price points were collected for March 11-17 for the Load Zone South, which includes Austin, TX (Figure 5.3). The settlement price points all had very similar profiles throughout the day, with the most variation occurring in the late afternoon and early evening. There was also daily deviations, with some days having a slightly higher average cost than other days. Due to the limited data available on the ERCOT website, settlement prices for July were unavailable. However, using data from the average DAM settlement price points for the month of July [12], a normally distributed random variable with mean of zero and standard deviation of 3 was added to the data to generate seven days of price points (Figure 5.3).

5.8 Solution Algorithm: Moving Horizon Scheduling

To calculate the operational cost to run the CHP plant to meet the neighborhood utility demands, taking into account the possibility to sell electricity to or purchase electricity from the grid, a moving horizon scheduling

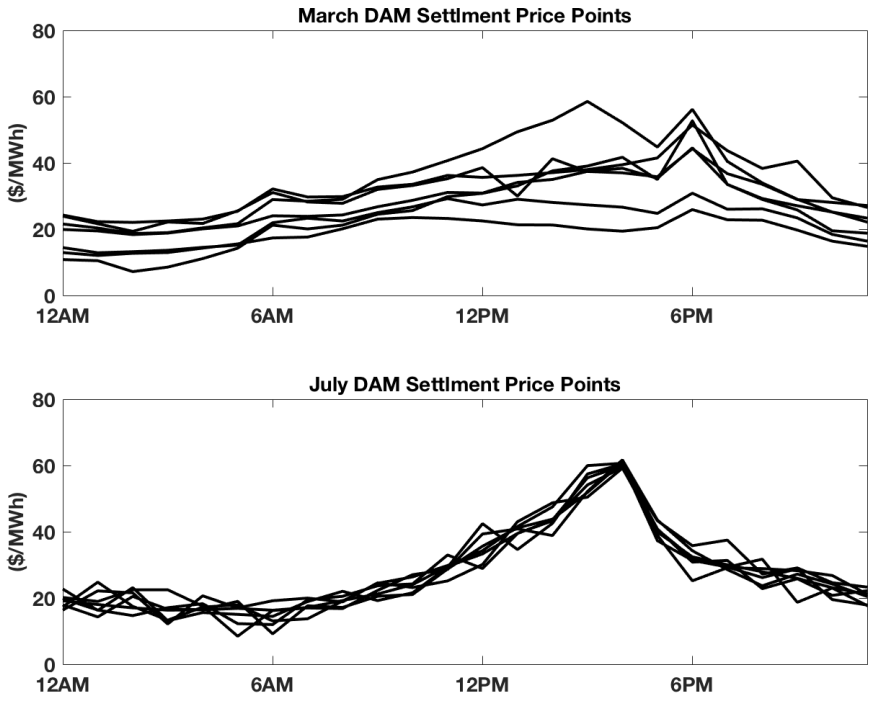

Figure 5.3: Seven days of DAM settlement prices used to calculate the cost of selling electricity to and buying electricity from the grid in March and July (data from [11, 12]).

was constructed. With the overarching goal of minimizing the total operational costs, the equipment can be scheduled every day to take into account the new DAM settlement price points, assuming that the price points are known and fixed.

An overview of the moving horizon scheduling is depicted in Figure 5.4. Every day when the DAM settlement price points are released (before *h=1*), the plant operation is re-scheduled for the next three days to capture the equipment and TES dynamics, incorporating the newly obtained data. This

includes the DAM settlement price points (*Price (DAM)*) plus two more days of price points that are calculated by adding a normally distributed random variable with mean of zero and standard deviation of 2 to the data (*Price (Optimized)*). Also, the expected utility demand of the neighborhood for the next three days is included. To account for plant dynamics and warm and cold start-up calculations, the last seven hours of plant operation of the current day (*Power (Current)*) are added to the beginning of the scheduling as fixed operating values. When solved, the future plant operation (*Power (Estimate)*) that minimizes the operational costs can be computed, including how much electricity should be sold to or purchased from the grid.

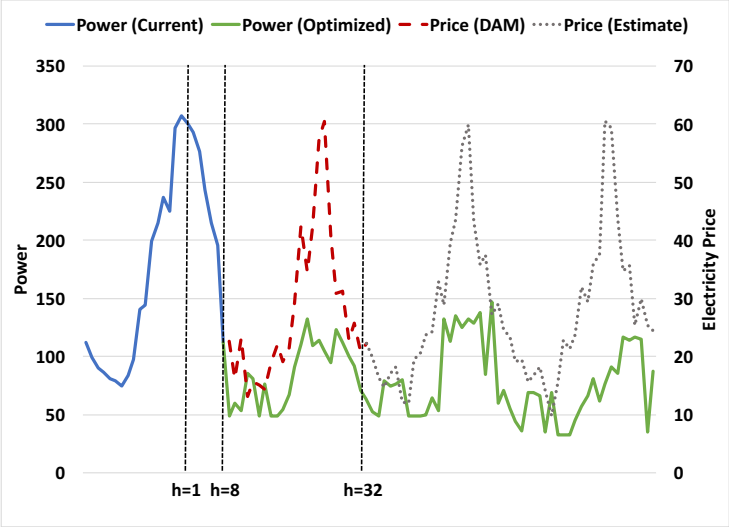

Figure 5.4: Schematic of the algorithm used to solve the simultaneous optimization of design and operational strategies.

With the moving horizon scheduling, one TES constraint is changed to allow more freedom in the model. Originally, the TES was forced to contain the same amount of chilled water at 12:00 AM as it did at 11:00 PM the same day, to guarantee that the optimization did not extort the scheduling and start with a full tank in the morning and leave it empty in the evening (Equation (4.5)). However, since the scheduling has increased to 79 hours, the constraint is now reformulated as the following, so that the tank constraint holds true from the first hour of the first full day optimized ($h = 8$) to the last day of the scheduling horizon ($h = 79$):

$$L_{TH}^{8} = L_{TH}^{79} \tag{5.15}$$

Using the following description of the moving horizon algorithm and incorporating the methodology shown in Figure 5.4, the CHP plant's operational strategies for meeting the residential neighborhood utility demand and interacting with the grid through the day ahead market is solved. First, all residential utility demand data and DAM settlement price points are collected and noise is added to the DAM settlement price points to estimate the next two days of price points. Next, the CHP plant operation is "initialized" by scheduling the CHP plant in island mode, i.e., not open to purchase or sell electricity from/to the grid, incorporating one day of residential utility demand . This is equivalent to the CHP plant (operating in island mode) receiving its first day of DAM settlement price points and scheduling its next three days of operation with participation in the DAM. The last seven hours of equipment

operation ($h^{init} = 18 - 24$) from the initialization solution are stored, and used to fix the 1st seven hours of the moving horizon scheduling ($h = 1 - 7$). The moving horizon scheduling is solved for all seventy-nine hours ($H = 79$), with the plant operation solutions from $h = 8 - 31$ being the plant operation for the next day. The last seven hours of the implemented plant operation, $h = 25 - 31$, are stored and used to fix the first seven hours of the next moving horizon scheduling, new DAM settlement price points are obtained, and the process iterates for 6 more days of DAM price points.

5.9 Case Study

To determine the effect of connecting the CHP plant with rooftop PV generation and TES to the grid, the moving horizon scheduling was applied to a case study using data from the Mueller neighborhood in Austin, TX. Two different months (March and July), with vastly different residential energy demands and slightly different DAM market prices were used to determine how the two main seasons in Texas effect the operational costs and the plant's interaction with the grid.

The scheduling was solved with GAMS 24.4.6 using the commercial solver CPLEX (12.6.2.0) on a PC Intel Core i7, 3.40 GHz, 16 GB RAM, 64 bit and Windows 10.

5.9.1 March Results

The moving horizon scheduling, with one initialization day and seven days of DAM settlement price points from March, was able to be solved to completion in 17 seconds. As can be seen in Figure 5.5, initially when the CHP plant is operating in island mode (3/10), the small 5 MW gas turbine and the larger 15 MW gas turbine are needed to meet the electricity demand of the neighborhood, . However, once the plant starts participating in the DAM, only the small gas turbine is used until March 14th. This is done because the optimization found it economical to purchase electricity form the grid to help meet the electricity demand. On March 14th in the later afternoon/early evening, both gas turbines are used at their maximum capacity to generate as much electricity as possible. This can be attributed to the price of electricity for the DAM, which rises to almost 60 $/MWh, as shown in Figure 5.6. On 3/15, 3/16, and 3/17, the optimization found it economic to generate more electricity by turning up the power produced by the 5 MW gas turbine. However, the DAM prices were not high enough to warrant turning on the 15 MW gas turbine. On the remaining days (3/12 and 3/13), the gas turbine is kept running at its minimum capacity and any additional electricity from the 5 MW gas turbine or PV panels is sold to the grid.

After examining the electricity generation results (Figure 5.5), there seemed to be an inconsistency in the evenings when electricity is purchased from the grid. If the optimization is purchasing electricity from the grid instead of running the gas turbine at a higher level to produce more power,

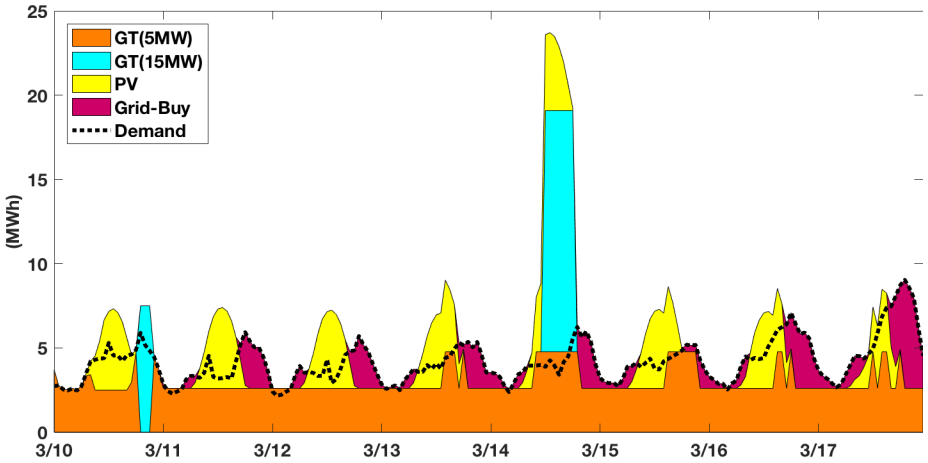

Figure 5.5: Electricity production in March to meet the electricity demand of the neighborhood and to be sold to the grid.

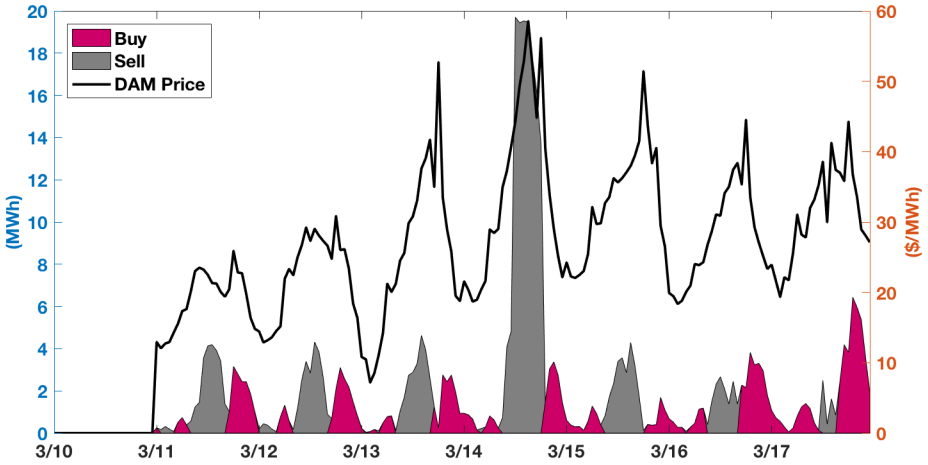

Figure 5.6: Electricity sold to and purchased from the grid, optimized using March DAM settlement price points (data from [11]).

the optimization should logically turn off the gas turbine and obtain all the electricity from the grid. However, with the current CHP plant design, this is impossible. Shown in Figure 5.7, there is minimal, but existent heating in

the month of March. The HRSGs are the only available piece of equipment that can produce heat, and they need their associated gas turbine running to produce the exhaust gas for the HRSG. Thus, the smaller 5 MW gas turbine must be kept running at all hours, even though it might be more economical to turn it off.

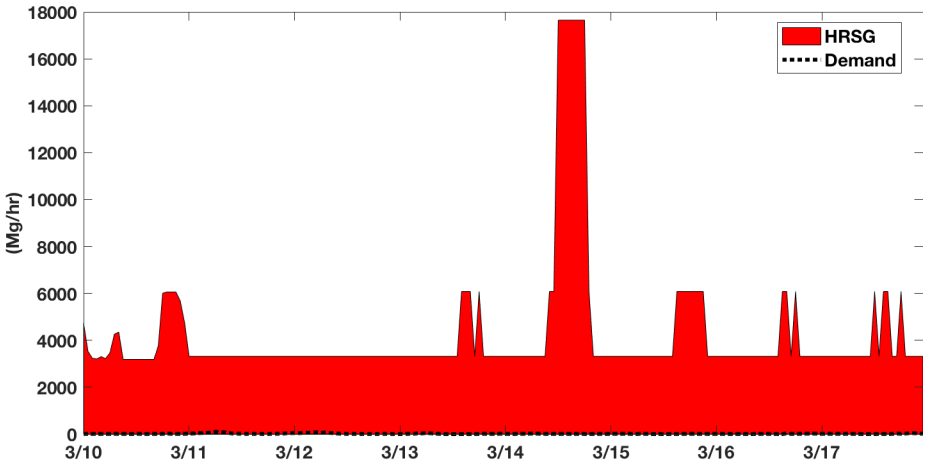

Figure 5.7: Steam production in March to meet the heat demand of the neighborhood.

Overall, with one day of operating in island mode and seven days of participating in the DAM market, the total operational cost of running the CHP plant to meet all of the residential utility demands is $30,276 over eight days. The hourly fuel costs, divided up by source, are displayed in Figure 5.8, which includes the total cost which is equal to the cost to generate electricity, plus the cost to purchase electricity from the grid, minus the revenue from selling electricity to the grid. While the overall operational cost is positive, the plant is able to make money participating in the DAM by selling electricity

to the grid when there is over-generation of electricity or when the DAM settlement price point gets between \$50 - \$60/MWh. On March 14[14], the plant is able to make enough money from the DAM to offset the operational costs of generating utilities for the neighborhood and electricity to be sold to the grid. Comparing the operating cost to the base case, i.e., if the CHP plant operated in island mode for all eight days, the total operating cost would be \$42,862. The CHP plant is able to save over \$12,500 by participating in the DAM for seven days in March.

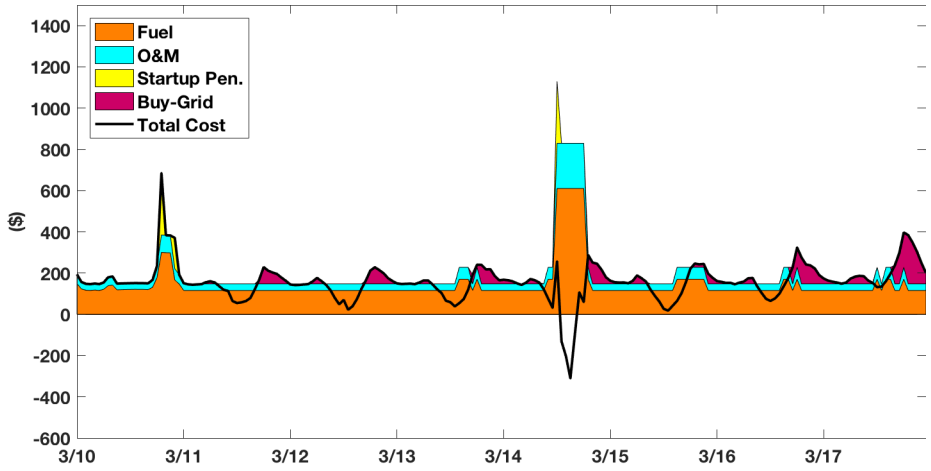

Figure 5.8: Hourly operational cost to run the CHP plant for a week in March when participating in the DAM.

5.9.2 July Results

For the month of July, the moving horizon scheduling, with one initialization day and seven days of DAM settlement price points, was able to be solved to completion in 9 seconds. As shown in Figure 5.9, the electricity

generation profile in July is greatly different from that of March. For the initial day when the plant was operating in island mode, the larger gas turbine is needed for a longer period of time to help meet the electricity demands of the neighborhood and electric chillers. However, when the CHP plant was participating in the DAM, the optimization found it economical to purchase almost all of the electricity from the grid to meet the neighborhood and electric chiller demands. The 15 MW gas turbine was only run for a very short amount of time in the late afternoon/early evening, making the CHP plant act like a "peaker plant" for the grid. In July, it was not necessary to have a gas turbine running at all hours because there was no heating present in the July residential utility demand data.

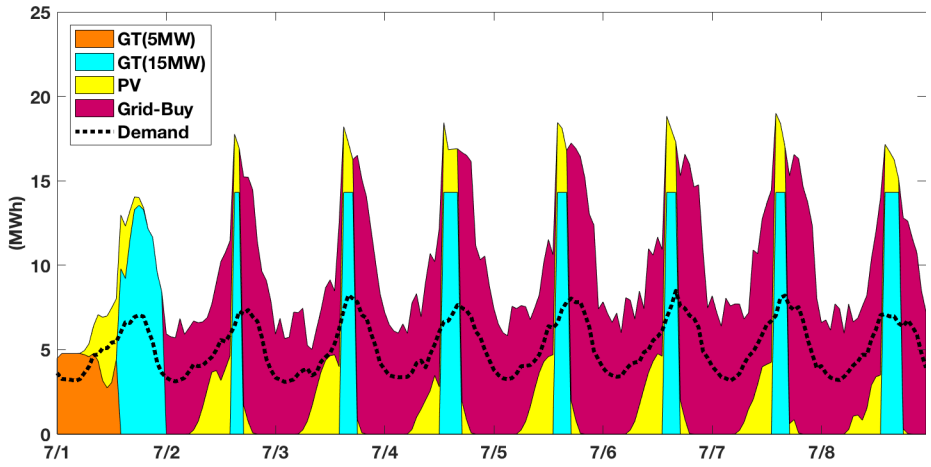

Figure 5.9: Electricity production in July to meet the electricity demand of the neighborhood, power the electric chillers, and to be sold to the grid.

When the CHP plant was participating in the DAM, the 15 MW gas turbine, running at full capacity, corresponded with the peaks in DAM settle-

ment price points, which all reach a high of at least $60/MWh (Figure 5.10). However, not all of the electricity generated by the CHP plant is sold to the grid. Part of the generation is used to supply the neighborhood and electric chiller demands, as it saves the plant money to generate its own electricity versus buying it from the grid at $60/MWh. One benefit of participating in the DAM, using this set of settlement price points, is the slight offset of the peak electricity and cooling demands from the peak in the DAM prices. After the drop in DAM prices, the optimization turns off the gas turbine and purchases a vast amount of electricity from the grid to meet the still high electricity demand, at a lower economic cost.

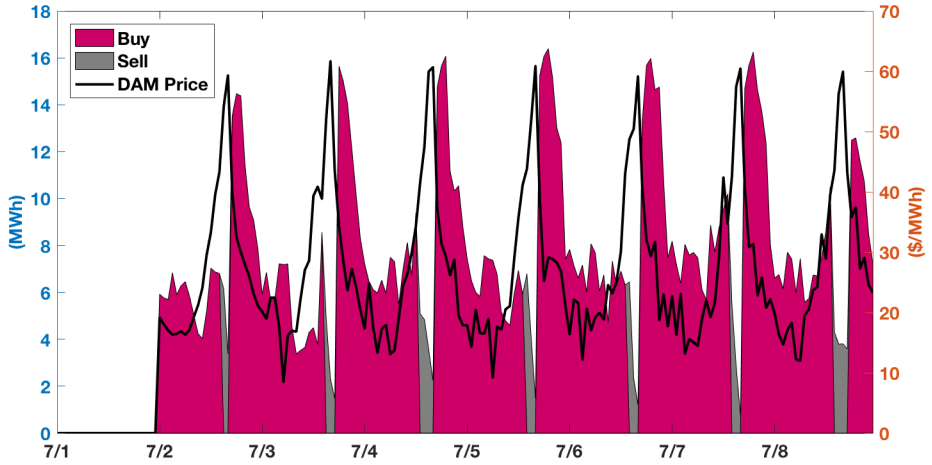

Figure 5.10: Electricity sold to and purchased from the grid, optimized using March DAM settlement price points (data from [12]).

To meet the cooling demand of the neighborhood in July, both electric chillers are needed, as shown in Figure 5.11. The optimization chooses too avoid a startup penalty and run both electric chillers at their minimum capac-

ity in the early morning hours when the cooling demand is minimal. However, any over generation of chilled water is loaded into the TES tank to avoid loss of energy (and money).

The plant revenue would be lower if the TES tank was not present. The chilled water was discharged from the TES tank towards the beginning of peak cooling demand hours, and to a lesser degree during the later evening hours when electricity was cheaper. After discharging all of its cooling in the evening, the TES tank waited until the next morning and afternoon to reload, when there was over generation of chilled water from the electric chillers, electricity was cheaper, and PV generation was available.

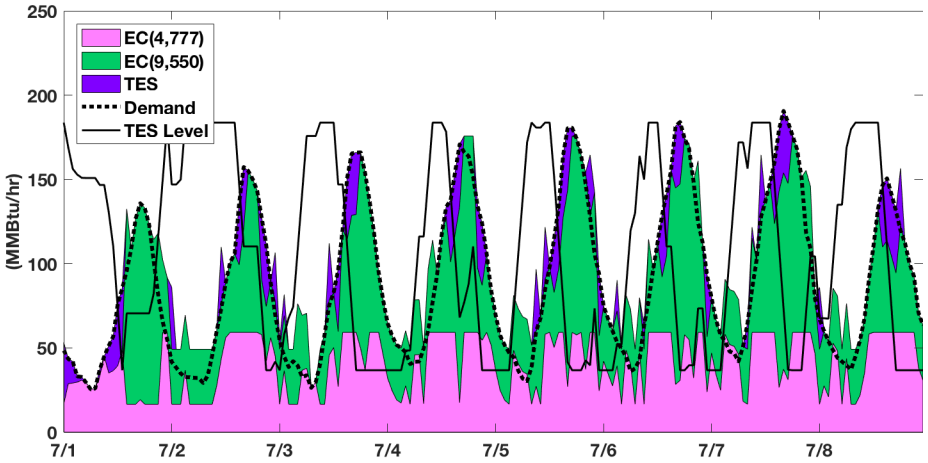

Figure 5.11: Chilled water production in July to meet the cooling demand of the neighborhood.

Overall, with one day of operating in island mode and seven days of participating in the DAM market, the total operational cost of running the CHP plant to meet all of the residential utility demands in July is $67,602. The

hourly fuel costs, divided up by source, are displayed in Figure 5.12, as well as the total cost, minus the revenue from selling electricity to the grid. Unlike in March when the CHP plant was able to cover the utility generation costs with its profit from the DAM, the plant in July was able to lessen the operational costs but never broke even. If the CHP plant did not participate in the DAM, and operated in island mode for all eight days, the total operating cost would be $97,910. The CHP plant is able to save over $30,300 by participating in the DAM over a period of seven days in July.

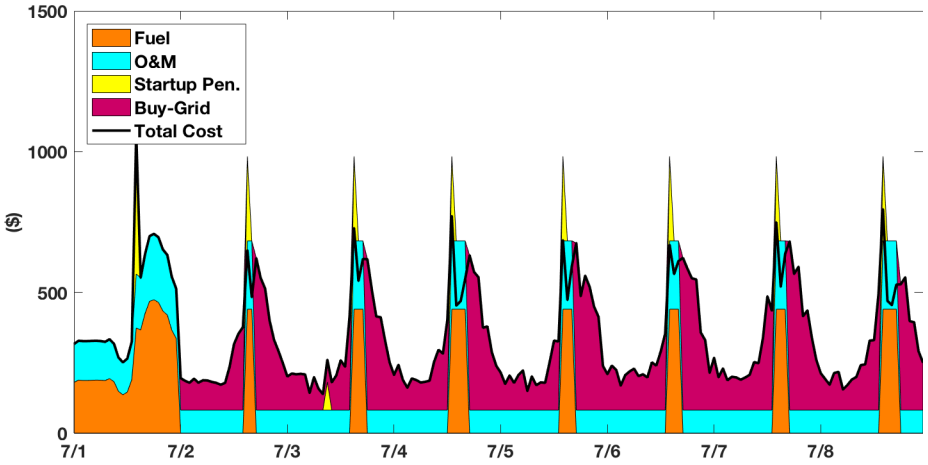

Figure 5.12: Hourly operational cost to run the CHP plant for a week in March when participating in the DAM.

5.10 Conclusions

In conclusion, we successfully optimized the operation of a CHP plant with rooftop PV panels and TES tank, as well as its participation in the day ahead market using a moving horizon scheduling strategy. Utilizing residential

energy demand and PV generation data from Austin, Texas, as well as day ahead market settlement price points from ERCOT, we were able to determine the optimal operation, capturing the hourly and seasonal variability of the energy demand and the day ahead market. While the CHP plant is able to occasionally make enough revenue from the day ahead market to cover the operational costs of the CHP plant meeting all residential utility demands, the high residential energy demand in July prohibits the plant from generating profit. However, the CHP plant's participation in the day ahead market does save the plant money in overall operating costs both in March and July.

Chapter 6

Conclusions and recommendations

6.1 Summary of Contributions

This section presents the key findings from this research on district-level Combined Heat and Power with PV generation and energy storage for a residential neighborhood. The intent is to highlight the major contributions and conclusions from this dissertation.

In Chapter 2, we described the optimal integration of a CHP plant as a utility producer for a residential neighborhood, and the potential for using photovoltaics, implemented in a centralized fashion, to provide additional electricity for the CHP plant. The residential energy demand data, collected from Pecan Street Inc., highlighted the decoupling of peak PV generation and cooling demand in the summer. However the electricity generation from the rooftop PV panels was large enough to power the neighborhood and the electric chillers, which provided cooling for the neighborhood. When given the option to sell electricity to the grid, the optimization chose to have the CHP plant sell electricity in the afternoon when there was extra PV generation, and in the evening when prices made it economical to run the gas turbine at its maximum capacity. While the plant was able to make money from the

electricity market, the results highlighted the fact that the gas turbine was not sized for the residential neighborhood's utility demands. The electricity demand of the neighborhood was always less than the minimum capacity of the gas turbine, so the turbine would be guaranteed to operate inefficiently if the CHP plant were to operate in island mode. This realization of plant oversizing led to the research contained in the next chapter.

Based on the oversizing of CHP plant equipment seen in Chapter 2, we constructed a novel simultaneous optimization of design and operation strategies for a CHP plant as a utility producer for a residential neighborhood operating in island (i.e., grid-disconnected) mode, incorporating residential photovoltaics, implemented in a centralized fashion. In order to more accurately capture the seasonal variability and uncertainty of residential energy demand, eight days of residential energy demand data were included in the optimization. Due to the large problem size created by using eight days of data, a temporal Lagrangean decomposition method was used to solve the optimization in a short period of time. The optimal plant design and its' equipment operation matched well to the residential energy demand, with smaller amounts of over-generation in electricity and cooling, compared to that of Chapter 2. Although the operational costs were extrapolated to encompass 20 years of operation (i.e., the lifetime of the plant), 50% of the plant cost was from purchasing the equipment.

In Chapter 4, motivated by the presence of extra energy generation in the Chapter 3 results, and the possibility that PV generation may not

be present, we studied the same system operating in an islanded (i.e., grid-disconnected) mode, and considered the impact of PV generation and centralized energy storage facilities on the CHP plant design and operations. The temporal Lagrangean decomposition method constructed in Chapter 3 was unable to solve the new optimization formulation with the additional equipment models. Thus, a bilevel decomposition method was implemented to help solve the optimization problem. While rooftop PV panels did aid in decreasing the operational costs of the plant, the savings were not enough to cover the capital cost of the panels, making them currently uneconomical. Also, despite the high efficiency of lithium-ion batteries, the current cost makes it an uneconomical choice for energy storage. Instead, a 2.2 million gallon TES tank was found to provide economic benefit by shifting some of the chilled water generation from the peak in the evening, to the morning when more PV generation is present and the electricity demand is not as high.

Lastly, in Chapter 5, we gave the CHP plant with TES and PV generation (from Chapter 4) the option to purchase electricity from and sell electricity to the grid. A moving horizon scheduling was used to schedule the operation of the CHP plant every day when updates on the DAM market prices are published. To capture the dynamics of the equipment operation and the DAM market prices, the scheduling included initializing the scheduling with the fixed operation from the current day, and looked ahead two days in the future beyond the day associated with the published DAM prices. We found that whenever heating is needed by the neighborhood, a gas turbine must always

be running, limiting the amount of electricity that can be purchased from the grid. However, in the summer when heating is not present, the CHP plant acts similar to a peaker plant, purchasing electricity from the grid for most hours except when the DAM settlement price points reach over $50/MWh. While the plant only acts as an electricity provider to the neighborhood for a few hours each day, the moving horizon scheduling with DAM participation does save the plant over $30,000 in operational costs in one week.

6.2 Future Work

From this dissertation, an economic formulation has been created to calculate the optimal design of a CHP plant with PV generation and energy storage taking into account the operation, capturing the uncertainty and variability of residential energy demand. The capacity of the equipment modeled may limit the number of applications that could utilize the research in this dissertation. For example, an economical optimization of a micro-CHP plant could have any number of residential homes as a potential client, versus a medium scale CHP could only be applied to a large group of homes. However, this work may be beneficial to growing cities with a need for residential neighborhoods (e.g., Dallas), military bases that need a reliable source of energy no matter the state of the grid, or could be extended to the commercial sector, where it could improve the energy efficiencies of commercial parks and company campuses (e.g., ExxonMobil or Google). In all of these cases, the energy demand profiles to be met by the CHP plant (e.g., electricity, heating,

and cooling) should be very similar.

If this work is to be continued and/or extended to another area, the number of equipment sizes available in the CHP plant superstructure should be increased to allow a better selection of equipment sizes. All of the equipment analyzed are available many sizes, in addition to the sizes selected. Also, the major assumptions made in this work should be improved to generate a better model. These major assumptions that need revision include: 1) the district heating/cooling model, which assumed no efficiency losses and a constant enthalpy of the return water, and ignored electricity to pump the utilities; 2) the steam adsorption chiller and electric chiller COPs, which did not consider the change of efficiency based on operating conditions; 3) the CHP plant network, which assumed all thermal energy was generated with the same enthalpy; and 4) the CHP plant interaction with the grid, which was only studied through the DAM - there might be additional value if the plant also participated in the real-time market. With these improvements, the feasibility of using CHP to provide local-utilities on a medium-scale may become more realizable in the future.

Although the simultaneous optimization of the design and operation of the CHP plant included residential energy demand uncertainty and variability, other inputs in the optimization were assumed be constant, even though in reality they carry some degree of uncertainty. The price of natural gas is very difficult to predict, considering it can be affected by factors on both the supply (e.g., production, net imports into the United States, etc.) and demand sides

(e.g., weather, petroleum prices, etc.) of the market. For this research, the price of natural gas was assumed to be constant for the lifetime of the CHP plant (20 years). However, this is not likely to happen and as a result, the solutions from the economical optimization may be skewed when determining if a certain technology is economically advantageous or disadvantageous.

Also, when determining whether certain technologies are economically feasible, such as rooftop PV generation and lithium-ion batteries, a constant price using current values was assumed, and the technology had to be implemented when the CHP plant was built. These two technologies have both received a lot of attention in the research community, and the prices have decreased while the efficiency has improved. Future estimated prices as a function of time should be included in the optimization to give more accuracy to the economic results, and their installation should be a function of time as well.

Lastly, the price of real and reactive power at the grid-level has a great effect on the CHP plant's interaction with the grid. Electricity prices are heavily influenced by the electricity demand, as well as the cost to generate electricity, i.e., the type of generation available. If future electricity demand increases during peak hours, the cost of electricity could be higher during peak hours, possibly making other energy storage methods, such as battery storage, economic. Also, if renewable energy generation continues to increase, the grid will need a fast-reacting, controllable source of energy, such as a CHP plant, to be present incase the renewable generation fails or fades. This would increase

the value of reactive power for the grid, allowing the CHP plant to have a higher value if it participates in the real-time market.

Appendices

Appendix A

Nomenclature - Chapter 2

Nomenclature

Sets

- H (index h): The set of hours used in the scheduling
- C (index c): The set of components scheduled, {*GT, BR, EC, SA*}
- M (index m): The set of modes, {*on, off, cold startup, warm startup*}

Variables

Binary variable

- $y^h_{c,m}$ Component c is in mode m at hour h
- $V^h_{c,cold}$: Cold startup has begun at hour $h-1$ for component c, and continues at hour h
- $V^h_{c,warm}$: Warm startup has occurred at hour $h-1$ for component c

Continuous variables

- IGV^h: Inlet guide vane angle of the inlet air cooler at hour h
- Vw^h: Volume of water entering the inlet air cooler at hour h

- m_{air}^{h}: Mass of the air exiting the inlet air cooler at hour h
- $T_{air,out}^{h}$: Temperature of the air exiting the inlet air cooler at hour h
- Fd^{h}: Fuel signal of the gas turbine at hour h
- P_{GT}^{h}: Power generated by the gas turbine at hour h
- T_{f}^{h}: Firing temperature of the gas turbine at hour h
- T_{e}^{h}: Temperature of the exhaust gas exiting the gas turbine at hour h
- $W_{f,HRSG}^{h}$: Fuel flow into the HRSG at hour h
- $W_{sh,HRSG}^{h}$: Mass flow of steam exiting the HRSG at hour h
- $T_{sh,HRSG}^{h}$: Temperature of steam exiting the HRSG at hour h
- $T_{e,HRSG}^{h}$: Temperature of exhaust gas exiting the HRSG at hour h
- $W_{f,BR}^{h}$: Fuel flow into the boiler at hour h
- $W_{sh,BR}^{h}$: Mass flow of steam exiting the boiler at hour h
- $W_{sh,SA}^{h}$: Mass flow of steam entering the steam absorption chiller at hour h
- Q_{SA}^{h}: Cooling produced by the steam absorption chiller at hour h
- P_{EC}^{h}: Power supplied to the electric chiller at hour h
- Q_{EC}^{h}: Cooling produced by the electric chiller at hour h

- $PowerRev.Ext.^h$: Revenue from selling electricity to the grid at hour h
- $PowerRev.Int.^h$: Revenue from selling electricity to the neighborhood at hour h
- $CoolingRev.^h$: Revenue from selling cooling to the neighborhood at hour h
- $HeatingRev.^h$: Revenue from selling heating to the neighborhood at hour h
- P_{ext}^h: Electricity sold to the grid at hour h
- $FuelCost^h$: Cost to purchase fuel at hour h
- $CostTimeLost_c^h$: Cost of transitioning from off to on for component c at hour h

Parameters

- $T_{w,in}^h$: Temperature of the water entering the inlet air cooler at hour h
- $T_{air,in}^h$: Temperature of the air entering the inlet air cooler at hour h
- IGV^{max}: Maximum angle of the inlet guide vane
- IGV^{min}: Minimum angle of the inlet guide vane
- Vw^{max}: Maximum volume of water to enter the inlet air cooler
- Fd^{max}: Maximum fuel signal

- Fd^{min}: Minimum fuel signal
- P_{GT}^{max}: Maximum power from the gas turbine
- kNL: Fuel valve lower limit for the gas turbine
- $W_{f,0}$: Fuel flow at nominal operating condition
- $W_{f,HRSG}^{max}$: Maximum fuel flow entering the HRSG
- $W_{f,BR}^{max}$: Maximum fuel flow entering the boiler
- $W_{f,BR}^{min}$: Minimum fuel flow entering the boiler
- P_{EC}^{max}: Maximum power supplied to the electric chiller
- P_{EC}^{min}: Minimum power supplied to the electric chiler
- $W_{sh,SA}^{max}$: Maximum steam supplied to the steam absorption chiller
- COP_{SA}: Coefficient of performance for the steam absorption chiller
- $H_{out,HRSG}$: Enthalpy of steam exiting the HRSG
- $H_{out,SA}$: Enthalpy of steam exiting the steam absorption chiller
- $\hat{H}_{sh,BR}$: Enthalpy of the steam exiting the boiler
- $\hat{H}_{i,BR}$: Enthalpy of the water entering the boiler
- P_{int}^{h}: Electricity needed by the neighborhood at hour h
- Q_{int}^{h}: Cooling needed by the neighborhood at hour h

- $W^h_{sh,HT}$: Steam needed by the neighborhood for heating at hour h
- P^h_{solar}: PV generation from the neighborhood at hour h
- $Trans\ Cost_c$: $m' \times m$ matrix with the costs to transition from mode m' to mode m for component c
- $WarmCost_c$: Cost to turn on a component through a warm startup for component c
- $ColdCost_c$: Cost to turn on a component through a cold startup for component c

Appendix B

Original Equipment Models

Three pieces of equipment originally were modeled using sets of nonlinear equations [66]. The nonlinear models are described below.

Inlet Air Cooler

Volume of air (V_{air}^h):

$$V_{air}^h = V_{air,0} \times \frac{sin(IGV^h - IGV^{min})}{sin(IGV^{max} - IGV^{min})} \tag{B.1}$$

where:

$V_{air,0}$ is the volumetric air flow at nominal operating conditions

IGV^h is the inlet guide vane angle

IGV^{min} is the minimum inlet guide vane angle

IGV^{max} is the maximum inlet guide vane angle

Lumped variable 1 (A^h):

$$A^h = P_{out}^h \times V_{air}^h \times \frac{MW_{air} \times C_{pc}}{R_g} \tag{B.2}$$

where:

P^h_{out} is the pressure of air exiting the inlet air cooler

MW_{air} is the molecular weight of air

C_{pc} is the specific heat of air

R_g is the ideal gas constant

Lumped variable 2 (B^h):

$$B^h = 1000 \times \rho_w \times V^h_w \times C_{p,w} \tag{B.3}$$

where:

ρ_w is the water density

V^h_w is the volumetric flow rate of chilled water entering the inlet air cooler

$C_{p,w}$ is the specific density of water

Minimum possible air temperature at the outlet of the inlet air cooler ($T^h_{air,TIAC,min}$):

$$T^h_{air,TIAC,min} = \frac{\left(B^h \times T^h_{w,in}\right) - A^h + (A^h)^2 - \left(2 \times A^h \times B^h \times T^h_{w,in}\right)}{2 \times B^h} + \frac{\left(4 \times T^h_{air,in} \times A^h \times B^h\right) + (T^h_{w,in})^2 \times (B^h)^2}{2 \times B^h} \tag{B.4}$$

where:

$T^h_{w,in}$ is the temperature of water entering

$T^h_{air,in}$ is the temperature of the air entering

Temperature of the water exiting the inlet air cooler ($T^h_{w,out}$):

$$T^h_{w,out} = \eta_{HX} \times \left(T^h_{air,TIAC,min} - T^h_{w,in}\right) + T^h_{w,in} \tag{B.5}$$

where:

η_{HX} is the efficiency of the heat exchanger

Temperature of the air exiting the inlet air cooler ($T^h_{air,out}$):

$$T^h_{air,out} = \frac{A^h \times T^h_{air,in}}{A^h + \left(B^h \times \left(T^h_{w,out} - T^h_{w,in}\right)\right)} \tag{B.6}$$

Mass of the air exiting the inlet air cooler (m^h_{air}):

$$m^h_{air} = \frac{V^h_{air} \times MW_{air} \times P^h_{out}}{1000 \times R_g \times T^h_{air,out}} \tag{B.7}$$

Temperature difference between the compressor outlet and inlet (Td^h_{Ti}):

$$Td^h_{Ti} = \left(\frac{PR_0 \times m^h_{air}}{W_0}\right)^{\frac{rc-1}{rc}-1} \times \frac{T^h_{air,out}}{\eta_{CP}} \tag{B.8}$$

where:

PR_0 is compression ratio

W_0 is the air flow at nominal operating condition

rc is the cold end ratio of specific heats

η_{CP} is the compressor efficiency

Gas Turbine

Volume flow rate of fuel entering the gas turbine ($W_{f,GT}$):

$$W^h_{f,GT} = \left(Fd^h \times (1 - kNL) + kNL\right) \times W_{f,0} \tag{B.9}$$

where:

Fd^h is the fuel signal

kNL is the fuel valve lower limit

$W_{f,0}$ is the gas turbine fuel flow at nominal operating condition

Lumped variable 3 (X^h_h):

$$X^h_h = \left(PR_0 \times \frac{W^h_{f,GT} + m^h_{air}}{W_{f,0} + W_0}\right)^{\frac{rh-1}{rh}} \tag{B.10}$$

where:

W_0 is the air flow at nominal operating conditions

rh is the hot end ratio of specific heats

Firing temperature (T^h_f):

$$T^h_f = T^h_{air,out} + \left(\frac{\eta_{comb,GT} \times LHV}{C_{ph}}\right) \times \left(\frac{W^h_{f,GT}}{W^h_{f,GT} + m^h_{air}}\right) \tag{B.11}$$

where:

$\eta_{comb,GT}$ is the combustor efficiency

C_{ph} is the specific heat of exhaust gas flow

LHV is the lower heating value of the fuel

Temperature of the exhaust (T_e^h):

$$T_e^h = T_f^h \times \left(1 - \left(1 - \frac{1}{X_h^h}\right) \times \eta_t\right) \tag{B.12}$$

where:

η_t is the turbine efficiency

Power generated by the gas turbine (P_{GT}^h):

$$P_{GT}^h = \left(m_{air}^h + W_{f,GT}^h\right) \times C_{ph} \times \left(T_f^h - T_e^h\right) - \left(m_{air}^h \times C_{pc} \times Td_{Ti}^h\right) \tag{B.13}$$

Heat Recovery Steam Generator

Temperature of the steam after supplementary firing ($T_{e,raised}^h$):

$$T_{e,raised}^h = T_e^h + \frac{\beta_{HRSG}}{\alpha_{HRSG}} \times \left(\frac{W_{f,HRSG}^h}{W_{f,HRSG}^h + m_{air}^h + W_{f,GT}^h}\right) \tag{B.14}$$

with:

$$\beta_{HRSG} = \eta_{HRSG} \times \eta_{HRSG,comb} \times LHV \tag{B.15}$$

$$\alpha_{HRSG} = \eta_{HRSG} \times C_{ph} \tag{B.16}$$

where:

η_{HRSG} is the overall HRSG efficiency

$\eta_{HRSG,comb}$ is the duct burner combustion efficiency

$W^h_{f,HRSG}$ is the duct burner fuel flow

HRSG steam flow ($W^h_{sh,HRSG}$):

$$W^h_{sh,HRSG} = \frac{\alpha_{HRSG} \times \left(m^h_{air} + W^h_{f,GT} + W^h_{f,HRSG}\right)\left(T^h_{e,raised} - T_{e,out}\right) - \Delta_{FWHTR}}{\Delta_{HRSG}} \quad \text{(B.17)}$$

where:

$T_{e,out}$ is the temperature of the exhaust gas at the outlet of the HRSG

Δ_{FWHTR} is the heat duty for the feedwater preheater

Δ_{HRSG} is the different in enthalpy at the inlet and outlet of the economizer

Appendix C

Linearization of CHP Equipment

To obtain linear representations of the highly nonlinear inlet air cooler, gas turbine, and HRSG models, the nonlinear models, located in Appendix B, were approximated using Microsoft Excel and the LINEST function. The ranges of the manipulated variables (IGV^h, Vw^h, Fd^h, $W^h_{f,HRSG}$) and the variable parameters ($T^h_{w,in}$, $T^h_{air,in}$, $T^h_{air,out}$) used in the approximation were selected based on the minimum and maximum values of the operating ranges and the minimum and maximum values of the input parameters.

The following table contains the values of the parameters obtained from the linear approximation for the inlet air cooler, gas turbine, and HRSG models described in Section 2.4.1:

Approx. Parameters	i = 1	i = 2	i = 3	i = 4	i = 5
α_i	78.7313	0.0017	-0.2655	-0.1568	146.9265
β_i	2.8078	-0.0041	0.6209	.3645	5.9316
γ_i	43.4225	0.0165	-0.0211	2.7703	-
δ_i	748.9867	-3.2473	2.2190	519.4641	-
ζ_i	446.6062	-3.3625	1.3253	464.6612	-
κ_i	9.0831	24.4140	-0.0530	0.0733	-16.9129
λ_i	164.7688	445.6615	-3.7707	1.3253	516.5225

Appendix D

Efficiency vs. Capacity Data

Elec. Capacity (MW)	Electrical Eff. (%)	Maker	Source
3.30	23.95	Solar Turbines	[104]
5.05	30.20	Siemens	[154]
5.40	31.00	Siemens	[154]
6.75	31.50	Siemens	[154]
7.04	28.90	Solar Turbines	[104]
7.90	30.60	Siemens	[154]
9.95	27.34	Solar Turbines	[104]
12.90	34.80	Siemens	[154]
14.33	35.40	Siemens	[154]
18.00	35.00	GE	[155]
19.06	33.70	Siemens	[154]
20.34	33.24	Solar Turbines	[104]
24.00	37.00	GE	[155]
24.48	33.60	Siemens	[154]
29.00	39.00	GE	[155]
32.82	37.20	Siemens	[154]
34.00	41.00	GE	[155]
37.03	39.50	Siemens	[154]
44.00	33.50	GE	[155]
44.49	35.96	GE	[104]
47.50	37.70	Siemens	[154]
50.50	38.30	Siemens	[154]
51	38.00	GE	[155]

Table D.1: Data collected to relate gas turbine electrical efficiency to nominal capacity.

Appendix E

Linearization of Gas Turbine Fuel Equation

McCormick relaxation of Equation 3.8, used to relate the power produced by a gas turbine of size v at hour h to the product of the gas turbine parameter α_{GT}, the natural gas flow rate $W^h_{f,GT,v}$, and the efficiency $\eta^h_{GT,v}$:

$$P^h_{GT,v} = (W_f \eta)^h_{GT,v} \times \alpha_{GT} \tag{E.1}$$

such that

$$(W_f \eta)^h_{GT,v} \geq \left(\eta^h_{GT,min,v}\right) W^h_{f,GT,v} + \left(W^{min}_{f,GT,v}\right) \eta^h_{GT,v} - \left(\eta^h_{GT,min,v} \times W^{min}_{f,GT,v}\right) \tag{E.2}$$

$$(W_f \eta)^h_{GT,v} \geq \left(\eta^h_{GT,max,v}\right) W^h_{f,GT,v} + \left(W^{max}_{f,GT,v}\right) \eta^h_{GT,v} - \left(\eta^h_{GT,max,v} \times W^{max}_{f,GT,v}\right) \tag{E.3}$$

$$(W_f \eta)^h_{GT,v} \leq \left(\eta^h_{GT,min,v}\right) W^h_{f,GT,v} + \left(W^{max}_{f,GT,v}\right) \eta^h_{GT,v} - \left(\eta^h_{GT,min,v} \times W^{max}_{f,GT,v}\right) \tag{E.4}$$

$$(W_f \eta)^h_{GT,v} \leq \left(\eta^h_{GT,max,v}\right) W^h_{f,GT,v} + \left(W^{min}_{f,GT,v}\right) \eta^h_{GT,v} - \left(\eta^h_{GT,max,v} \times W^{min}_{f,GT,v}\right) \tag{E.5}$$

where the maximum ($W^{max}_{f,GT,v}$) and minimum ($W^{min}_{f,GT,v}$) fuel consumed and the maximum ($\eta^h_{GT,v,max}$) and minimum ($\eta^h_{GT,v,min}$) efficiencies are calculated by the following:

$$\eta^h_{GT,min,v} = \eta^{min}_{GT,rt} \times \eta^h_{GT,temp,v} \tag{E.6}$$

$$\eta^h_{GT,max,v} = \eta^{max}_{GT,rt} \times \eta^h_{GT,temp,v} \tag{E.7}$$

$$W^{max}_{f,GT,v} = \frac{1000 \times P^{max}_{GT,v}}{\alpha_{GT} \times \eta^h_{GT,v,max}} \tag{E.8}$$

$$W^{min}_{f,GT,v} = 0.5 \times W^{max}_{f,GT,v} \tag{E.9}$$

Appendix F

Minimum Electric Chiller Operation Data

Equipment Name	Maximum Cooling Capacity (ton)	Minimum Unloaded Capacity (ton)	Fraction
TCW300C	83.8	27	0.322
TCW300E	86.8	27	0.311
TCW300J	90.5	27	0.298
TCW300M	93.3	27	0.289
TWC350Q	132.1	30	0.227
TCW350S	133.3	30	0.225
		Average	**0.28**

Table F.1: Data used to calculate the average minimum amount of cooling produced from the electric chillers [2].

Appendix G

Nomenclature - Chapters 3, 4, and 5

Sets

- S (index s): The set of integers used to track the sizes of equipment available
- Υ (index υ): The set of integers used to track the sizes of the gas turbine
- Φ (index ϕ): The set of integers used to track the sizes of the steam turbine
- X (index χ): The set of integers used to track the sizes of the boiler
- Ψ (index ψ): The set of integers used to track the sizes of the steam absorption chiller
- Ω (index ω): The set of integers used to track the sizes of the electric chiller
- H (index h): The set of hours scheduled
- E (index e): The set of equipment scheduled, {*GT/HRSG, ST, BR, EC, SA*}

- D (index d): The set of days scheduled
- K (index k): The set of iterations in the Lagrangean Decomposition
- B (index b): The set of energy storage devices
- Y_0^i: The set of pieces of equipment that were not used in the upper level optimization of the bilevel decomposition
- Y_1^i: The set of pieces of equipment that were used in the upper level optimization of the bilevel decomposition

Variables

Binary variables

- $y_{e,s}^h$: Equipment e of size s is on (equal to 1) or off (equal to 0) at hour h
- $U_{e,s}$: Equipment e of size s has been used (Chapter 4)

Continuous variables

- $P_{GT,pr,\upsilon}^h$: Partial load of power generated from gas turbine of size υ at hour h (nu)
- $P_{GT,\upsilon}^h$: Power produced by gas turbine of size υ at hour h (kW)
- $\eta_{GT,pr,\upsilon}^h$: Ratio of actual efficiency to nominal efficiency based on the partial load of a gas turbine of size υ at hour h (nu)

- $\eta^h_{GT,\upsilon}$: Efficiency of a gas turbine of size υ at hour h (%)
- $(W_f\eta)^h_{GT,\upsilon}$: Substitute for fuel times efficiency for a gas turbine of size *size* at hour h (MMBtu/hr)
- $W^h_{HRSG,\upsilon}$: Amount of steam produced by the HRSG associated with a gas turbine of size υ at hour h (kg/hr)
- $P^h_{ST,\phi}$: Power produced by a steam turbine of size ϕ at hour h (MW)
- $W^h_{ST,\phi}$: Amount of steam consumed by a steam turbine of size ϕ at hour h (kg/s)
- $W^h_{BR,\chi}$: Amount of steam produced by a boiler of size χ at hour h (kg/hr)
- $W^h_{f,BR,\chi}$: Amount of fuel consumed by a boiler of size χ at hour h (kg/hr)
- $Q^h_{SA,\psi}$: Amount of cooling produced by a steam absorption chiller of size ψ at hour h (Btu/hr)
- $W^h_{SA,\psi}$: Amount of steam consumed by a steam absorption chiller of size ψ at hour h (kg/hr)
- $Q^h_{EC,\omega}$: Amount of cooling produced by an electric chiller of size ω at hour h (Btu/hr)
- $P^h_{EC,\omega}$: Amount of power consumed by an electric chiller of size ω at hour h (kWh)

- $warm^h_{e,s}$: Equipment e of size s is in the last hour of a warm startup at hour h (nu)
- $cold^h_{e,s}$: Equipment e of size s is in the last hour of a cold startup at hour h (nu)
- $StartCost^h_{e,s}$: Cost from transitioning equipment from one mode to the next for equipment e of size *size* at hour h ($)
- $C_{GT,\upsilon}$: Capital cost of a gas turbine of size υ ($)
- $C_{ST,\phi}$: Capital cost of a steam turbine of size ϕ ($)
- $C_{BR,\chi}$: Capital cost of a boiler of size χ ($)
- $C_{SA,\psi}$: Capital cost of a steam absorption chiller of size ψ ($)
- $C_{EC,\omega}$: Capital cost of an electric chiller of size ω ($)
- $M^h_{GT,\upsilon}$: Hourly maintenance cost for a gas turbine of size υ at hour h ($/hr)
- $M_{ST,\phi}$: Yearly maintenance cost for a steam turbine of size ϕ ($)
- $M^h_{BR,\chi}$: Hourly maintenance cost for a boiler of size χ at hour h ($/hr)
- $M_{SA,\psi}$: Maintenance cost for a steam absorption chiller of size ψ ($)
- $M_{EC,\omega}$: Maintenance cost for an electric chiller of size ω ($)
- $U_{e,s}$: Equipment e of size s has been used (Chapter 3)

- $Capital$: Total capital cost for all used equipment ($)
- $Main_1$: Total maintenance costs for the lifetime of the plant of all used equipment except gas turbines (Chapters 3 and 4) ($)
- $Main_{2,d}$: Total maintenance costs for all used gas turbines for the lifetime of the plant ($)
- $Fuel_d$: Overall cost to purchase fuel to run the plant for its entire lifetime ($)
- $Trans.Pen._d$: Total cost spent on turning equipment on for the lifetime of the plant ($)
- Z: Objective of optimization (Lagrangean decomposition) ($)
- L: Long-term plant costs ($)
- R_d: Short-term plant costs for day d ($)
- g_d: Short-term variable separated into days (nu)
- j_d: Short-term variable separated into days (nu)
- $U^d_{e,s}$: Equipment e of size s used on day d (nu)
- L_d: Long-term plant costs broken into d days ($)
- λ_d: Lagrange multiplier for day d ($)
- f_d: Penalization function for lower bound optimization for day d ($)

- Z^{LB}: Lower bound optimization solution (Lagrangean decomposition) ($)
- Z^{UB}: Upper bound optimization solution (Lagrangean decomposition) ($)
- ζ: Objective of hybrid lagrange multiplier updating optimization ($)
- L_b^h: Energy stored in each energy storage device (BTU/hr or kWh)
- in_b^h: Energy put into the energy storage device (BTU/hr or kWh)
- out_b^h: Energy removed from the energy storage device (BTU/hr or kWh)
- C_b: Capital cost of the energy storage device ($)
- M_b: Yearly maintenance cost for the energy storage device ($)
- Z^{UL}: Objective of the upper level optimization (bilevel decomposition) ($)
- Z_d^{LL}: Daily objective of the lower level optimization (bilevel decomposition) ($)
- Z^{LL}: Total objective of the lower level optimization (bilevel decomposition) ($)
- E_{out}^h: Electricity sold to the grid (kWh)
- E_{in}^h: Electricity purchased from the grid (kWh)

- $Main_1$: Hourly maintenance costs for the lifetime of the plant of all used equipment except gas turbines (Chapter 5) ($)
- $Main_2$: Maintenance costs for the gas turbines over the optimization horizon ($)
- $Fuel$: Cost to purchase fuel to run the plant over the optimization horizon ($)
- $Trans.Pen.$: Cost spent on turning equipment on over the optimization horizon ($)
- C_{in}: Cost of purchasing electricity from the grid over the optimization horizon ($)
- C_{out}: Revenue from selling electricity to the grid over the optimization horizon ($)

Parameters

- $Elec^h$: Neighborhood electricity demand at hour h (kWh)
- PV^h: Neighborhood PV generation at hour h (kWh)
- $Heat^h$: Neighborhood heating demand at hour h (kWh)
- $Cool^h$: Neighborhood cooling demand at hour h (Btu/hr)
- $P_{GT,\upsilon}^{max}$: Maximum capacity of a gas turbine of size υ (MW)

- N_{GT}: Number of sizes of gas turbine available (nu)
- $\eta^{nom}_{GT,\upsilon}$: Nominal efficiency of a gas turbine of size υ (%)
- $\eta^{h}_{GT,temp,M50}$: Efficiency of Mercury 50 gas turbine at hour h (%)
- T^{h}_{air}: Temperature of the air outside (^{o}C)
- $\eta^{h}_{GT,temp,\upsilon}$: Efficiency of a gas turbine of size υ at hour h influenced by the temperature (%)
- $T_{air,nom}$: Temperature of the air when nominal efficiency recorded (^{o}C)
- $\eta^{min}_{GT,rt}$: Minimum value for $\eta^{h}_{rt,\upsilon}$ for a gas turbine (nu)
- $\eta^{max}_{GT,rt}$: Maximum value for $\eta^{h}_{rt,\upsilon}$ for a gas turbine (nu)
- α_{GT}: Constant used to related the efficiency and fuel consumed to power produced (kJ/MMBtu)
- $\eta^{h}_{GT,min,\upsilon}$: Minimum efficiency possible for a gas turbine of size υ at hour h (%)
- $\eta^{h}_{GT,max,\upsilon}$: Maximum efficiency possible for a gas turbine of size υ at hour h (%)
- $W^{min}_{f,GT,\upsilon}$: Minimum amount of fuel consumed by a gas turbine of size υ (MMBtu/hr)
- $W^{max}_{f,GT,\upsilon}$: Maximum amount of fuel consumed by a gas turbine of size υ (MMBtu/hr)

- $W^{nom}_{HRSG,\upsilon}$: Nominal amount of steam produced by the steam turbine using exhaust gas from a gas turbine of size υ (kg/hr)
- $P^{max}_{ST,\phi}$: Maximum capacity of a steam turbine of size ϕ (MW)
- N_{ST}: Number of sizes of steam turbine available (nu)
- n_{ϕ}: Slope of steam turbine model for a steam turbine of size ϕ (MJ/kg)
- $P_{int,\phi}$: Intercept of steam turbine model for a steam turbine of size ϕ (MW)
- A_{ϕ}: Parameter used to model operation of a steam turbine of size ϕ (MW)
- B_{ϕ}: Parameter used to model operation of a steam turbine of size ϕ (nu)
- Δh: Isentropic enthalpy change in the steam turbine
- $W^{max}_{ST,\phi}$: Maximum amount of steam consumed by a steam turbine of size ϕ (kg/s)
- $a_{i,stsize}$: Regression coefficient of a steam turbine model of size *stsize*, i = {*1, 2, 3, 4*}
- $T_{sat,in,\phi}$: Temperature of the steam entering a steam turbine of size ϕ (^{o}C)
- $W^{max}_{BR,\chi}$: Maximum amount of steam generated by a boiler of size χ (kg/hr)

- N_{BR}: Number of sizes of boiler available (nu)
- η_{BR}: Efficiency of the boiler (%)
- LHV: Lower heating value of natural gas (kJ/kg)
- H_{BRout}: Enthalpy at the outlet of the boiler (kJ/kg)
- H_{BRin}: Enthalpy at the inlet of the boiler (kJ/kg)
- $W^{max}_{f,BR,\chi}$: Maximum amount of fuel consumed by a boiler of size χ
- $Q^{max}_{SA,\psi}$: Maximum amount of cooling provided by a steam absorption chiller of size ψ (Btu/hr)
- N_{SA}: Number of sizes of steam absorption chiller available (nu)
- COP_{SA}: COP of the steam absorption chiller (nu)
- $H_{s,in}$: Enthalpy of steam at the inlet of the steam absorption chiller (kJ/kg)
- $H_{s,SA}$: Enthalpy of steam at the outlet of the steam absorption chiller (kJ/kg)
- $W^{max}_{SA,\psi}$: Maximum amount of steam consumed by a steam absorption chiller of size ψ (kg/hr)
- $Q^{max}_{EC,\omega}$: Maximum amount of cooling provided by an electric chiller of size ω (Btu/hr)

- N_{EC}: Number of sizes of electric chiller available (nu)
- COP_{EC}: COP of the electric chiller (nu)
- $P^{max}_{EC,\omega}$: Maximum amount of power consumed by an electric chiller of size ω (kWh)
- $\gamma_{cold,e}$: Cost to turn on a piece of equipment e via a cold startup
- $\kappa_{warm,e}$: Cost to turn on a piece of equipment e via a warm
- $Cost_{BR}$: Cost of the boiler (\$/MMBtu/hr)
- $Cost_{EC}$: Cost of the electric chiller (\$/Btu/hr)
- $Main_{e,s}$: Maintenance cost for equipment e, $e \neq GT$, of size s
- MC_{BR}: Maintenance price based on size of boiler (\$/MBtu/hr)
- MC_{SA}: Maintenance price based on cooling capacity of the steam absorption chiller (\$/ton)
- MC_{EC}: Maintenance price based on cooling capacity of the electric chiller (\$/ton)
- Y: Projected lifetime of the plant (yrs)
- τ_d: Scaling parameter for each day, d, optimized (nu)
- NG_{cost}: Industrial price for natural gas in Texas (\$/ thousand ft^3)
- $U^d_{e,s,LB}$: Final value of $U^d_{e,s}$ in the lower bound optimization solution (nu)

- $U^{d}_{e,s,UB}$: Fixed value of $U^{d}_{e,s}$ in the upper bound optimization problem (nu)
- $U^{tot}_{e,s}$: Number of total days d a piece of equipment e of size s was used in the lower bound optimization solution (nu)
- Δ^{k}_{d}: Difference between asymmetric linking variables for iteration k (nu)
- θ^{k}: Step length parameter for iteration k (nu)
- β^{-}: 'Negative' adjustment parameter for the step length parameter (nu)
- β^{o}: 'Neutral' adjustment parameter for the step length parameter (nu)
- β^{+}: 'Positive' adjustment parameter for the step length parameter (nu)
- G^{LB}: Global (highest) lower bound optimization solution (Lagrangean decomposition) ($)
- G^{UB}: Global (lowest) upper bound optimization solution (Lagrangean decomposition) ($)
- η_{b}: Efficiency of the energy storage device (%)
- L^{max}_{b}: Maximum capacity of the energy storage device (BTU/hr or kWh)
- m_{b}: Parameter dictating the minimum capacity of the energy storage device (%)
- f^{in}_{b}: Parameter dictating maximum energy into the energy storage device (%)

- f_b^{out}: Parameter dictating the minimum energy into the energy storage device (%)
- $Cost_b$: Cost of the energy storage device ($/unit energy)
- MC_b: Maintenance price based on the size of the energy storage device ($/unit energy)
- G^{UL}: Global (lowest) lower bound optimization solution ($)
- G^{LL}: Global (highest) upper bound optimization solution ($)
- C_{DAM}^h: Day ahead market settlement price point ($/kWh)

Bibliography

[1] S. Treddinnick. Benefits of Economic Analysis (part 2): Real-world examples, 2011.

[2] Thermal Care. Installation, Operation, and Mainntenance TC Series Centrifugal Central Chillers with Panasonic PLC.

[3] World Coal Association. Improving efficiencies.

[4] C. Collins. Case studies: Mueller energy center at Dell Children's Medical Center, Austin, TX, 2010. In *Combined Heat & Power Conference*.

[5] NREL. Right-size heating and cooling equipment.

[6] D. Steen, T. Le, O. Carlson, and L. Bertling. Evaluating the customers' benefits of how published pricing based on day-ahead spot market. In *CIRED 22nd International Conference on Electricity Distribution*, 2013.

[7] U.S. Energy Information Administration. Annual Energy Outlook 2015 with projections to 2040, report DOE/EIA-0383(2015), 2015.

[8] Pecan Street Inc. Research.

[9] Electropaedia. Electricity Demand.

[10] Centre for Low Carbon Futures. Pathways for Energy Storage in the UK.

[11] ERCOT. Day-Ahead Market.

[12] ERCOT. ERCOT Monthly Operational Overview, 2016.

[13] National Archives and Records Administration. Fact Sheet: Obama Administration Announces Additional Steps to Increase Energy Security.

[14] Smart Manufacturing Leadership Coalition. DOE - Innovative Manufacturing Initiative.

[15] P. Wattles and J. Adams. Renewables, DERs and Reliability in the Evolving Grid. Presentation, 2016.

[16] A.D. Ondeck, T.F. Edgar, and M. Baldea. Optimal operation of a residential district-level combined photovoltaic/natural gas power and cooling system. *Applied Energy*, 2015.

[17] U.S. Energy Information Administration. AEO 2014 early release: Delivered energy by sector, 2013.

[18] The Association for Decentralised Energy. What is CHP?

[19] Energy and Environmental Analysis Inc. Combined heat and power units located in Texas.

[20] D. Williams. 3 MW biomass power plant commissioned in India, 2014.

[21] International Energy Agency. CHP/DHC country scorecard: Finland.

[22] Energy and Environmental Analysis Inc. Combined heat and power units located in Louisiana.

[23] P.M. Sartorelli. The integration of a cogeneration plant in a textile company, 2013.

[24] AGC Glass Europe. Cogeneration installation at AGC Fleurus automotive plant.

[25] International Energy Agency. CHP and DHC applications.

[26] U.S. EPA CHP Partnership. CHP in the hotel and casino market sectors, 2005.

[27] U.S. DOE. Hospitals discover advantages to using CHP systems, 2011.

[28] International District Energy Association. University of Texas at Austin 137-MW CHP & district energy system, 2012.

[29] Stadtwerke München. Combined heat and power.

[30] WorldWatch Institute. One twelfth of global electricity comes from combined heat and power systems.

[31] Weather Online. Sweden.

[32] U.S. Energy Information Administration. Annual Energy Review 2011, report DOE/EIA-0384(2011), 2012.

[33] State of Arizona Department of Revenue. Residential solar energy credit, 2013.

[34] State Energy Conservation Office. Texas tax code incentives for renewable energy §11.27 and §171.056.

[35] North Carolina State University. New Mexico incentives/policies for renewables & efficiency: Property tax exemption for residential solar systems.

[36] NREL. Open PV state rankings.

[37] M. Bianchi, A. De Pascale, and P.R. Spina. Guidelines for residential micro-CHP systems design. *Applied Energy*, 97:673–683, 2011.

[38] M. Maghanki, B. Ghobadian, G. Najafi, and R.J. Galogah. Micro combined heat and power (MCHP) technologies and applications. *Renewable and Sustainable Energy Reviews*, 28:510–24, 2013.

[39] O.A. Shaneb, G. Coates, and P.C. Taylor. Sizing of residential μCHP systems. *Energy and Buildings*, 43:1991–2001, 2011.

[40] M. De Paepe, P. D'Herdt, and D. Mertens. Micro-CHP systems for residential applications. *Energy Conversion and Management*, 47:3435–3446, 2006.

[41] E.S. Barbieri, P.R. Spina, and M. Venturini. Analysis of innovative micro-CHP systems to meet household energy demands. *Applied Energy*, 97:723–733, 2012.

[42] C. Brandoni and M. Renzi. Optimal sizing of hybrid solar micro-CHP systems for the household sector. *Applied Thermal Engineering*, 75:896–907, 2015.

[43] M. Bianchi, A. De Pascale, F. Melino, and A. Peretto. Performance prediction of micro-CHP systems using simple virtual operating cycles. *Applied Thermal Engineering*, 71:771–779, 2014.

[44] T.C. Fubara, F. Ceclja, and A. Yang. Modelling and selection of micro-CHP systems for domestic energy supply: The dimension of network-wide primary energy consumption. *Applied Energy*, 114:327–334, 2014.

[45] F. TeymouriHamzehkolaei and S. Sattari. Technical and economic feasibility study of using micro CHP in the different climate zones of Iran. *Energy*, 36:4790–4798, 2011.

[46] H. Ren and W. Gao. Economic and environmental evaluation of micro CHP systems with different operating modes for residential buildings in Japan. *Energy and Buildings*, 42:853–861, 2010.

[47] A. Hawkes and M. Leach. Impacts of temporal precision in optimization modeling of micro-combined heat and power. *Energy*, 30:1759–1779, 2005.

[48] M. Bianchi, L. Branchini, A. De Pascale, F. Melino, and A. Peretto. Preliminary investigations on a test bench for integrated micro-CHP energy systems. *Energy Procedia*, 45:1275–1284, 2014.

[49] M. Dentice d'Accadia, M. Sasso, S. Sibilio, and L. Vanoli. Micro-combined heat and power in residential and light commercial applications. *Applied Thermal Engineering*, 23:1247–1259, 2003.

[50] M.F. Torchio. Comparison of district heating CHP and distributed generation CHP with energy, environmental and economic criteria for Northern Italy. *Energy Conversion and Management*, 92:114–128, 2015.

[51] A.P. Prato, F. Strobino, M. Broccardo, and L.P. Giusino. Integrated management of cogeneration plants and district heating networks. *Applied Energy*, 97:590–600, 2012.

[52] G. Sundberg and D. Henning. Investments in combined heat and power plants: influence of fuel price on cost minimised operation. *Energy Conversion and Management*, 43:639–650, 2001.

[53] B. Rolfsman. Combined heat-and-power plants and district heating in a deregulated electricity market. *Applied Energy*, 78:37–52, 2004.

[54] H. Ren, W. Gao, and Y. Ruan. Optimal sizing for residential CHP system. *Applied Thermal Engineering*, 28:514–523, 2008.

[55] A. Hawkes and M. Leach. Cost-effective operating strategy for residential micro-combined heat and power. *Energy*, 32:711–723, 2007.

[56] M.H. Moradi, M. Hajinazari, S. Jamasb, and M. Paripour. An energy management system (EMS) strategy for combined heat and power

(CHP) systems based on a hybrid optimization method employing fuzzy programming. *Energy*, 49:86–101, 2013.

[57] D. Ziher and A. Poredos. Economics of a trigeneration system in a hospital. *Applied Thermal Engineering*, 26:680–687, 2006.

[58] S.M. Lai and C.W. Hui. Feasibility and flexibility for a trigeneration system. *Energy*, 34:1693–1704, 2009.

[59] E. Cardona and A. Piacentino. A methodology for sizing a trigeneration plant in mediterranean areas. *Applied Thermal Engineering*, 23:1665–1680, 2003.

[60] J. Bassols, B. Kuckelkorn, R. Schneider, and H. Veelken. Trigeneration in the food industry. *Applied Thermal Engineering*, 22:595–602, 2002.

[61] S. Mitra, L. Sun, and I.E. Grossmann. Optimal scheduling of industrial combined heat and power plants under time-sensitive electricity prices. *Energy*, 54:194–211, 2013.

[62] Mueller. Mueller green resources guide.

[63] Mueller Megawatt Project. Mueller megawatt project: About us.

[64] K.X. Perez, W.J. Cole, J.D. Rhodes, A. Ondeck, M. Webber, M. Baldea, and T.F. Edgar. Nonintrusive disaggregation of residential air-conditioning loads from sub-hourly smart meter data. *Energy and Buildings*, 81:316–325, 2014.

[65] The University of Texas at Austin: Utilities & Energy Management. Sustainability.

[66] J.S. Kim. *Modeling, Control, and Optimization of Combined Heat and Power Plants*. PhD thesis, University of Texas at Austin, 2014.

[67] A.I. Cohen and G. Ostrowski. Scheduling units with multiple operating modes in unit commitment. *IEEE Transactions on Power Systems*, 11:497–503, 1996.

[68] Austin Energy. Rates: Residential electric rates & line items.

[69] P. Ulloa. *Potential for Combined Heat and Power and District Heating and Cooling from Waste-to-Energy Facilities in the U.S.—Learning from the Danish Experience*. PhD thesis, Columbia University, 2007.

[70] ERCOT. Day-ahead market.

[71] U.S. Energy Information Administration. Texas natural gas industrial prices.

[72] A. Ondeck, T.F. Edgar, and M. Baldea. A Multi-Scale Framework for Simultaneous Optimization of the Design and Operating Strategy of Residential CHP Systems. *Applied Energy*. Submitted.

[73] American Society of Civil Engineers. 2013 Report Card for America's Infrastructure.

[74] K. Cooney, S. Schare, and et al. Combined Heat and Power in Texas: Status, Potential, and Policies to Foster Investment.

[75] California Independent System Operator. What the Duck Curve Tells us about Managing a Green Grid.

[76] E. Cardona and A. Piacentino. A new approach to exergoeconomic analysis and design or variable demand energy systems. *Energy*, 31:490–515, 2006.

[77] Y. Fumero, G. Corsano, and J.M. Montagna. A Mixed Integer Linear Programming model for simultaneous design and scheduling of flowshop plants. *Applied Mathematical Modelling*, 37:1652–1664, 2013.

[78] Y. Fumero, J.M. Montagna, and G. Corsano. Simultaneous design and scheduling of a semicontinuous/batch plant for ethanol and derivatives production. *Computers and Chemical Engineering*, 36:342–357, 2012.

[79] B.P.M Duarte, L.O. Santos, and J.S. Mariano. Optimal sizing, scheduling and shift policy of grinding section of ceramic tile plant. *Computers & Operations Research*, 36:1825–1834, 2009.

[80] G. Corsano and J.M. Montagna. Mathematical modeling for simultaneous design of plants and supply chain in the batch process industry. *Computers and Chemical Engineering*, 35:149–164, 2011.

[81] G.S.K. Priya and S. Bandyopadhyay. Optimum sizing of supply equipment for time varying demand. *Computers and Chemical Engineering*, 83:72–78, 2015.

[82] J. Wang, Y. Jing, and C. Zhang. Optimization of capacity and operation for CCHP system by genetic algorithm. *Applied Energy*, 87:1325–1335, 2010.

[83] M.A. Lozano, J.C. Ramos, and L.M. Serra. Cost optimization of the design of CHCP (combined heat, cooling and power) systems under legal constraints. *Energy*, 35:794–805, 2010.

[84] A.H. Azit and K.M. Nor. Optimal sizing for a gas-fired grid-connected cogeneration system planning. *IEEE Transactions on Energy Conversion*, 24(4):950–958, 2009.

[85] M. Rivarolo, A. Cuneo, A. Traverso, and A.F. Massardo. Design optimisation of smart poly-generation energy districts through a model based approach. *Applied Thermal Engineering*, 99:291–301, 2016.

[86] M.H. Moradi, M. Eskandari, and H. Showkati. A hybrid method for simultaneous optimization of DG capacity and operational strategy in microgrids utilizing renewable resources. *Electrical Power and Energy Systems*, 56:241–258, 2014.

[87] F. Capra and E. Martelli. Numerical optimization of combined heat and power Organic Rankine Cycles - Part B: Simultaneous design &

part-load optimization. *Energy*, 90:329–343, 2015.

[88] N.K. Shah and M.G. Ierapetritou. Lagrangian decomposition approach to scheduling large-scale refinery operations. *Computers and Chemical Engineering*, 79:1–29, 2015.

[89] A. Piacentino and F. Cardona. On thermoeconomics of energy systems at variable load conditions: Integrated optimization of plant design and operation. *Energy Conversion and Management*, 48:2341–2355, 2007.

[90] F. Oliveira, S. Hamacher V. Gupta, and & I.E. Grossmann. A Lagrangean decomposition approach for oil supply chain investment planning under uncertainty with risk considerations. *Computers & Chemical Engineering*, 50:184–195, 2013.

[91] A.G. Marín. Airport taxi planning: Lagrangian decomposition. *Journal of Advanced Transportation*, 47(4):461–474, 2013.

[92] S.A. Van den Heever, I.E. Grossmann, S. Vasantharajan, and K. Edwards. A Lagrangean decomposition heuristic for the design and planning of offshore hydrocarbon field infrastructures with complex economic objectives. *Industrial & engineering chemistry research*, 40(13):2857–2875, 2001.

[93] H. Hajabdollahi, A. Ganjehkaviri, and M.N.M. Jaafar. Assessment of new operational strategy in optimization of CCHP plant for different

climates using evolutionary algorithms. *Applied Thermal Engineering*, 75:468–480, 2015.

[94] J. Ortiga, J.C. Bruno, and A. Coronas. Operational optimisation of a complex trigeneration system connected to a district heating and cooling network. *Applied Thermal Engineering*, 50:1536–1542, 2013.

[95] N.A. Diangelakis, C. Panos, and E.N. Pistikopoulos. Design optimization of an internal combustion engine powered CHP system for residential scale application. *Computational Management Science*, 11(3):237–266, 2014.

[96] S. Gamou, R. Yokoyama, and K. Ito. Optimal unit sizing of cogeneration systems in consideration of uncertain energy demands as continuous random variables. *Energy Conversion and Management*, 43:1349–1361, 2002.

[97] K.C. Kavvadias, A.P. Tosios, and Z.B. Maroulis. Design of a combined heating, cooling and power system: Sizing, operation strategy selection and parametric analysis. *Energy Conversion Management*, 51:833–845, 2010.

[98] T. Wakui, H. Kawayoshi, and R. Yokoyama. Optimal structural design of residential power and heat supply devices in consideration of operational and capital recovery constraints. *Applied Energy*, 163:118–133, 2016.

[99] D. Buoro, M. Casisi, P. Pinamonti, and M. Reini. Optimal synthesis and operation of advanced energy supply systems for standard and domotic home. *Energy Conversion and Management*, 60:96–105, 2012.

[100] C. Marnay, G. Venkataramanan, M. Stadler, A. Siddiqui, R. Firestone, and B. Chandran. Optimal technology selection and operation of commercial-building microgrids. *IEEE Transactions on Power Systems*, 23(3):975–982, 2008.

[101] S. Oh, H. Lee, J. Jung, and H. Kwak. Optimal planning and economic evaluation of cogeneration system. *Energy*, 32:760–771, 2007.

[102] Solar Turbines. Mercury 50.

[103] R. Kurz. Introduction to Gas Turbines and Applications.

[104] U.S. Environmental Protection Agency Combined Heat and Power Partnership. Catalog of CHP Technologies, 2015.

[105] P.S. Varbanov, S. Doyle, and R. Smith. Modelling and optimization of utility systems. *Chemical Engineering Research and Design*, 82:561–578, 2004.

[106] S.P. Mavromatis and A.C. Kokossis. Conceptual optimisation of utility networks for operation variations - I. Targets and level optimisation. *Chemical Engineering Science*, 53:1585–1608, 1998.

[107] R. Baldick. The Generalized Unit Commitment Problem. *IEEE Transactions on Power Systems*, 10(1):465–475, 1995.

[108] EPA. Fact Sheet: CHP as a Boiler Replacement Opportunity.

[109] Sacramento Municipal Utility District. Compare - Installed Costs - Chillers.

[110] R.L. Arnold and W.P. Bahnfleth. Peak shaving: Using natural gas engine-driven chillers. *Heating, piping and air conditioning*, 70(9):51–59, 1998.

[111] A.G. Awn and S. Murai. Absorption Chiller Applications and Efficiency. *2nd International District Cooling Symposium*, 2007.

[112] Mueller. The Plan.

[113] Mueller Megawatt Project.

[114] F. Barahona and R. Anbil. The volume algorithm: Producing primal solutions with a subgradient method. *Mathematical Programming*, 87(3):385–399, 2000.

[115] WeatherSpark. Historical Weather for 2012 in Austin, Texas, USA.

[116] U.S. Energy Information Administration. Electric Power Monthly, 2016.

[117] I.A. de Oliveria, R. Schaeffer, and A. Szklo. The impact of energy storage in power systems: The case of Brazil's Northeastern grid. *Energy*, 122:50–60, 2017.

[118] A. Nú nez Reyes, D.M. Rodríguez, C.B. Alba, and M.A.R. Carlini. Optimal scheduling of grid-connected PV plants with energy storage for integration in the electricity market, 2017.

[119] R. Hemmati and H. Saboori. Short-term bulk energy storage system scheduling for load leveling in unit commitment: modeling, optimization, and sensitivity analysis. *Journal of Advanced Research*, 7:360–372, 2016.

[120] S.S. Reddy. Optimal scheduling of thermal-wind-solar power system with storage. *Renewable Energy*, 101:1357–1368, 2017.

[121] D. McConnell, T. Forcey, and M. Sandiford. Estimating the value of electricity storage in an energy-only wholesale market. *Applied Energy*, 159:422–432, 2015.

[122] D. Buoro, P. Pinamonti, and M. Reini. Optimization of a Distributed Cogeneration System with solar district heating. *Applied Energy*, 124:298–308, 2014.

[123] R.C. Pattison, C.R. Touretzky, T. Johansson, I. Harjunkoski, and M. Baldea. Optimal process operations in fast-changing electricity markets: framework for scheduling with low-order dynamic models and an air separation application. *Industrial & Engineering Chemistry Research*, 55(16):4562–4584, 2016.

[124] S. Chakraborty and T. Okabe. Robust energy storage scheduling for imbalance reduction of strategically formed energy balancing groups.

Energy, 114:405–417, 2016.

[125] G. Pagliarini and S. Rainieri. Modeling of thermal energy storage system coupled with combined heat and power generation for the heating requirements of a University Campus. *Applied Thermal Engineering*, 30:1255–1261, 2010.

[126] T. Nuytten, B. Claessens, K. Paredis, J. Van Bael, and D. Six. Flexibility of a combined heat and power system with thermal energy storage for district heating. *Applied Energy*, 2014:583–591, 2013.

[127] D. Steen, M. Stadler, G. Cardoso, M. Groissb ́ock, and N. DeForest. Modeling of thermal storage systems in MILP distributed energy resource models. *Applied Energy*, 137:782–792, 2015.

[128] C. Finck, R. Li, and W. Zeiler. An optimization strategy for scheduling various thermal energy storage technologies in office buildings connected to smart grid. *Energy Procedia*, 78:806–811, 2015.

[129] M. Fiorentini, P. Cooper, Z. Ma, and D.A. Robinson. Hybrid model predictive control of a residential HVAC system with PVT energy generation and PCM thermal storage. *Energy Procedia*, 83:21–30, 2015.

[130] E.S. Barbieri, F. Melino, and M. Morini. Influence of thermal energy storage on the profitability of micro-CHP systems for residential building applications. *Applied Energy*, 97:714–722, 2012.

[131] C. Shang, D. Srinivasan, and T. Reindl. Generation and storage scheduling of combined heat and power. *Energy*, 2017.

[132] V. Verda and F. Colella. Primary energy savings through thermal storage in district heating networks. *Energy*, 36:4278–4286, 2011.

[133] E. Carpaneto, P. Lazzeroni, and M. Repetto. Optimal integration of solar energy in a district heating network. *Renewable Energy*, 75:714–721, 2015.

[134] H. Wang, E. Abdollahi, R. Lahdelma, W. Jiao, and Z. Zhou. Modelling and optimization of the smart hybrid renewable energy for communities (SHREC). *Renewable Energy*, 84:114–123, 2015.

[135] H. Wang, W. Yin, E. Abdollahi, R. Lahdelma, and W. Jiao. Modelling and optimization of CHP based district heating system with renewable energy production and energy storage. *Applied Energy*, 159:401–421, 2015.

[136] G. Streckienė, V. Martinaitis, A.N. Andersen, and J. Katz. Feasibility of CHP-plants with thermal stores in the german spot market. *Applied Energy*, 86:2308–2316, 2009.

[137] T. Tveit, T. Savola, A. Gebremedhin, and C. Fogelholm. Multi-period MINLP model for optimising operation and structural changes to chp plants in district heating networks with long-term thermal storage. *Energy Conversion and Management*, 50:639–647, 2009.

[138] K. Li and K.J. Tseng. Energy efficiency of lithium-ion battery used as energy storage devices in micro-grid. In *Industrial Electronics Society, IECON 2015-41st Annual Conference of the IEEE*, pages 5235–5240. IEEE, 2015.

[139] K.C. Divya and J. Østergaard. Battery energy storage technology for power systems - An overview. *Electric Power Systems Research*, 79:511–520, 2009.

[140] W.P. Bahnfleth and A. Musser. Thermal performance of a full-scale stratified chilled-water thermal storage tank. *ASHRAE Transactions*, 104:377, 1998.

[141] Lazard Ltd. Lazard's Levelized Cost of Storage Analysis v1.0, 2015.

[142] Z. Zhang, W.D. Turner, Q. Chen, C. Xu, and S. Deng. A method to determine the optimal tank size for a chilled water storage system under a time-of-use electricity rate structure. 2010.

[143] R.R Iyer and I.E. Grossmann. Synthesis and operational planning of utility systems for multiperiod operation. *Computers & Chemical Engineering*, 22(7):979–993, 1998.

[144] B.A. Calfa, A. Agarwal, I.E. Grossmann, and J.M. Wassick. Hybrid Bilevel-Lagrangean Decomposition Scheme for the Integration of Planning and Scheduling of a Network of Batch Plants. *Industrial & Engineering Chemistry Research*, 52:2152–2167, 2013.

[145] T. Nishi, Y. Hiranaka, and I.E. Grossmann. A bilevel decomposition algorithm for simultaneous production scheduling and conflict-free routing for automated guided vehicles. *Computers & Operations Research*, 38:876–888, 2011.

[146] M. Erdirik-Dogan and I.E. Grossmann. Simultaneous planning and scheduling of single-stage multi-product continuous plants with parallel lines. *Computers and Chemical Engineering*, 32:2664–2683, 2008.

[147] S. Terrazas-Moreno and I.E. Grossmann. A multiscale decomposition method for the optimal planning and scheduling of multi-site continuous multiproduct plants. *Chemical Engineering Science*, 66:4307–4318, 2011.

[148] M. Munsell. Solar PV Prices Will Fall Below $1.00 per Watt by 2020.

[149] Mueller Green Resources Guide, 2012.

[150] S. Lacey. Stem CTO: Lithium-Ion Battery Prices Fell 70% in the Last 18 Months, June 2016.

[151] Z. Shahan. EV Battery Prices: Looking Back A Few Years, & Forward Yet Again, May 2016.

[152] M.H. Brown and R.P. Sedano. Electricity Transmission: A Primer, 2004. National Council on Electricity Policy (NCEL).

[153] ERCOT. Module 2: Day-Ahead Operations, 2010.

[154] Siemens. Industrial Gas Turbines: The comprehensive product range from 5 to 50 megawatts.

[155] GE Power & Water Distributed Power. Power Generation Products.

Vita

Abigail Devin Ondeck is from Pittsburgh, Pennsylvania. She graduated from Carnegie Mellon University in 2012 with honors, and received a B.S. in Chemical Engineering and B.S. in Biomedical Engineering. She started her graduate studies in Chemical Engineering at the University of Texas at Austin in the autumn of 2012. While at UT, she earned a coursework M.S. degree in Chemical Engineering in 2014 and completed a graduate internship at ExxonMobil as an applications engineer in the summer of 2016. After graduating, Abigail has accepted a post-doctoral position and will be headed back to Pittsburgh and Carnegie Mellon University.

Permanent address: abigailondeck@gmail.com

This dissertation was typeset with LaTeX[†] by the author.

[†]LaTeX is a document preparation system developed by Leslie Lamport as a special version of Donald Knuth's TeX Program.